GEOLOGIC INVESTIGATION OF ROOF AND FLOOR STRATA: LONGWALL DEMONSTRATION, OLD BEN MINE NO. 24. PREDICTION OF COAL BALLS IN THE HERRIN COAL

FINAL TECHNICAL REPORT: PART 2

by

Philip J. DeMaris, Robert A. Bauer, Richard A. Cahill, and Heinz H. Damberger

Principal Investigators:

Heinz H. Damberger
Harold J. Gluskoter (to 6/78)

Illinois State Geological Survey
Natural Resources Building
615 East Peabody Drive
Champaign, Illinois 61820

Date Published, April 1983

Contract No. U.S.D.O.E. DE-FG01-78ET12177
(Formerly U.S.B.M. G0166207)

This report represents work on a program
that was originated by the Interior Department's Bureau of Mines
and was transferred to the Department of Energy on October 1, 1977.

U.S. DEPARTMENT OF ENERGY
Assistant Secretary for Energy Technology
Division of Fossil Fuel Extraction
Mining Research and Development

CONTENTS

TABLES

FIGURES

ABSTRACT

Coal-ball areas, large deposits of mineralized peat in the coal seam, obstructed longwall mining in the Herrin Coal at Old Ben Mine No. 24. In-mine mapping located coal balls under transitional roof--areas where the roof lithology alternates between the Energy Shale and the Anna Shale/Brereton Limestone. Specifically, coal balls occur under eroded exposures or "windows" of the marine Anna Shale/Brereton Limestone in the Energy Shale.

Two types of coal-ball areas have been identified, based on stratigraphic position in the coal seam: type I is restricted to the top of the seam, and type II occurs at midseam and below. Type II occurrences are major mining problems. Although single and clustered coal balls also occur in the coal seam, they present no major difficulties for mining.

To predict the distribution of coal balls, as well as explain their formation, a depositional model was developed: First, freshwater sediments buried the Herrin peat. Decomposition of the sealed peat continued, producing high CO_2 partial pressures; then selective erosion took place as a river removed the cover along sinuous paths, cutting through to the peat in some places. With the seal broken, CO_2 was released, and freshwaters that contained Ca and Mg ions flushed out organic acids. These events increased the pH and shifted the equilibrium toward carbonate precipitation. Later, marine mud buried both the freshwater sediments and the exposed peat, which accounts for the transitional roof over the Herrin Coal and the coal balls under the marine shale "windows" in the Energy Shale.

The depositional model was supported by the first comprehensive set of geochemical data for coal balls. Coal balls generally contained less than 4 percent organic carbon and very low levels of detrital minerals. Distributions of minor elements generally showed no clear imprint of the original peat composition, with the possible exception of the rare earth elements. Carbon isotope data suggested a terrestrial source for the carbonate in type II coal balls from one area, and a marine source for samples of type I (top-of-seam) coal balls.

Although individual sites of concentrated coal balls cannot be predicted, the specific linear roof exposures associated with these coal-ball areas can be identified by mapping. Based on previously mapped areas, the trends of these linear exposures can be projected.

KEYWORDS: coal balls, Herrin Coal, depositional model, transitional roof, geochemistry, sedimentary rocks, trace elements, C-13/C-12, longwall mining, Illinois Basin, Pennsylvanian

ACKNOWLEDGMENTS

This work was supported by U.S. Bureau of Mines Grant G0166207 from September 1976 to March 1978, by Department of Energy Grant ET-76-G-01-9007, from April 1978 to December 1979, and by Department of Energy Grant DE-FG01-78ET12177 from February 1981 to July 1982.

The work was administered under the technical direction of the Pittsburgh Mining Technology Center with James R. White, Mary Ann Gross, and Jasinder Jaspal as Technical Project Officers.

We wish to thank the officials and employees of the Old Ben Coal Company for valuable information and assistance. We also wish to thank the following Illinois State Geological Survey staff members for their assistance: W. John Nelson and Steven K. Danner for assistance in underground mapping; Suzanne Costanza, Wesley Dillon and Mary H. Barrows for coal and organic petrography; Chen-Lin Chou for geochemical interpretations; James B. Risatti for geochemical interpretations of swamp conditions; and Randall E. Hughes for clay mineralogy. We are grateful to Thomas F. Anderson (University of Illinois) for providing stable isotope data, and T. L. Phillips (University of Illinois) and William A. DiMichele (University of Washington) for information and assistance during the project. We also wish to thank Harold J. Gluskoter, who was principal investigator during the first phase of the contract.

Geochemical analysts include John D. Steele (atomic absorption), Raymond S. Vogel (optical emission), L. R. Henderson (energy dispersive x-ray, optical emission, x-ray fluorescence), Josephus Thomas (ion-selective electrode), Joan K. Bartz (rock analysis), Lawrence B. Kohlenberger, Larry R. Camp and Chaven Chusak (coal analysis), Elisabeth I. Fruth (atomic absorption, x-ray fluorescence), Richard A. Cahill (instrumental neutron activation analysis), Herbert D. Glass (x-ray diffraction), and Jeanne Dunn (data analyst).

EXECUTIVE SUMMARY

This study documents the local geologic conditions at and near the longwall demonstration site, with special attention to coal balls: concretions of mineralized peat in the coal seam. To predict their locations was a principal goal, since massive coal balls disrupted mining operations. A better understanding of their depositional and formative environments was developed to achieve this goal. Our project involved mapping, sampling, and chemical analyses of coal balls, coal seams, and roof and floor strata - a continuation of the work presented in the U.S. Department of Energy Contract Report, Geologic Investigation of Roof and Floor Strata: Longwall Demonstration of Old Ben Mine No. 24 (NTIS No. DOE/ET/12177-1), Part 1.

Coal balls in the Herrin (No. 6) Coal are predictable at two levels: In general, they are associated with most Anna Shale/Brereton Limestone roof in transitional roof areas; transitional roof can be identified from typical drill hole densities (1 to 2 holes/mi^2) used during exploration. Specifically, the type II coal ball areas which cause mining problems are located under a specific linear exposure of Anna Shale/Brereton Limestone roof at Old Ben Mine No. 24; preliminary evidence suggests other such linear exposures may be linked to type II coal ball occurrences found elsewhere. These linear exposures can be mapped in mine without difficulty.

A depositional model is proposed which explains the distribution of coal balls at Old Ben Mine No. 24. The model is based on detailed geological observations and mapping, together with geochemical data on major, minor and trace element distributions from coal, coal balls, roof and floor lithologies, as well as carbon and oxygen isotope data for selected coal balls and other materials. The model has the peat covered with fresh or brackish water sediments, sealing the top of the peat. Continued decomposition of the peat produces high partial CO_2 pressures in the sealed peat. Erosion of the cover in selected areas by fresh waters from a river containing Ca and Mg ions flushes out the organic acids, increases the pH, and along with the CO_2 degassing, shifts the equilibrium toward carbonate precipitation. Later a marine mud was deposited on the fresh water sediments and on the peat exposed by the removal of the fresh water sediments, producing the association of coal balls and marine shale roof.

Further work suggested by our results includes investigations to evaluate the model at other coal-ball sites in the Herrin and other seams, and refinement of the model through further geochemical investigations.

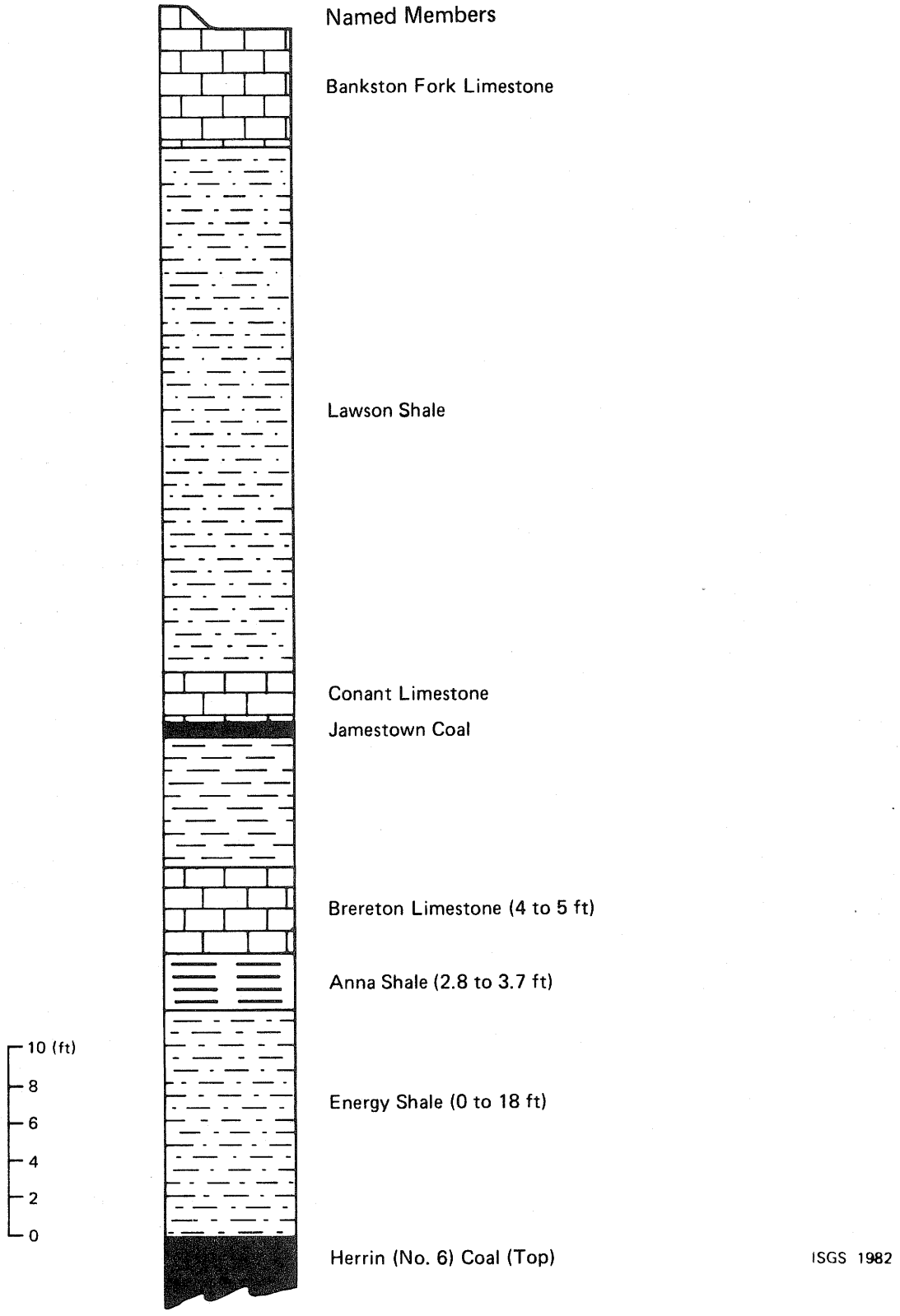

Figure 1
Composite stratigraphic section of the roof of the longwall panels, representing a portion of the Carbondale Formation, Kewanee Group, Pennsylvanian System.

INTRODUCTION

This study documents the local geologic conditions at and near the longwall demonstration site, with special attention to coal balls: concretions of mineralized peat in the coal seam. To predict their occurrence was a principal goal, since massive coal balls disrupt mining operations. A better understanding of their depositional and formative environments was developed to help achieve this goal. This involved mapping, sampling, and chemical analyses of coal balls, coal seams, and roof and floor strata--a continuation of the work presented in the U.S. Department of Energy Contract Report, Geologic Investigation of Roof and Floor Strata: Longwall Demonstration of Old Ben Mine No. 24 (NTIS No. DOE/ET/12177-1), Part I.

The continued effort to investigate and explain coal balls in the Herrin (No. 6) Coal Member involved more mapping and sampling in Old Ben Mine No. 24 and in nearby mines. We reconnaissance-mapped in two nearby mines to compare previous findings with additional areas of transitional roof and coal-ball occurrences. At the same time we took samples of coal and associated lithologies to supplement those from Old Ben Mine No. 24, which was closed and inaccessible during much of the final phase of our work.

Samples of floor, roof, coal, shale partings, and coal balls were chemically analyzed to help define their environments of formation. The analyses included major, minor and trace elements. Selected samples were also analyzed for carbon and oxygen isotopes and clay mineral composition ($< 2\mu$). We reviewed previously published coal-ball models and compared them to our own findings at Old Ben Mine No. 24 and nearby mines.

GENERAL CHARACTERISTICS OF THE HERRIN COAL AND ASSOCIATED ROOF STRATA

This section expands the discussion that began in Part I on of the possible origins of various rock units associated with the Herrin Coal. Our main focus is the stratigraphic section consisting of four members: the Herrin Coal, the Energy Shale, the Anna Shale, and the Brereton Limestone Members of the Carbondale Formation, Kewanee Group, Pennsylvanian System (fig. 1). The following information on these and related lithologies and their depositional environments (table 1) provides a useful background for interpretation of our depositional model, which is discussed later.

Table 1. Major Depositional Periods and Events, and Spatial distribution of Units at Old Ben Mine No. 24.

Deposition of	Facies, events	Areal extent of rock units
E. Brereton Limestone Member	argillaceous, dark gray marine limestone (facies not studied)	100% coverage
	environment is host to several types of burrowing organisms	
D/E RESTRICTED MARINE ENVIRONMENT ENDS		
D. Anna Shale Member	upper portion of the Anna is highly bioturbated	ca. 98% coverage
	transported plant fragments are common components of lower portion	ca. 90% coverage
	very thin coal deposited as wave base erosion ceases	commonly seen on the Energy/Anna contact
C/D TOPS OF ROLLS AND PEAT ARE FURTHER ERODED; SOME OFF-SLOPE REDEPOSITION OF ENERGY SHALE		
C. Channel-fill Materials	as the transgression continues, tidal channels re-use the previous channels and develop new channels	fossiliferous shale and impure limestone, reworked peat fragments and coal balls are locally deposited in many channels.
	channels are cut into peat and filled with reworked Energy Shale	channels common in areas where Energy Shale was eroded
B/C ENERGY SHALE DEPOSITION CEASES; WIDESPREAD EROSION BEGINS		
B. Energy Shale Member	light gray, weakly laminated facies	thick; 100% coverage
	dark gray, carbonaceous facies	thin; ca. 20% coverage
A/B PEAT ACCUMULATION ENDS AS SHALE DEPOSITION BEGINS		
A. Herrin Peat	occasional flooding of peat swamp from Walshville channel to form partings	100% coverage by thick peat

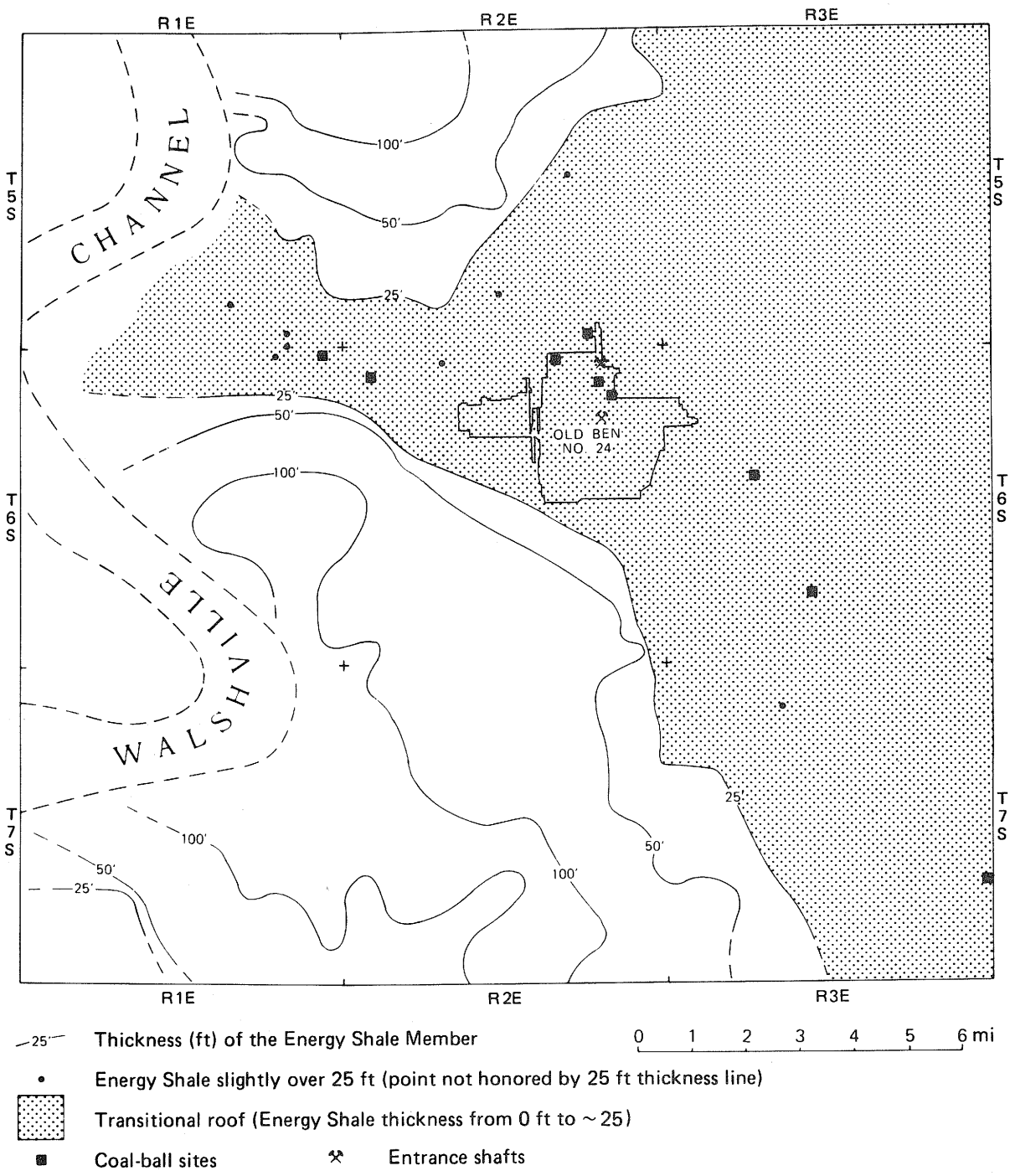

Figure 2

Distribution of transitional roof in a portion of Franklin County. All known coal-ball sites are also plotted.

Herrin Coal and Interbedded "Blue Band"

As discussed in Part I, the depositional environment of the Herrin Coal was a peat swamp in a broad, level coastal plain drained by a major river. The river flowed in a channel named the Walshville (D. O. Johnson, 1972), now represented primarily by shales, siltstones, and sandstones (fig. 2). Old Ben Mine No. 24 is located 6 to 10 miles east of the former riverbed.

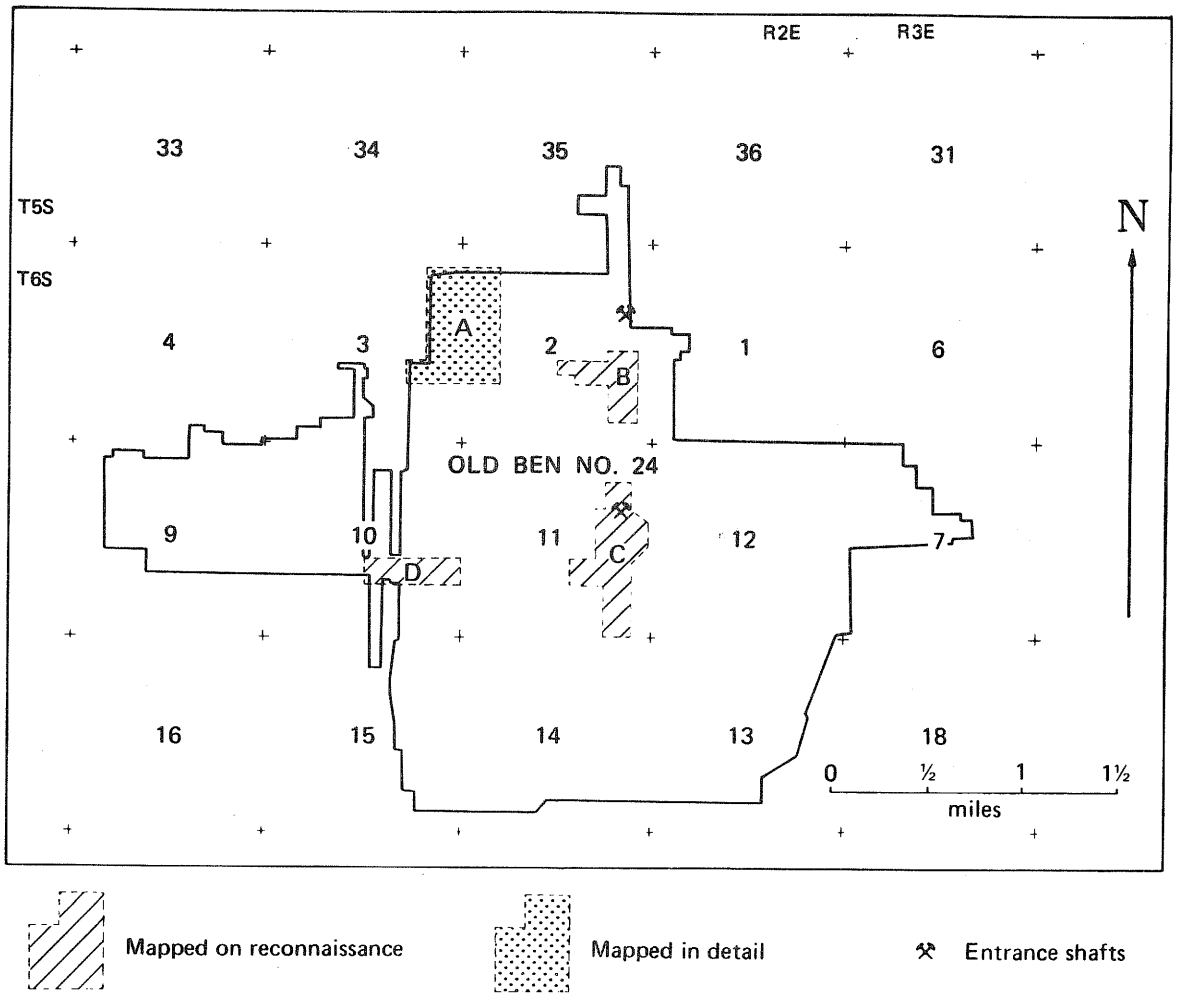

Figure 3
Index to mapped areas in the Old Ben Coal Company Mine No. 24. Numbers on the map are section numbers, located at the center of each square mile.

The origin of the "blue band," a prominent claystone parting in the lower part of the seam, appears to be closely related to the Walshville channel. Previous work by Survey geologists and a regional study by D. O. Johnson (1972) suggested the "blue band" thickened toward the channel. We checked this relationship on the west side of Old Ben Mine No. 21. Along a continuous exposure about 1 mile long, the "blue band" did thicken toward the channel from a normal 0.12 feet to nearly 2 feet. Approaching the channel, the "blue band" remained a claystone and retained its typically pelletoidal structure, first described by P. R. Johnson (1979). As the "blue band" probably originated during a major flood of the lowlands surrounding the river, it represents a useful time marker.

At numerous sites in study area A (fig. 3), the thickness of coal was measured between the underclay and the "blue band"; maximum variation was found to be about 0.6 feet. A peat-to-coal compaction ratio of 5:1 suggests that the original topographic relief of the underclay was 3 feet in the study area. The variation was unrelated to coal-ball occurrences, indicating that coal-ball formation was unrelated to local topography as suggested by Phillips, Kunz, and Mickish (1977) for sites in Saline County.

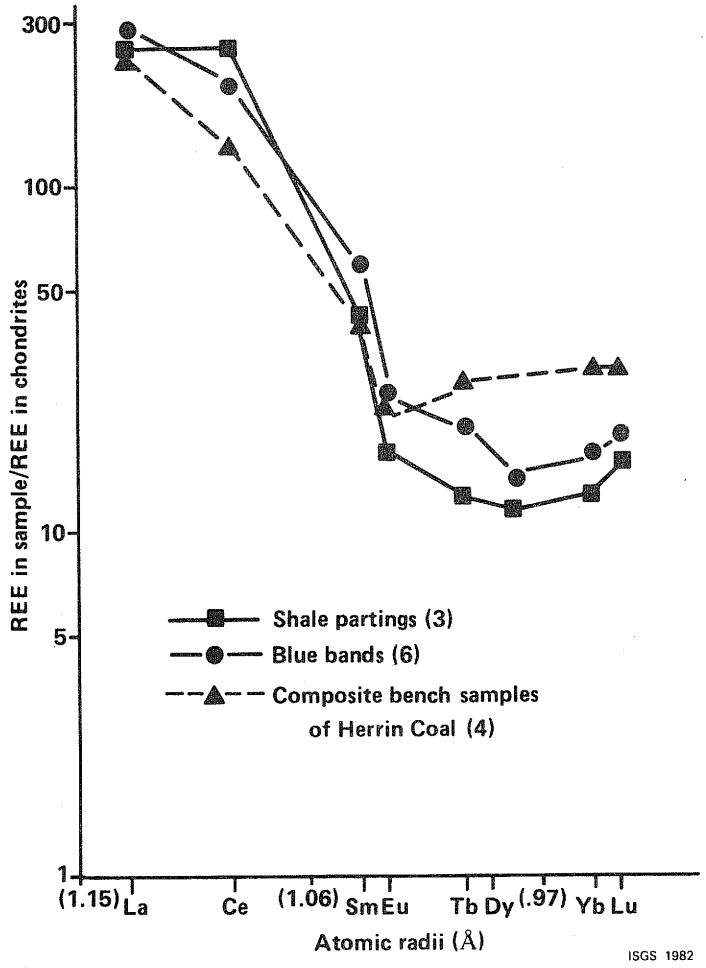

Figure 4
The rare earth element (REE) distributions in high-temperature ash (HTA) samples of the "blue band" and other claystone partings and in low-temperature ash (LTA) samples of the Herrin Coal from Old Ben Mine No. 24. The Herrin Coal values are averages of weighted bench composites (Harvey et al., 1983).

The "blue band" and other shale partings within the Herrin Coal are chemically similar to the finely disseminated mineral matter within the coal. Rare earth element (REE) distribution patterns (fig. 4) are similar for samples of the "blue band," other shale partings and low temperature ash of the Herrin Coal, suggesting a common source for these clay-rich materials.

Energy Shale

The Energy shale, which forms the immediate roof of the Herrin Coal over much of southern Illinois, is closely related to the Walshville channel. Since this shale consists of lobes or clastic wedges that thicken and coarsen toward the channel, D. O. Johnson (1972) interpreted the Energy Shale as crevasse-splay deposits, produced when the Walshville river repeatedly breached its levees and carried vast amounts of mud in suspension. We mapped these deposits as far as the eastern edge of Franklin County (fig. 2). He also noted abrupt truncation of isopach lines at the margins of the clastic wedges, probably caused by postdepositional erosion. When the river shifted and sea level rose, the edges of the clastic wedges were eroded.

Table 2. Flora of the carbonaceous facies of the Energy Shale Member

Taxa	Abundance	Occurrence
Lepidodendron dicentricum	common	full trunks to 30 cm wide and crown branches
Lepidodendron scleroticum	rare	scattered leaf cushions
Stigmaria ficoides	common	with rootlets attached, in situ
Pteridosperm petioles	average	in poor condition
Trigonocarpus	rare	only one found
Neuropteris ovata	rare	leaflets only
Pecopteris(?)	rare	leaflets only
Sphenophyllum emarginatum	rare	leaflets only

Interpretation This flora represents the final swamp forest; *L. dicentricum* is a typical swamp tree, and its roots (*Stigmaria*) are in situ in the peat (now coal). Other elements show poor preservation and may have been transported a short distance. The larger tree trunk fragments show no preferred orientation, suggesting slow drowning of the peat forest. Data gathered and interpreted by William A. DiMichele from 12 sites within mapped area A.

The end of the Herrin swamp and the beginning of Energy Shale deposition appear to be continuous in isolated areas. This transition is represented by a fossiliferous mud deposited over the Herrin Peat. It appears as a carbonaceous facies of the Energy Shale, forming about one-fifth of the immediate roof at Old Ben Mine No. 24; it contains a flora reflecting the end of forest vegetation (table 2).

Then the lighter gray facies of the Energy Shale was deposited over the carbonaceous facies. The sharp contact between them suggests either an interruption in deposition or possible erosion.

During the early distribution of the light gray facies, there was some rip-up of the underlying peat along small, shallow channels. The light gray facies is poorly bedded, indicating rapid deposition to some; however, at Old Ben Mine No. 27, a thin coal representing a short-lived swamp is locally found 0.4 feet from the base of the light gray facies. Thus, there were interruptions in its deposition. Fossils found in the light gray facies (including Dunbarella) indicate brackish water was present by this time.

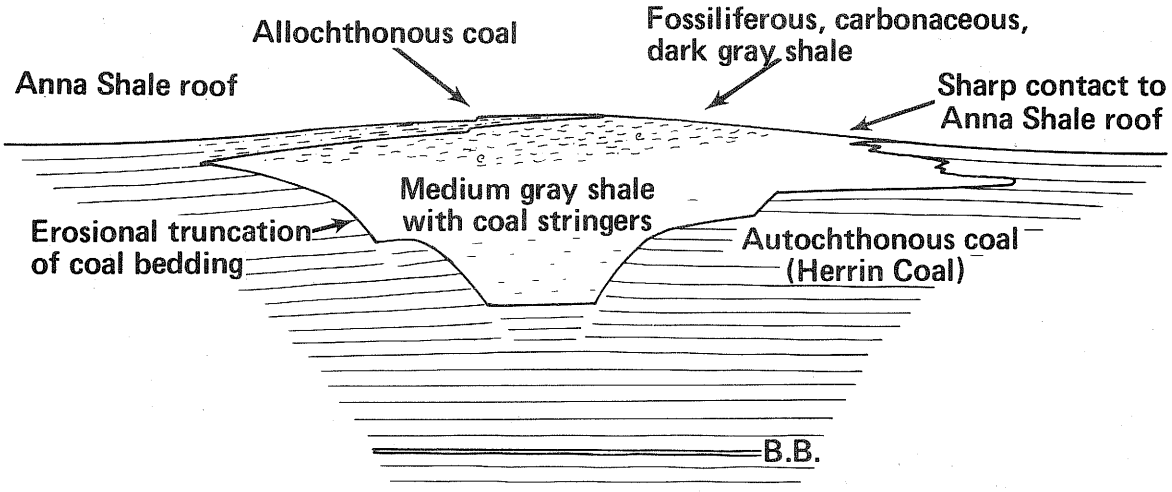

Figure 5
Sedimentary features of an idealized erosional channel ("roll") in the Herrin Coal. The contact between the medium gray shale and the fossiliferous dark gray shale is usually sharp, but may be gradational.

Four samples of Energy Shale from different localities in the Illinois Basin were chemically analyzed (Appendix C). Although they represent different lithologic facies, they are chemically similar, which suggests a common source. They vary primarily in organic carbon content, total sulfur, and chalcophile (sulfide-related) trace elements.

Channel-Fill Lithologies

After the Energy Shale mud was deposited, substantial erosion took place. Apparently the river that flowed in the Walshville channel (west of the mine; fig. 2) was diverted from its normal course. The Energy Shale was locally eroded--cut completely through to the top of the peat in a wide area of Franklin County, producing erosional "windows" in the Energy Shale. After the blanket deposition of marine units over both the Energy Shale and the Herrin peat, the formation of a transitional roof type was complete. In this case, the transitional roof is characterized by lateral variation between Energy Shale and Anna Shale/Brereton Limestone roof over short distances (Part I, p. 6).

Features that miners broadly call "rolls" are common to the areas where the Energy Shale has been removed. In Old Ben Mine No. 24, a few rolls were found that had been formed by soft-sediment deformation (Krausse et al., 1979); but most were erosional channels filled with sediments (DeMaris, 1982). Typically, the channels are sublinear, ranging from 10 to 20 feet wide and 1 to 4 feet thick. Many can be followed as far as the intermittent exposures permit; some are over 1000 feet in length. Smaller erosional channels were formed later by tidal action (table 1).

The channel-fill lithologies (fig. 5) include an older, light to medium gray shale interbedded with fine coal stringers, and a younger, medium to dark gray, carbonaceous shale locally grading into both an impure coal and a medium gray, calcareous shale (or impure, fossiliferous limestone) with shells of marine fossils and fragments of mineralized plants. The channel fill usually contains many compactional faults (fig. 6). In some places, soft-sediment deformation and plastic flow of fill material along bedding planes into adjacent coal has also occurred.

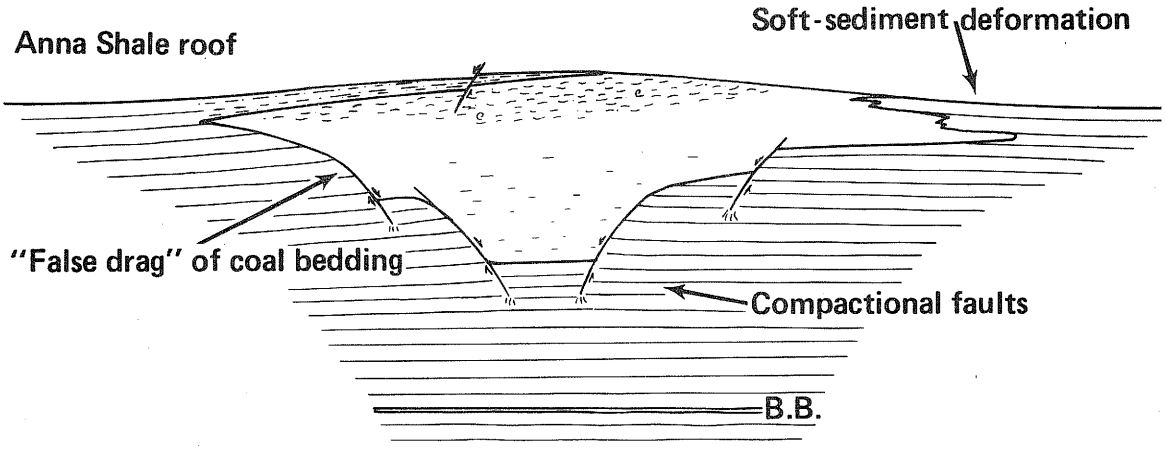

Figure 6
Structural features of an idealized erosional channel ("roll") in the Herrin Coal. Compactional faults may be numerous; they commonly affect the Anna Shale roof.

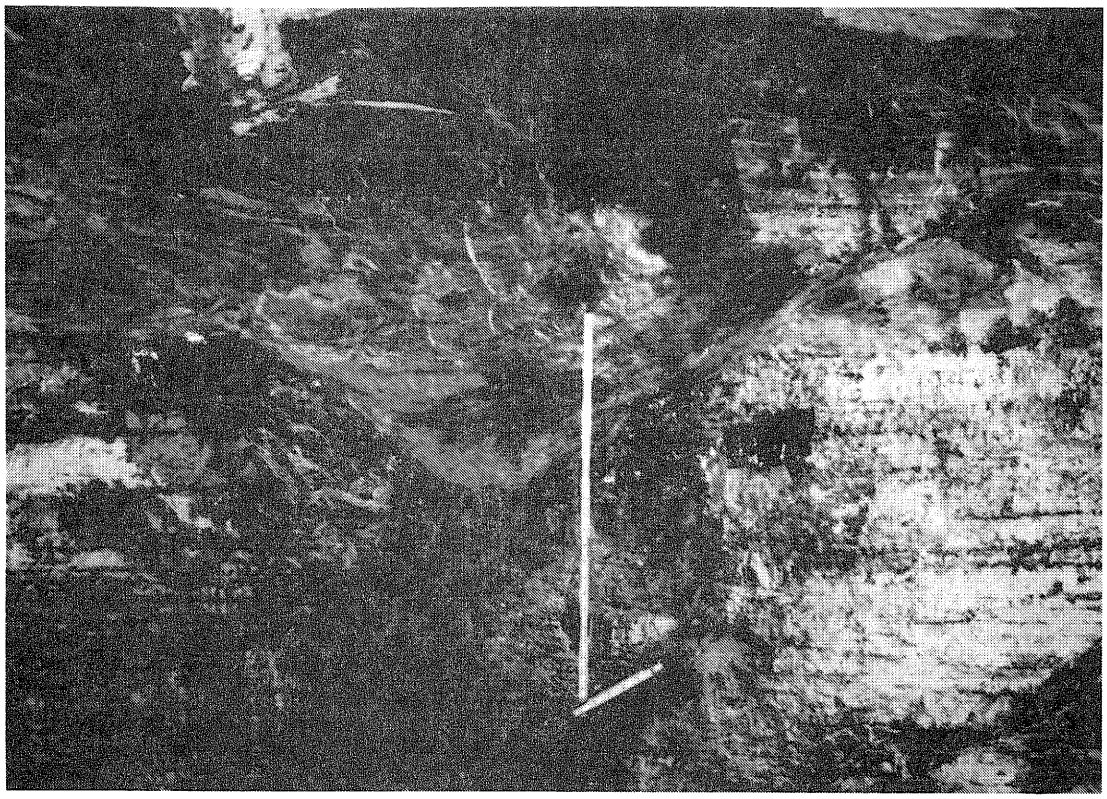

Figure 7
Detail of the center of an erosional channel in Old Ben Mine No. 27, showing "V" scoured into the peat. Vertical scale is a 2½ ft ruler.

Evidence for the erosional origin of these channels also distinguishes channel fill from the Energy Shale:

1. the light gray shale in the channels has a mineralogical composition distinct from that of the adjacent Energy Shale; coal stringers, representing peat fragments, frequently occur;
2. the channel-fill lithologies are found nowhere else and occur in predictable sequences;
3. the coal balls (with a normal peat matrix) occur as transported pebbles and cobbles in the fill materials;
4. a V-shape is occasionally found scoured into the seam below the fill material (fig. 7).

Five samples of channel-fill materials were chemically analyzed: 2 samples of light gray shale (C21634 and C21763), 1 sample of the impure coal (C21768), and 2 samples of the fossiliferous calcareous shale (C21627 and C21760). Results are given in Appendix C.

Since the 2 samples of light gray channel fill are very similar in composition to samples of the Energy Shale (Appendix C), but only slightly dissimilar in clay mineralogy (Part I, fig. 11a), these findings suggest this is slightly reworked Energy Shale. An analysis of dispersed organic matter in similar samples of light gray shale revealed two size populations of the organic fragments: a fine fraction from the original shale (Energy) and a coarser fraction from the organic material incorporated during transport. The impure coal sample

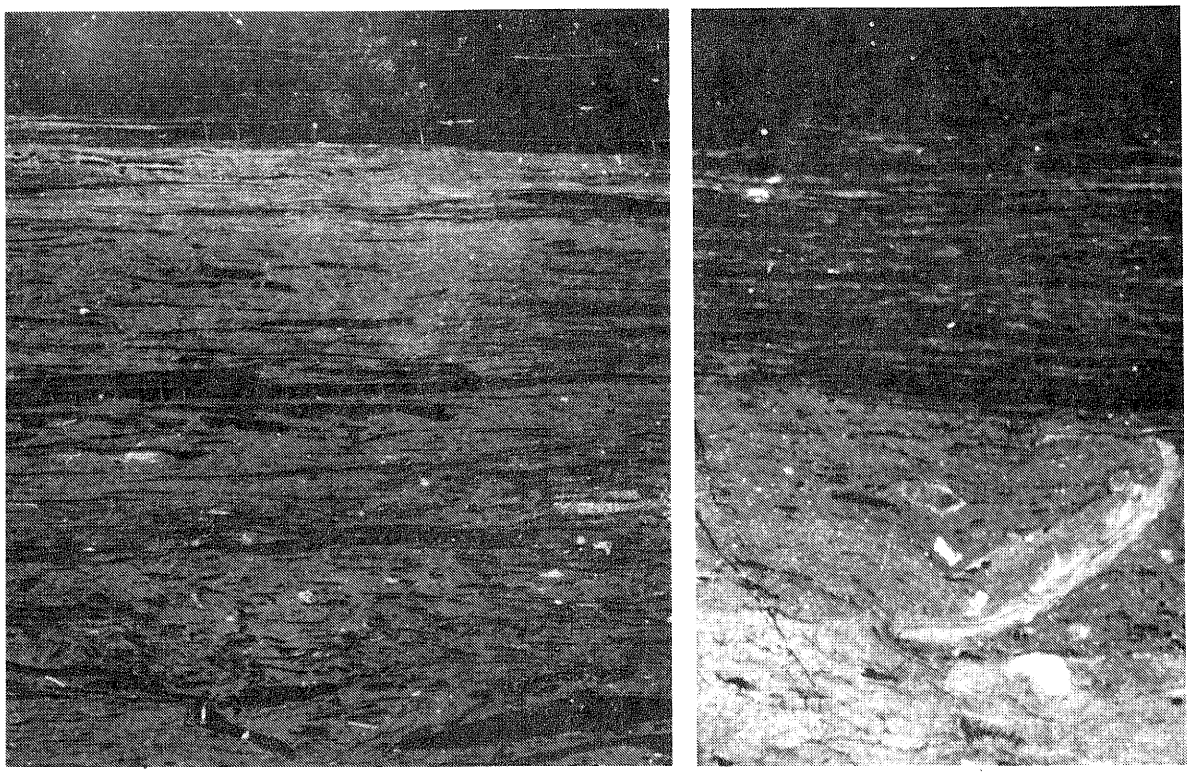

Figure 8
(Left) Transported vitrain fragments (black, cleated) in a gray claystone matrix, grading to an allochthonous coal, at top. (3 x, in air)
(Right) Contact between the fossiliferous shale at base and the impure allochthonous coal. (3 x, in air)

is composed of well preserved fragments of coal, largely vitrain, interbedded with thin clay partings (fig. 8). Although a coal in this setting could be interpreted as rafted peat redeposited in the channel fill, on closer examination it proved to be an allochthonous (transported) type of coal, composed of individual peat fragments mostly less than .03 feet long. The fossiliferous calcareous shale samples are similar to the other channel-fill materials in their clastic components but have higher calcium (12% to 25% more CaO) and total sulfur contents (3% to 6% more).

Anna Shale

The black Anna Shale (Part I, p. 9) was deposited in a marine environment with restricted circulation. There is disagreement over the depth of water: Zangerl and Richardson (1963) have argued that similar Pennsylvanian black shale originated in shallow marine waters where a floating algal mat reduced disturbances from waves and currents. Heckel (1977), on the other hand, thinks that such black shales were laid down in water as deep as 330 feet, well below the wave base.

Compressions of terrestrial plants are often seen near the base of the Anna Shale. Although organic material in the shale lacks diagnostic characteristics for visual identification, preliminary chemical analyses of the dispersed organic matter suggest it is primarily derived from terrestrial plants. Since animal fossils establish that the shale is marine, the terrestrial plant material must have been introduced from the land, probably as the sea advanced over the peat.

Eight samples of Anna Shale and 3 Anna Shale concretions were chemically analyzed and the results are given in Appendix C. Two of the samples (C21654 and C21759) contain portions of calcite/apatite bands typical of the base of the unit; this is the source of high levels of phosphorus in these samples.

On the average, the Anna Shale contains the highest levels of P, As, Cr, Cu, Se, Ni, Cd, and Zn (fig. 26 names these elements) of the rocks associated with the coal. The ranges of concentrations for the Anna Shale are comparable to those reported in Gluskoter et al. (1977); high levels of many elements relate to fluorapatite, pyrite, and other sulfide minerals in the shale. The uniform distribution of rare earth elements (REE) (fig. 26) in the 8 samples suggests a common sediment source.

In the Anna Shale of Franklin County, the concretions formed after deposition, often nucleating around plant material. Some plant fragments became mineralized, while others were transformed into coal. The findings of Woodland and Richardson (1975) are similar: in their discussion of the duration and timing of several processes involved in forming black-shale concretions, they found that mineralization of plant materials occurred late.

Two types of concretions, usually with a nucleus of plant material, are most common (fig. 9). A slice from each of 2 disc-shaped examples, representing the first type, were chemically analyzed (C21628 and C21629); they are quite variable in composition, especially in carbonate levels. A second type of concretion formed around in-filled bioturbation traces that passed into and sometimes through the Anna Shale (fig. 10). Only one of these (C21761) was analyzed, and it showed the lowest carbonate level. Despite their differences, the distribution of the rare earth elements in these two types of concretions is similar (Appendix C), suggesting that the REE distribution was unaffected during the concretion process.

Brereton Limestone

Analyses of 3 samples of Brereton Limestone (C21537, C21626, and C21767) show a highly argillaceous limestone, compatible with the shallow, near-shore marine environment suggested by Givens (1968). This environment was the habitat of the burrowing organism that produced the widely distributed trace fossils mentioned in the previous section.

Effects of Seawater on the Herrin Peat

Understanding the sequence of depositional events that produced coal balls (table 1) is important for predicting and locating them. Erosion occurred periodically after the Energy Shale sediments were deposited (B/C and C/D in table 1). These events closely relate to the introduction of large amounts of sulfur into the peat as well as the precipitation of carbonates that permineralized peat, forming coal balls.

Sulfur was introduced wherever seawater could penetrate the peat: (1) areas never covered by a thick, continuous layer of Energy Shale, (2) areas covered only by relatively thin, lenticular Energy Shale, or (3) areas where a thick layer of Energy Shale had been partially or completely removed by erosion. Coal lying under continuous Energy Shale, more than 20 feet thick, generally has less than 2.5 percent sulfur and often less than 1.5 percent. Without the Energy Shale cover, coal generally contains 3 to 5 percent sulfur or more.

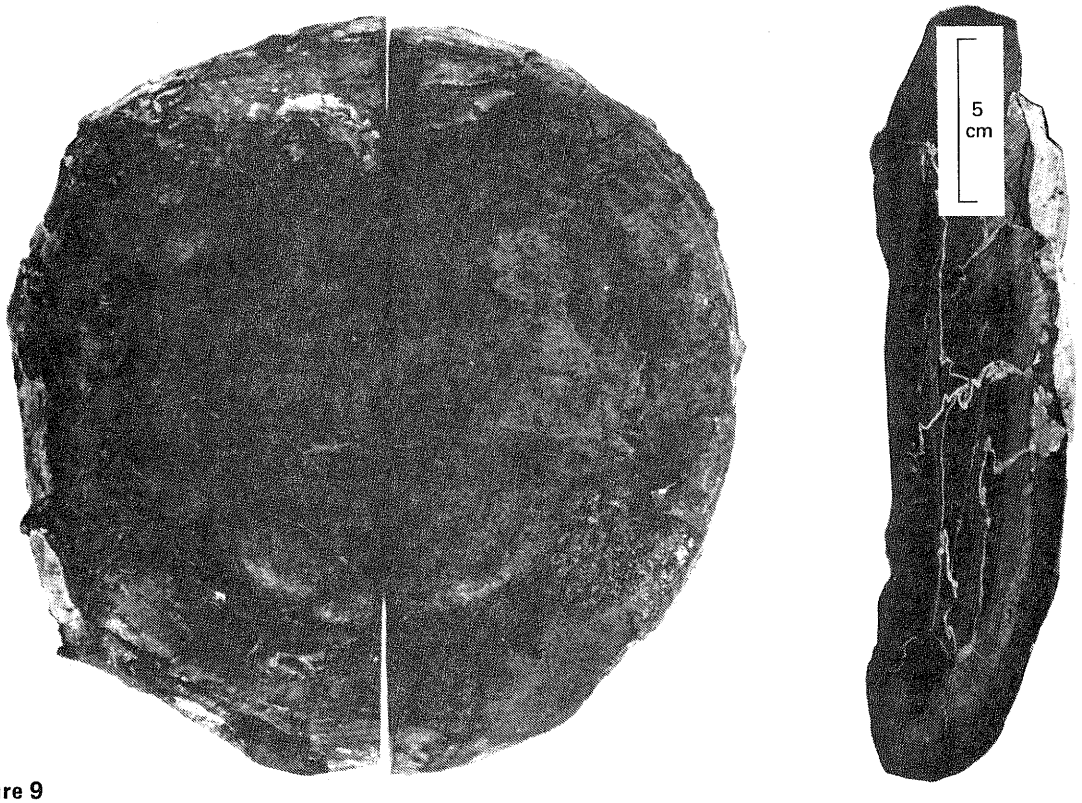

Figure 9
Typical disc-shaped Anna Shale concretion (C21628). (Left) top view; (right) view parallel to bedding showing calcite-filled fissures and the pyrite concentration around the rim and bottom of the concretion.

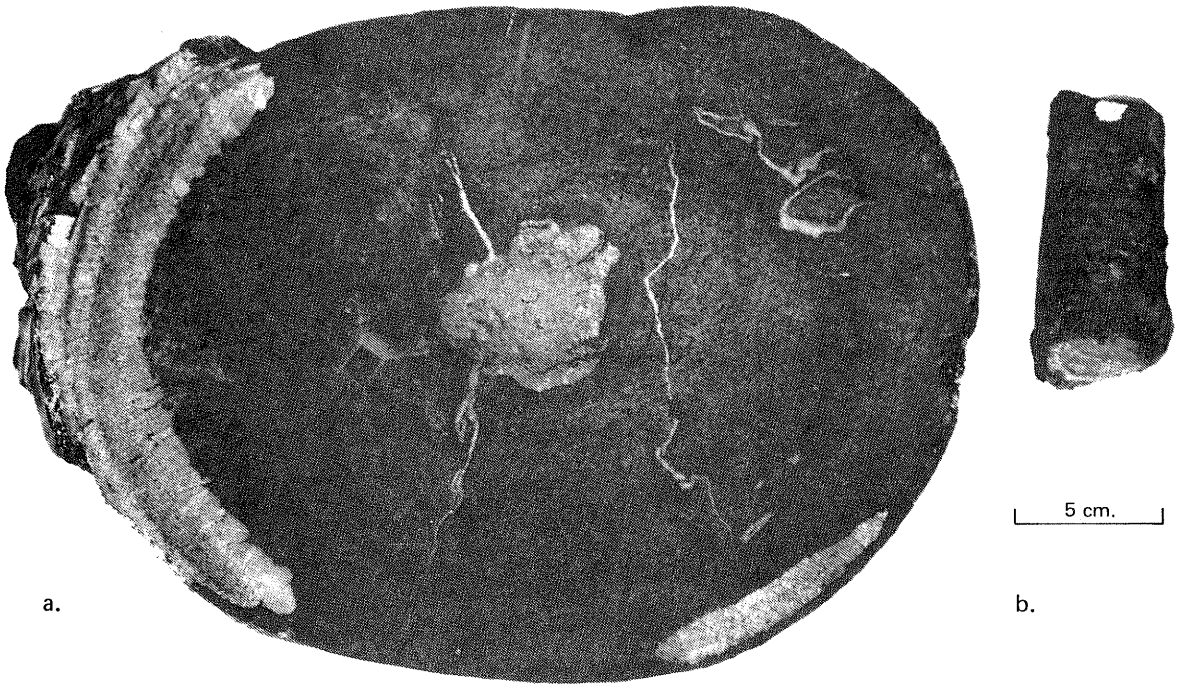

Figure 10
a. Anna Shale concretion formed on a segment of a bioturbation trace (at center). Bioturbation trace and portion of the rim have become strongly pyritized. (1 x)
b. A pyritized bioturbation trace without concretion formation.

To assess the short-range variation of total sulfur in the Herrin Coal, samples were taken at two different sites. We found an unusual site: an isolated area of Anna Shale/Brereton Limestone roof surrounded by thick Energy Shale roof. Channel samples taken 660 feet apart showed a drop of 1.8 percent total sulfur from the marine roof (3.2% total sulfur) to the thick Energy Shale roof (1.4% total sulfur). At a second site, representing the transitional roof (multiple windows in the Energy Shale roof) at Old Ben Mine No. 26, channel samples taken 400 feet apart showed a drop of 0.5 percent total sulfur from the Anna Shale/Brereton Limestone roof (C21721; 3.3% total sulfur) to the variable thickness Energy Shale roof (C21722; 2.8% total sulfur).

COAL BALLS

Permineralization of Peat

Coal balls are concretions of permineralized peat formed in place soon after peat deposition, but before significant alteration and compaction. Permineralization is a form of mineralization where plant cell lumens are often filled by the mineral while more resistant tissues such as cell walls are surrounded by the mineral. These resistant tissues are ultimately carbonized; and although they are prominent on a cut face of a coal ball, they generally represent less than 4 percent by weight of a carbonate coal ball (Appendix B). Because they form from peat in situ, coal balls generally contain very little detrital clay and quartz (Stopes and Watson, 1909). Our data set is composed of primarily carbonate coal balls and related materials; 2 silicate coal balls (C21591 and C21765) were included for comparison.

The fresh, broken surface of the carbonate coal balls has a light brown color that darkens only slightly with oxidation. Size and shape vary considerably. In general, coal balls range from less than 2 inches to more than 3 feet in width. Often they are elongated horizontally. Small coal balls (fist-sized and smaller) are usually spherical (fig. 11) or slightly ellipsoidal in shape. Medium-sized coal balls (up to 1.5 ft long) typically have height-to-width ratios from 1:3 to 1:6 (fig. 12). Where coal balls fill up 60 to 70 percent of the seam, they can have several different shapes and range from 1 to 4 feet thick (fig. 13).

The mineralization of the peat apparently began with the erosion of the Energy Shale (B/C in table 2). Field evidence shows that some coal balls had already formed by the time the fossiliferous channel-fill materials were deposited, and perhaps earlier. It is unclear when coal ball formation ended; bioturbation formed the last known coal balls after the deposition of the Brereton Limestone began.

During our studies of the Herrin Coal, we observed permineralized plant materials in a wide range of associations and locations. In the channel fill, coal balls the size of pebbles or cobbles were found deposited together with fossiliferous shale (fig. 14). They had no "rind" of bright coal typical of coal balls; but they could be confirmed as coal balls when cut open to show a peat matrix. We found over 60 transported coal balls in the channel fill. In other locations, plants and animal fossils were mixed within the same nodules (fig. 15) when carbonate mud intruded into peat deposits, combining plant parts with a fossiliferous, marine matrix. These are mixed coal balls (Mamay and Yochelson, 1962); further details are presented later.

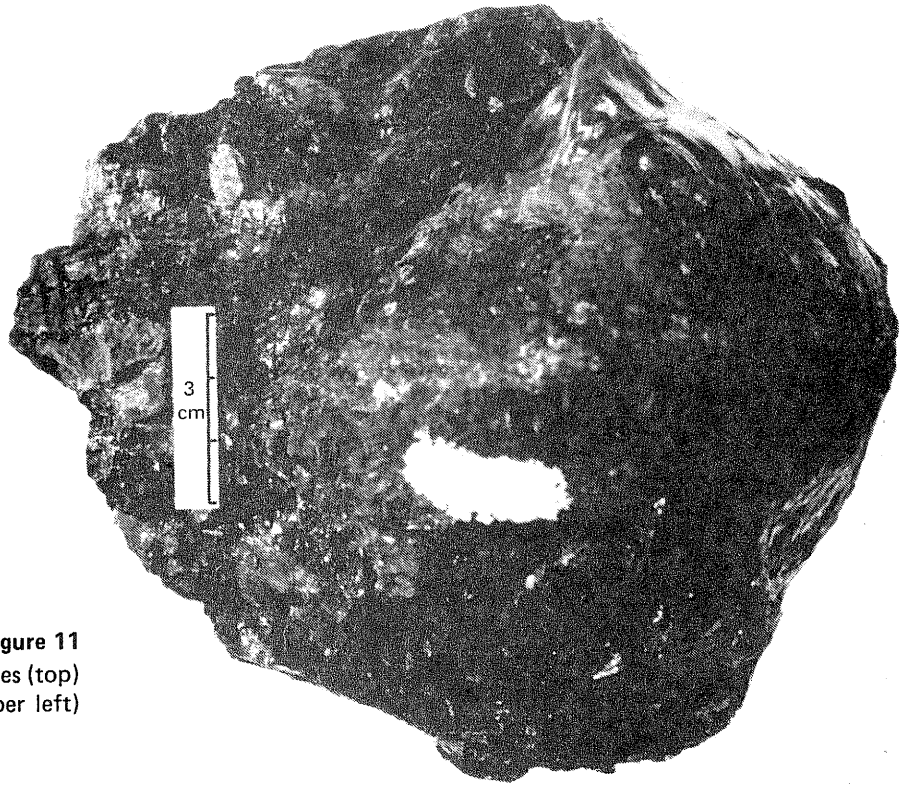

Figure 11
Round coal ball showing slickensides (top) and bending of coal laminae (upper left) due to compaction.

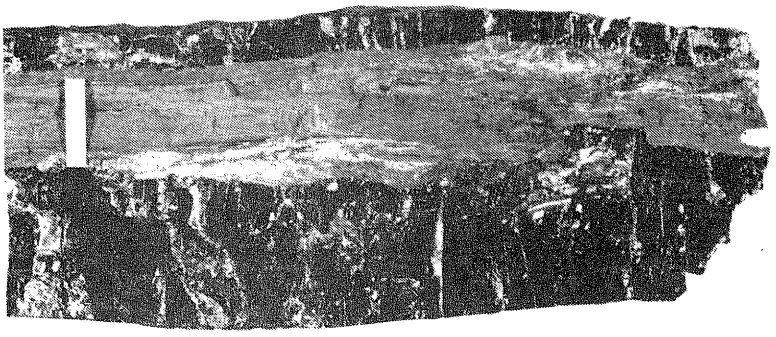

Figure 12
Long coal ball formed on a single plant axis. Scale bar: 3 cm.

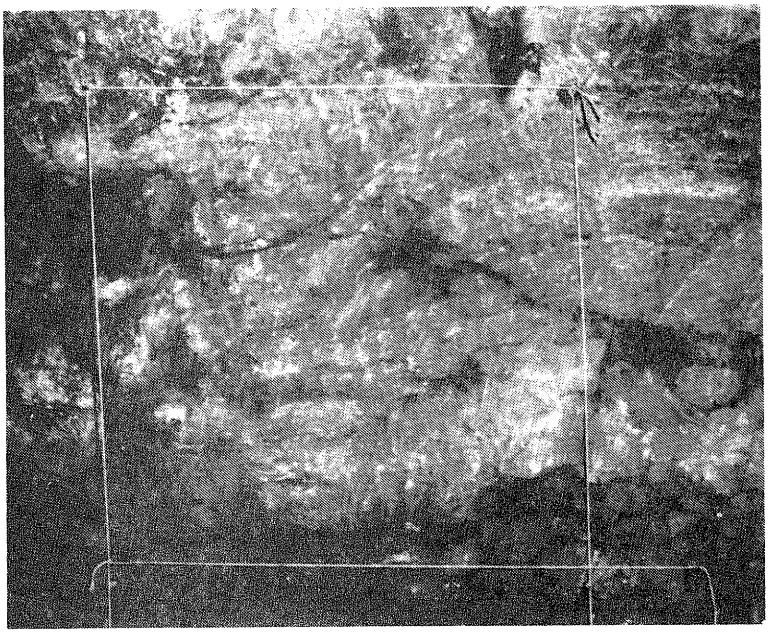

Figure 13
Concentrated coal balls near the center of coal-ball area L. This view overlaps that of figure 16, *Part 1*. Strings form a box 0.5 m on a side.

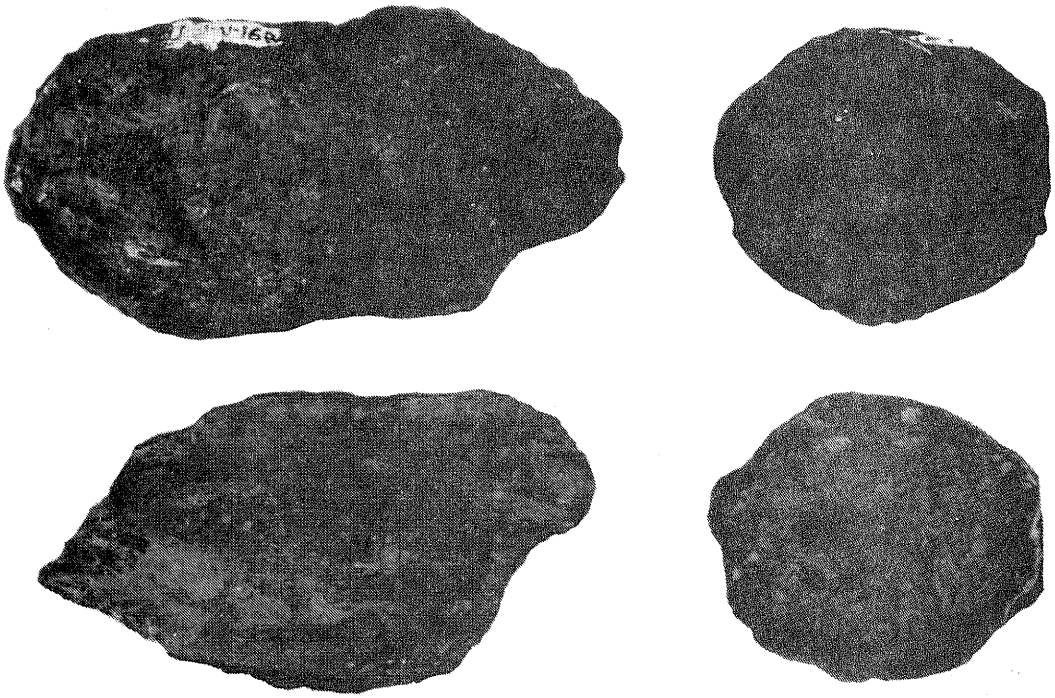

Figure 14
Exteriors (top) and cut faces (bottom) of two transported coal balls. Note the absence of a vitrain "rind" on these coal balls. (1.1 x)

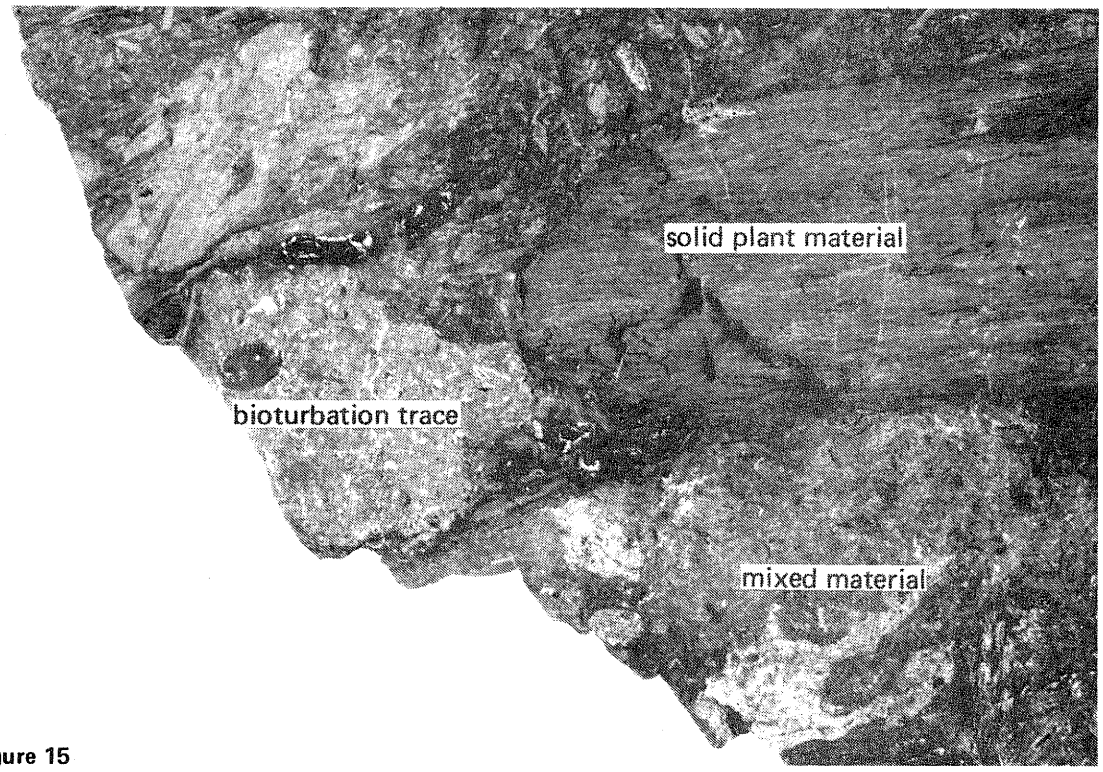

Figure 15
Mixed coal ball from Old Ben Mine No. 27 composed of a bioturbation trace surrounded by large and small pieces of permineralized plant material (including fusain fragments), coal traces, and fossiliferous marine limestone. Coal is out of view at both top and bottom; sample orientation is unknown. (1.1 x)

Figure 16
Permineralized plant fragments in a clastic matrix, obtained from a split in the Herrin Coal. The slab is about 6 cm wide.

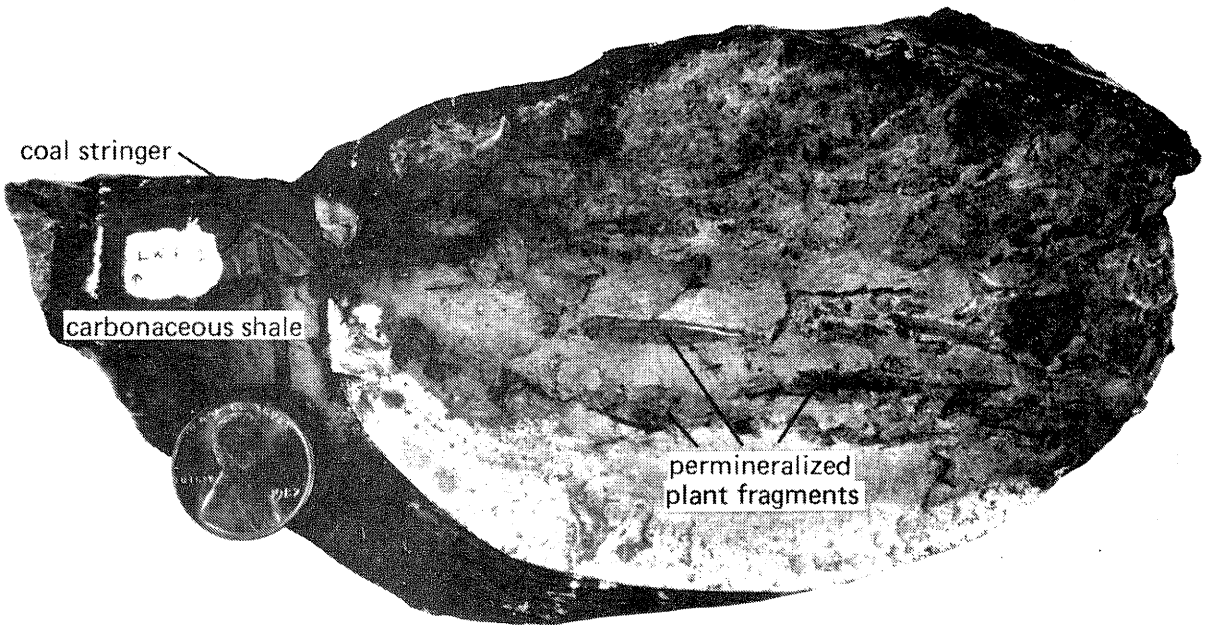

Figure 17
Concretion formed on channel-fill materials containing permineralized plant fragments in a clastic matrix. Outside the concretion (to the top and left), plant materials were coalified. Coin for scale. (1 x)

Permineralized plants were associated with a clastic matrix in two other cases; they were not considered coal balls. In the first case, the nodules represent an uncompacted precursor of a shale split in the seam, which was discovered by tracing the unit laterally to where it was not mineralized (fig. 16). The other case represents concretions formed around nuclei of redeposited plant material within channel-fill materials (fig. 17). Permineralization followed transport in both cases. Where unmineralized, both these types of plant materials are carbonaceous shale with coal stringers.

In summary, the eroded coal balls and mixed coal balls are representative of in situ peat, though of unusual genesis; the last two cases represent permineralized plants which are no longer representative of the peat due to selective transport and destruction of fragile plant parts. Transported and permineralized plants each represent a coal-seam flora, but as a group a transport-biased assemblage. In this paper our use of "coal ball" reflects the view that permineralized plants found in roof shale, seam splits, and channel-fills are not "coal balls" unless they can be established as indigenous to the coal seam.

Distribution of Coal Balls Within the Herrin Coal

Coal balls occur preferentially under Anna Shale or Brereton Limestone roof strata, which are of marine origin (figs. 18, 19, and 20). In study area A (fig. 3), only coal-ball areas B, H, I, and N straddle the boundary between black, Anna Shale and gray, Energy Shale roof (fig. 18). Otherwise, less than 1 dozen coal balls were seen under Energy Shale roof, while hundreds of thousands were present within the 18 mapped coal-ball areas under "windows" in the Energy Shale cover, with Anna Shale and Brereton Limestone immediately above the Herrin Coal.

Coal balls occur individually, in clusters, or in concentrated groups called "coal-ball areas," ranging from about 15 feet to more than 150 feet across. The distinction between a cluster and a coal-ball area depends on both the size of the accumulation and concentration of coal balls. Clusters, usually four or more balls within a few feet of each other, and individual coal balls have only been found near the top of the seam; only coal-ball areas have been found 2 or more feet below the top of the seam.

In large coal-ball areas with many, tightly packed coal balls, both size and number of coal balls tend to increase toward the core (fig. 21). If we observed no natural boundary, coal balls more than 5 feet apart were considered outside an area. The most highly permineralized exposure was found in coal-ball area L (fig. 25). In a measured section here, the seam with coal balls exceeded 12.5 feet thick where it normally would be 7.6 feet thick. The distance from the edge of a coal-ball area to the edge of its core ranged between 40 feet and 80 feet. In some coal-ball areas, such as area N, the core was not dense enough to severely hamper mining. On the other hand, the extremely dense core of area L was mined deeply because it was necessary to the layout of the longwall panel (fig. 22). Most coal-ball areas interfered with mining, both in the support entries (Part 1, fig. 17) and along the longwall face (Part 1, p. 25).

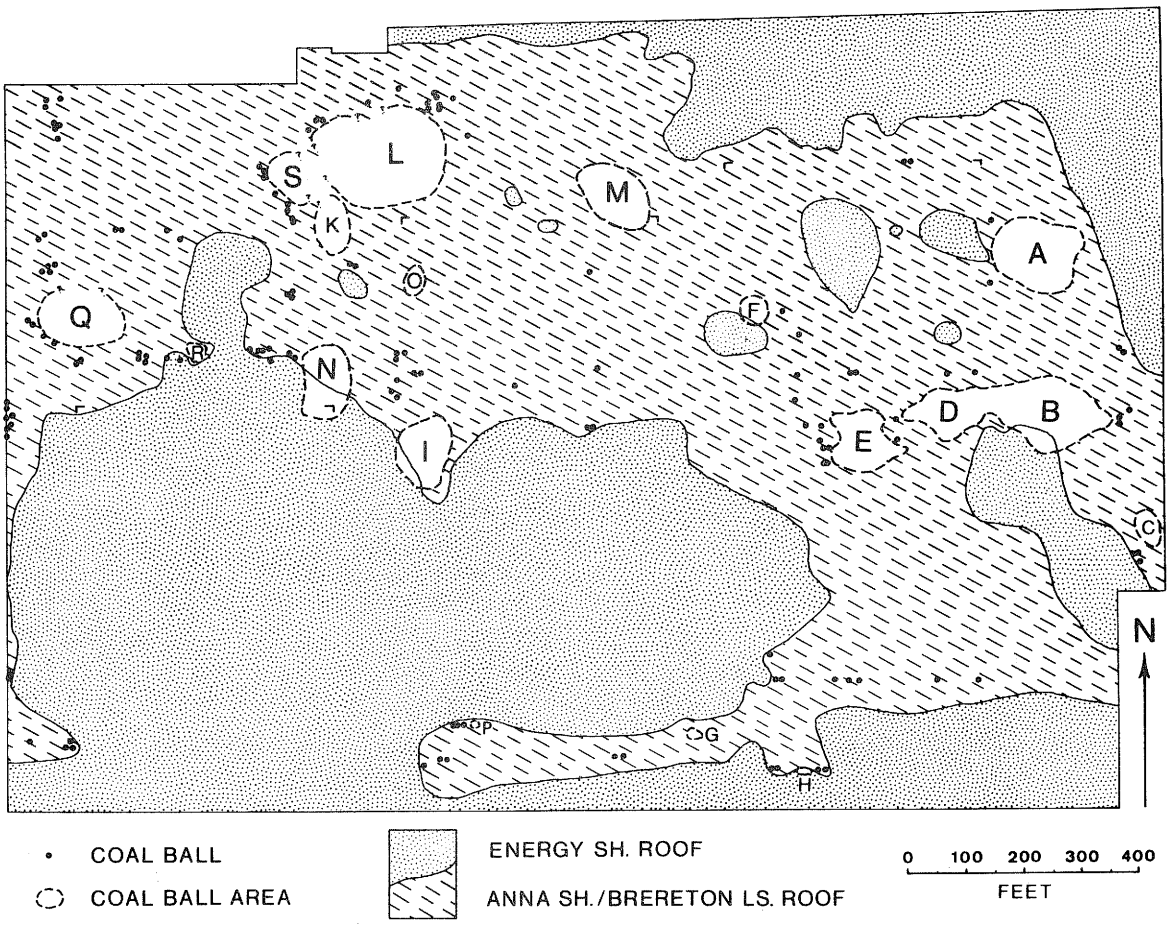

Figure 18
Coal balls, coal-ball areas, and roof lithologies identified in the northern half of mapped area A.

Coal-ball areas can be separated by stratigraphic location:

Type I areas have coal balls restricted roughly to the top 2 feet of the seam;

Type II areas have coal balls (a) below the top 2 feet of the seam; and (b) from the top to the floor of the seam.

At type I sites, coal balls occur right at the top of the seam; most are found within the top 1 to 1½ feet of the seam. Density may or may not increase toward the center of the area.

Type II sites generally become more tightly packed toward the center, but some have a low or moderate density throughout. Partial exposures of type II coal balls may only catch the edge of an area, exhibiting coal balls at the top of the seam, at midseam, below the "blue band," or any combination of these positions. Coal balls at one particular position may extend laterally for some distance, suggesting a pattern of mineralization based on the characteristics of various peat layers. In other places coal balls at a given stratigraphic positon may continue for only 6 to 10 feet.

The characteristics of the coal-ball areas within mapped area A (fig. 18) are recorded in table 3. The position of permineralized zones within the seam

Table 3. Some Characteristics of Coal-Ball Areas at Old Ben Mine No. 24

Coal-ball area	Size (ft x ft)	Type	Roof (Member)	Vertical development in seam	Zone of maximum development in seam
A	150 x 130	II	Anna Shale	middle-to-low seam	middle
B	200 x 140	II	Anna and Energy Shale	middle-seam	middle
C	50 x 60	II	Anna Shale	middle-to-low seam	middle
D	95 x 150	II	Anna Shale	top-to-low seam	middle
E	135 x 110	II	Anna Shale	top-to-low seam	middle
F	45 x 50	II	Anna Shale	top-to-low seam	low
G	30 x 10	I	Anna Shale	top-seam	top
H	15 x 10	I	Anna and Energy Shale	top-seam	top
I	90 x 125	II	Anna and Energy Shale	top-to-low seam	middle
K	50 x 100	II	Anna Shale	top-to-middle seam	middle
L	230 x 180	II	Anna Shale	top-to-low seam	middle
M	130 x 120	II	Anna Shale	top-to-low seam	middle
N	80 x 130	II	Anna and Energy Shale	top-to-middle seam	middle
O	35 x 55	I	Anna Shale	top-seam	top
P	15 x 15	I	Anna Shale	top-seam	top
Q	110 x 70	II	Anna Shale	top-to-low seam	middle
R	35 x 35	I	Anna Shale	top-seam	top
S	80 x 90	II	Anna Shale	top-to-middle seam	middle

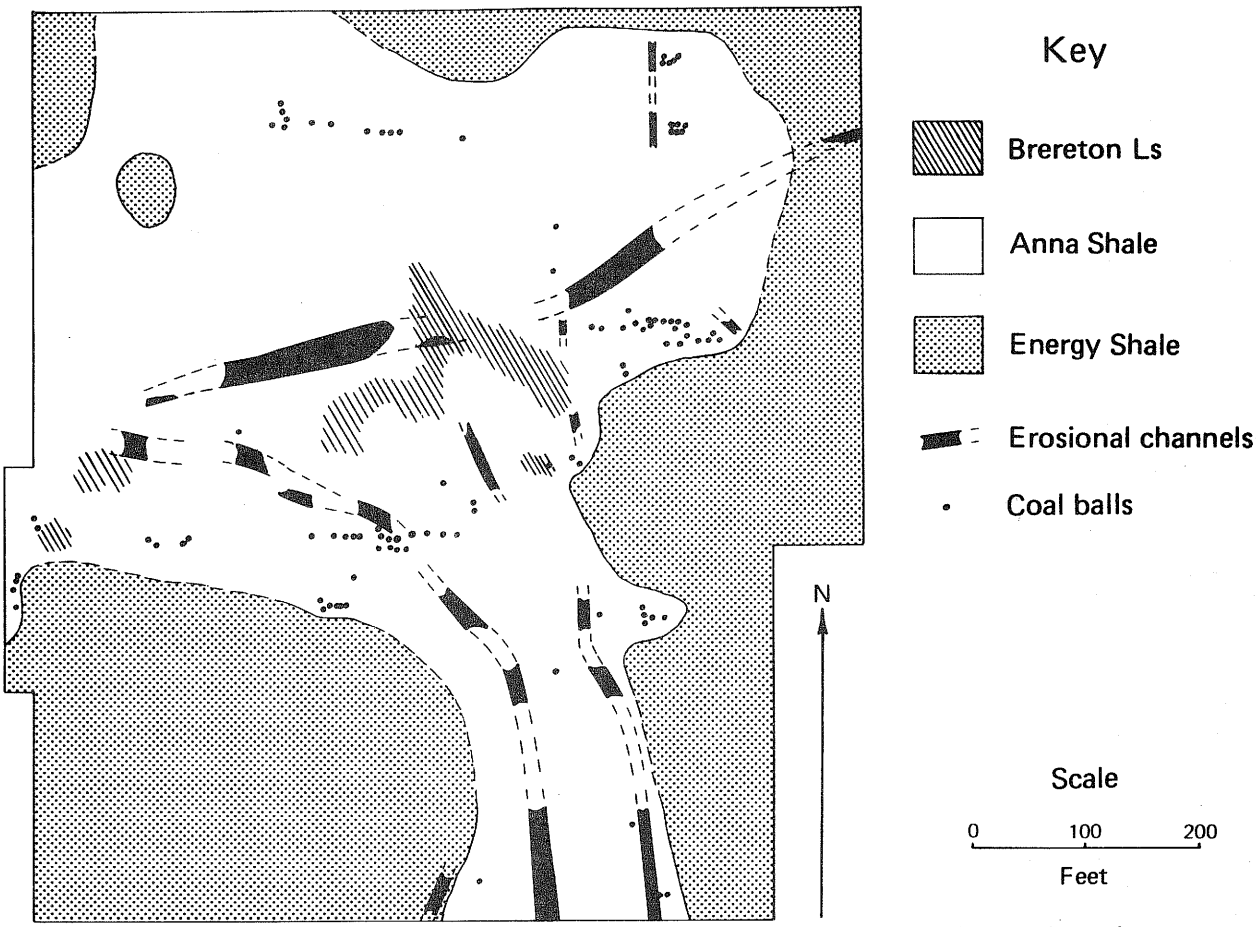

Figure 19 Coal balls, roof lithologies, and erosional channels in the southwest part of mapped area A.

varies substantially from site to site; for high concentrations of coal balls the most common stratigraphic position is midseam. Only in area F were coal balls best developed in the lower part of the seam.

Relationship to Roof Strata

As stated before, coal balls occur almost exclusively under Anna Shale/Brereton Limestone windows in the Energy Shale cover. Within the areas of Anna Shale/Brereton Limestone roof, there are often centrally located areas where Brereton Limestone alone forms the immediate roof. In several mapped areas we checked for spatial correlations of coal balls with these purely limestone areas. At Old Ben Mine No. 24, where there is little Brereton roof, the correlation was poor, with only an occasional isolated coal ball under limestone roof. At Old Ben Mine No. 27, the relationship is clearer: there is proportionally more Brereton Limestone roof, yet more coal balls are linked with the Anna Shale (fig. 20). Although there are some coal balls under Brereton roof, the general pattern of coal balls is largely independent of those areas. Evidently, coal-ball formation largely predates Brereton Limestone deposition.

Only a few mixed coal balls (Mamay and Yochelson (1962) were encountered during our study (fig. 15). As expected, they occurred only under Brereton Limestone and thin Anna Shale roof. The mixed coal balls were primarily mixed-heterogeneous with evidence of physical mixing only; no good examples were found where the burrow trace offered a clear nucleus for

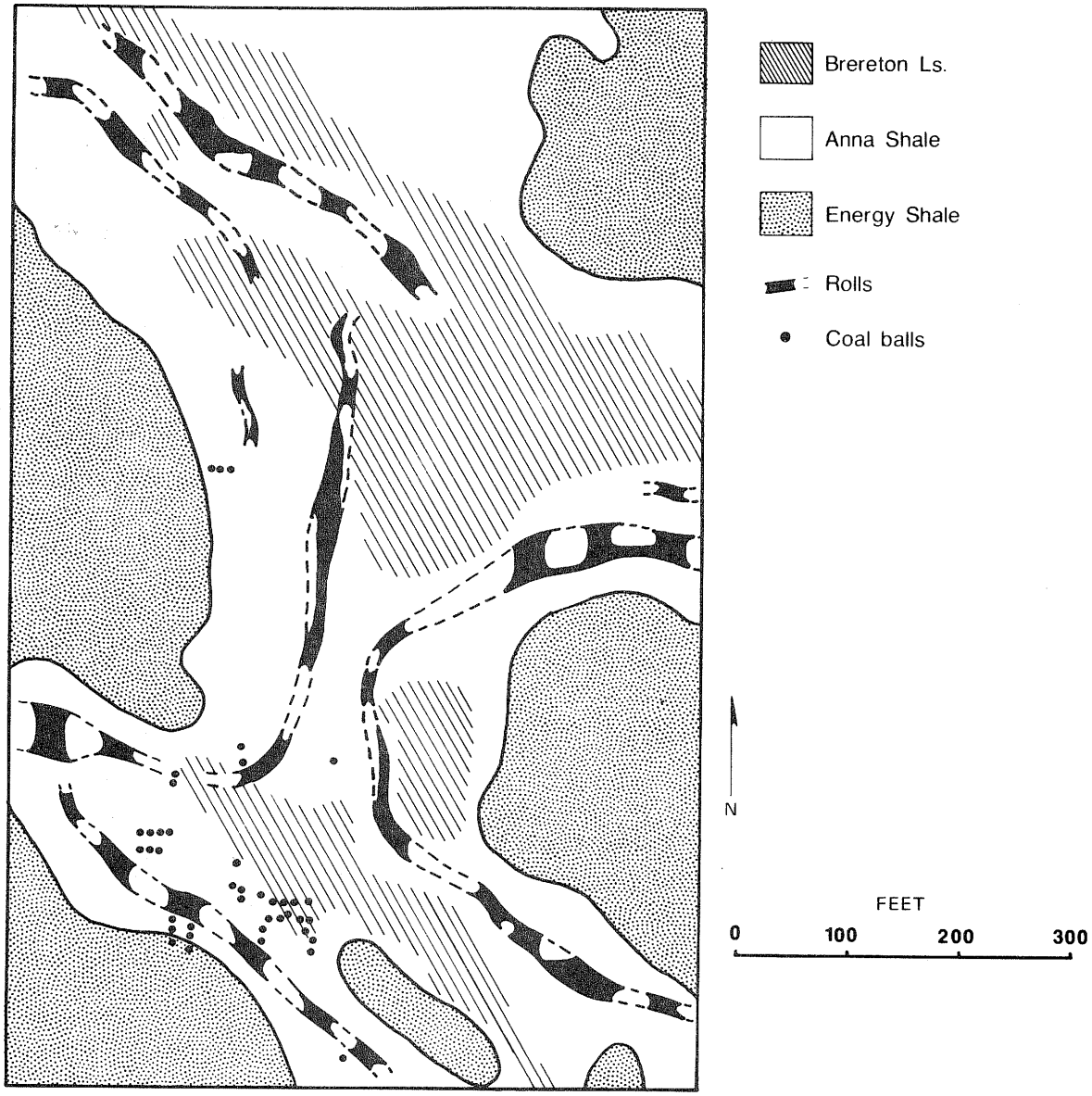

Figure 20
Coal balls, roof lithologies, and erosional channels in the mapped area in Old Ben Mine No. 27.

permineralization of the surrounding peat, as is the case for many Berryville, Illinois, coal balls. Two possible reasons for this scarcity are (1) the peat here may not have been as geochemically suitable for mineralization as in other regions, and (2) the burrowing organism may have been less common in the local facies of the Brereton Limestone in this area. Coal balls formed from marine bioturbation were rare, but caused a mining problem locally in Old Ben Mine No. 27. Despite their distinct origin, these coal balls are generally found in the same areas as normal coal balls.

Early Mineralization

As mentioned earlier, we found more than 60 coal-ball pebbles and cobbles in the younger of the channel-fill materials ("rolls"), all in the dark gray, fossiliferous shale (fig. 14). Quantities of coal balls had already formed in situ

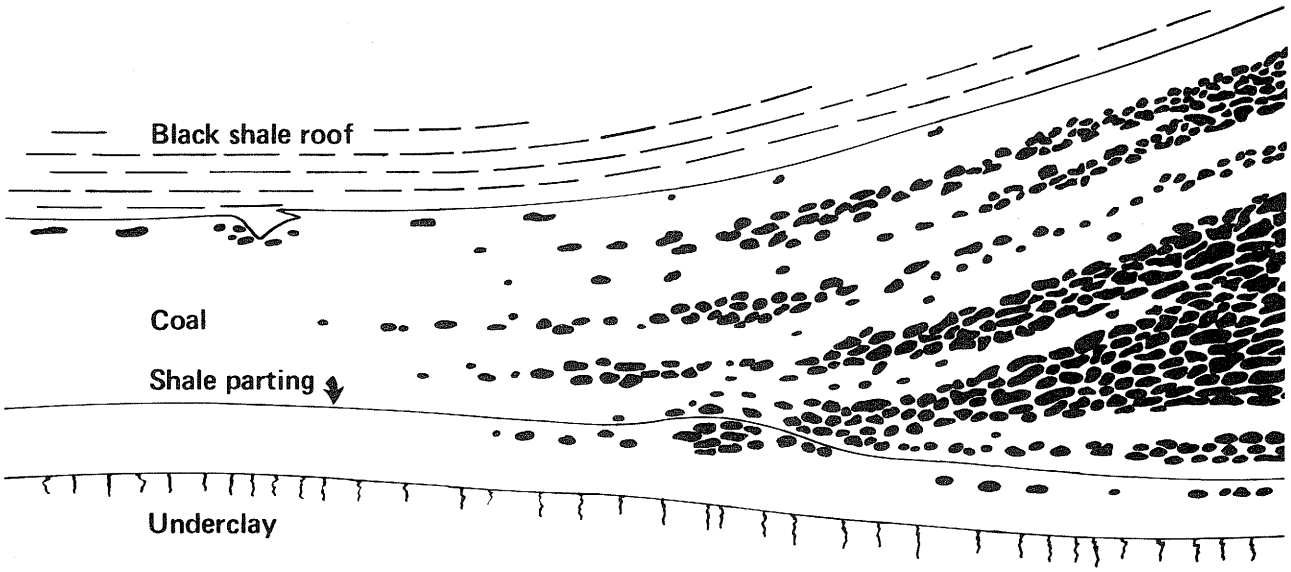

Figure 21
Diagram of generalized coal-ball distribution within coal-ball areas, based on observations of many such areas.

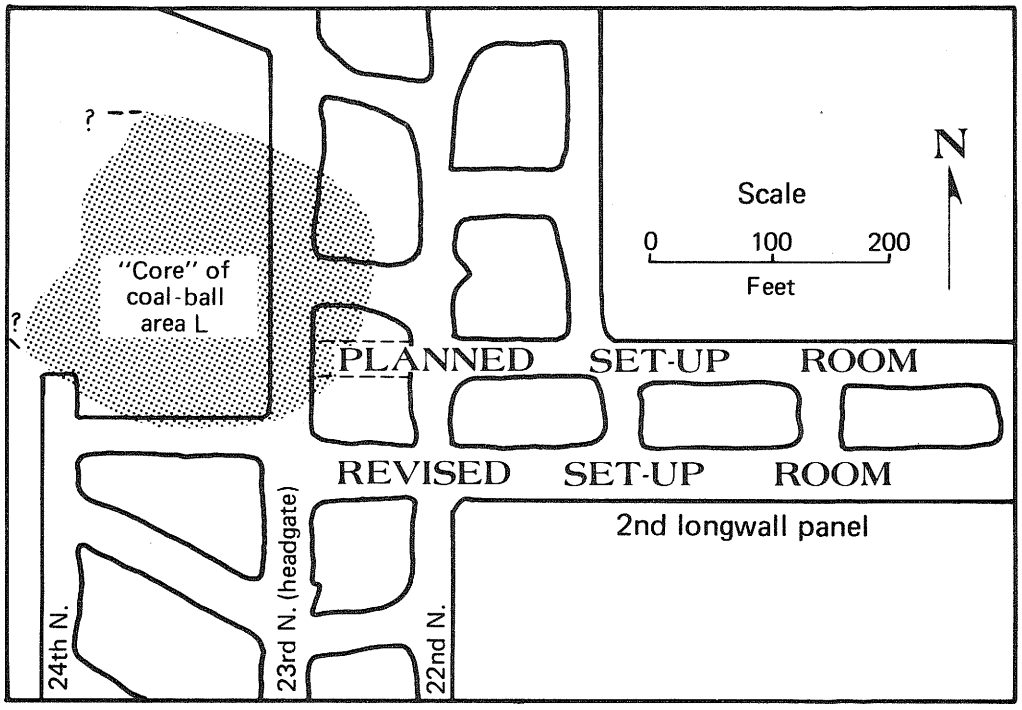

Figure 22
Adjustments made to the layout of the second longwall panel during mining as coal-ball area L was encountered.

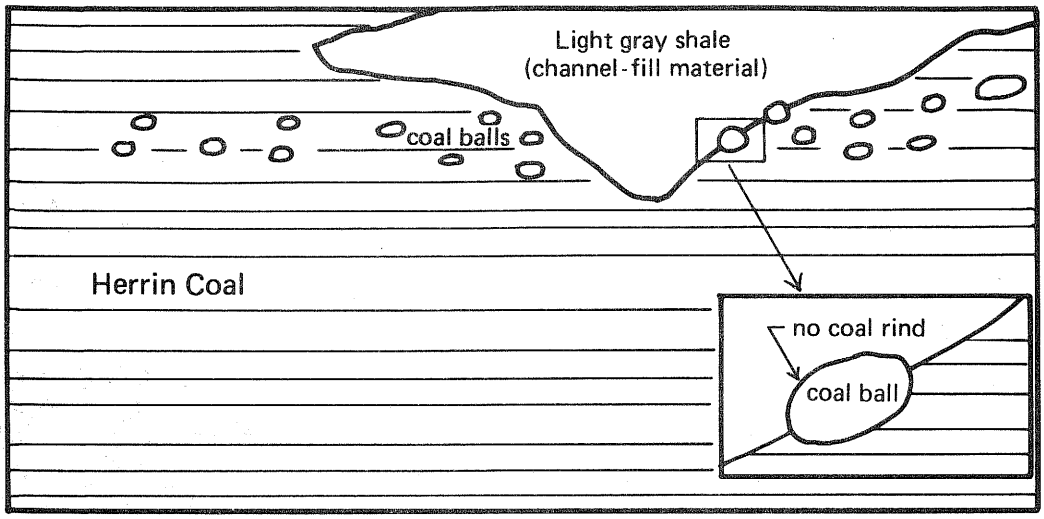

Figure 23 Relationship of type II coal balls to an erosional channel at one site.

before the tidal channels developed (before deposition of the Anna Shale), and the coal balls in the coal seam were redeposited in those channels. Clusters of coal balls were locally observed under and near the erosional channels filled only with the dark gray, fossiliferous, carbonaceous shale or impure limestone; this suggests a genetic link.

While coal balls were definitely present by the time the younger channel fill (fossiliferous or dark carbonaceous shale) was deposited, they may have also been present earlier during deposition of the older channel fill. For instance, in coal-ball areas L and Q the channel appeared to cut through preexisting coal-ball accumulations; where the coal balls protrude into the older light gray channel-fill, they have no rinds (fig. 23). Thus, evidence exists that permineralization of coal balls began soon after the Energy Shale mud was stripped from the peat.

Physical Appearance of Coal Balls

Coal-ball shapes vary considerably between stratigraphic zones in the seam. Some zones can be characterized by certain shapes, possibly reflecting the type of peat and its degree of degradation when permineralized. Round and oval coal balls are widely distributed, but many larger coal balls are preferentially mineralized in the horizontal plane along large pieces of lycopod periderm or the vascular portion of small stems (fig. 12).

Condition of peat in coal balls is not evaluated on a routine basis. William A. DiMichele (personal communication, 1979), who qualitatively evaluated the coal balls at vertical section 3 within coal-ball area L (figs. 24 and 25), found much interzonal variation but no stratigraphic trend in peat quality. The variation in quality of peat preserved in the coal balls records variations in local depositional environments of peat and alterations prior to mineralization. Some coal balls near the top of the seam exhibit shrinkage of plant tissue, suggesting tissue dehydration due to osmotic pressure during exposure to sea water.

Compaction of Peat Before Mineralization

Coal balls also record the degree of peat compaction. Fresh peat has as much as 90 percent moisture, much of it in the spaces between parts of

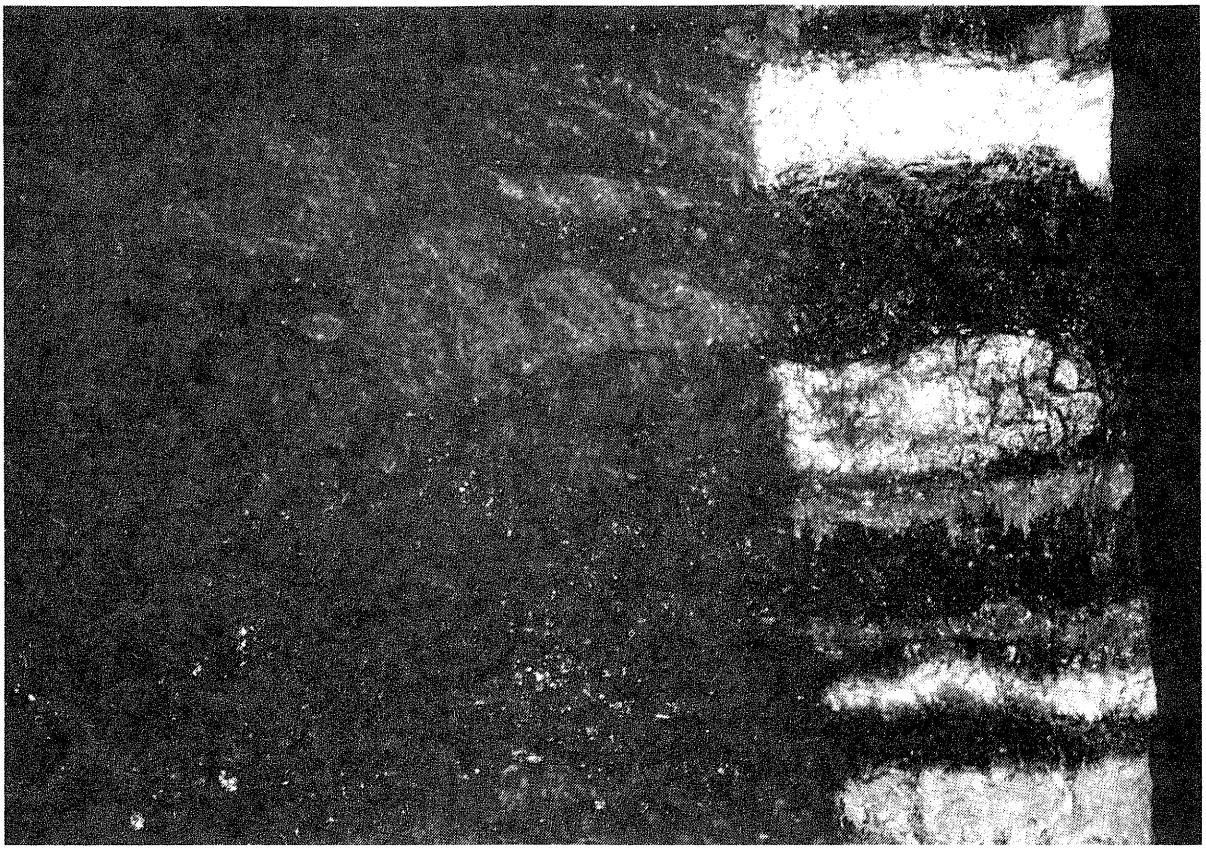

Figure 24
Detail of several coal-ball zones from vertical section 3 within area L. Coal balls were color coded by zone prior to sampling.

plants. The inter-tissue water must be largely removed before compaction of tissues can take place. The degree of dewatering can be estimated from the volume of voids that filled with minerals. In coal balls from the Herrin Coal in the Clarkson Mine, Washington County, Schopf (1938) found that mineral-filled voids represented 6.7 percent of the surface studied. A few such voids were seen in coal balls from Old Ben Mine No. 24.

The peat at vertical section 3 (fig. 24) showed only slight compaction from top to bottom (DiMichele, personal communication, 1979). In the case of the Clarkson Mine coal balls, which are from a depositional environment similar to that of Old Ben Mine No. 24, Schopf (Cady et al., 1940) noted "a general flattening ... but little cell distortion" of the peat, judged qualitatively.

Peat-to-Coal Compaction Ratios

Individual coal balls preserve peat in a largely uncompacted state and serve as a good indicator of the original thickness of the peat deposit at the time of mineralization. Peat-to-coal compaction ratios can be derived by comparing the thickness of coal next to a single coal ball to the corresponding thickness of permineralized peat in the coal ball (Teichmueller, 1955; Zaritsky, 1975). This is the only method that produces a valid measure of peat-to-coal compaction.

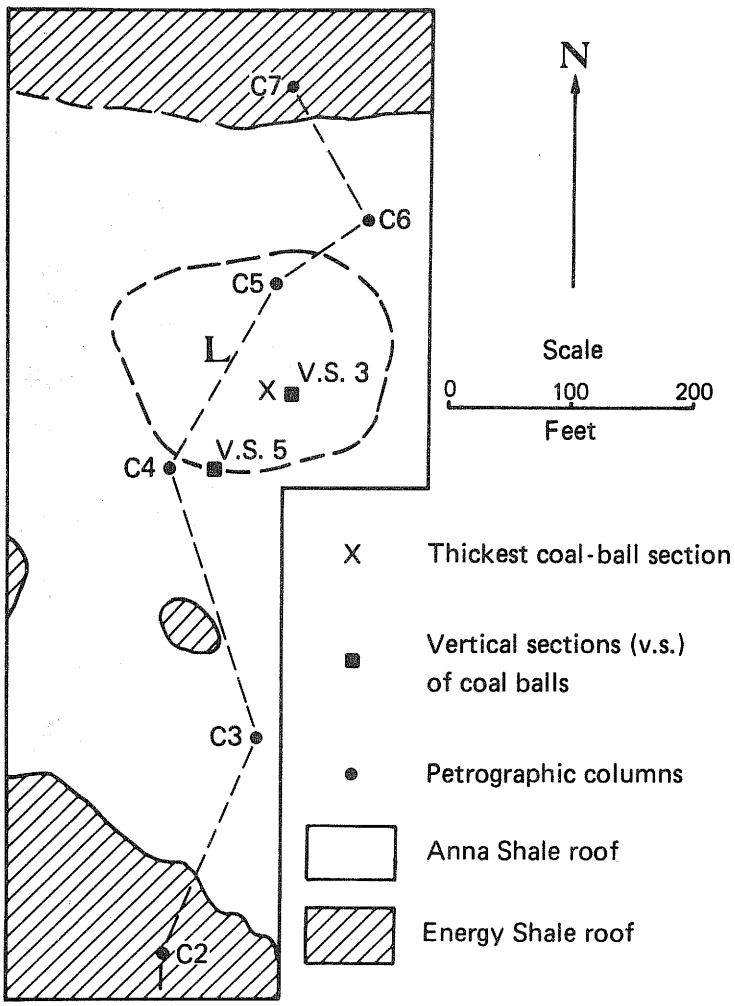

Figure 25
Coal-ball area L and selected sample sites. Detail from mapped area A.

During our investigations we made over a dozen such measurements; the peat-to-coal ratios ranged from roughly 3:1 to 7:1. Because of the lateral variation of coal lithotypes, the variation in coal-ball shapes, and the difficulty in following banding around the coal balls, multiple measurements were necessary to obtain reliable estimates. The average peat-to-coal compaction ratio for coal balls of Old Ben Mine No. 24 is 5:1, which is similar to values found by Zaritsky (1975) for coal balls of similar age and type in the Donets Basin (USSR).

Another set of measurements between stratigraphic markers in the seam in an area of many coal balls gave a value of about 2:1 (Part I, fig. 19a). The coal immediately above and below coal balls often displays extra compaction; slippage of coal is commonly indicated by slickensides (Part I, fig. 19b). Such factors result in lower compaction ratios in sections with many coal balls. Because of compaction and deformation within the coal, a seam with large lenticular coal balls may be only 2½ to 3 times thicker than the seam nearby without coal balls.

GEOCHEMISTRY OF COAL BALLS

The geochemical investigations constituted a significant part of the last phase of our investigations of coal balls at Old Ben Mine No. 24 and nearby mines. We hoped the geochemical investigations would assist in developing a number of parameters that any model of the origin of these coal balls would have to account for.

Our major interest was in the conditions locally favoring the precipitation of carbonate minerals and preserving delicate plant structures. The precipitation of carbonate minerals depends upon specific pH, pCO_2 and Ca boundary conditions. The interstitial water in the peat would have contained dissolved CO_2 from two sources. A certain amount of dissolved CO_2 would have been present in any water percolating through the peat; the amount would be controlled by temperature, pH, and the type of rock and minerals that the water had been in contact with. A second source of CO_2 would have been from bacterial degradation of the organic matter in the peat under anaerobic conditions. The amount of pCO_2 (partial pressure) could be quite high, and if so, produce conditions of supersaturation; supersaturation would result in a low pH and increase the solubility of carbonate minerals. There would be little calcite formation until the pH rose, for instance, after the removal of CO_2 from the system. Reduction in the amount of CO_2 would raise the pH with the same effect as a reduction in the confining pressure. Also an influx of alkaline water could raise the pH above 8 and promote rapid calcite precipitation. If sufficient magnesium were present, dolomite could form.

During deposition, the sulfate content in the peat and pore waters would be much lower in freshwater than in marine water; and thus the bacterial reduction of sulfate to sulfide would not be significant. As marine water intruded into the freshwater system, the sulfate levels would increase and the bacterial reduction of sulfate would result in pyrite formation. Thorough discussions of carbonate and pyrite equilibria are provided in Garrels and Christ (1965) and Berner (1971). Schopf (1980) cites useful criteria for determining paleosalinity with chemical data.

The following sections present the geochemical data on the coal balls and associated rocks and their interpretation in detail: this is the first comprehensive set of chemical analyses of coal balls to be reported in the literature.

Sample Sets

The 36 samples of coal balls selected for chemical study are described in Appendix A: 31 of the samples were analyzed for up to 53 major, minor, and trace elements as well as loss on ignition, moisture, and percent of insoluble residue on selected samples; 5 samples of limited quantity were analyzed for major chemical constituents only. Appendix B lists the results of the coal-ball analyses. Also analyzed for the same major and minor elements (Appendix C) were 41 samples of materials associated with the coal balls, such as the underclay and roof lithologies.

Examined for mineral composition by x-ray diffraction were 18 coal balls and 7 associated carbonate rock materials.

A suite of coal balls and carbonate roof materials were evaluated for their δC^{13} and δO^{18} values (table 9) by T. F. Anderson of the University of Illinois. Coal balls from vertical sections 3 and 5, selected by T. L. Phillips, were supplemented by other coal balls and roof material selected by the authors. There is some overlap between these samples selected for carbon and oxygen isotopes and those selected for full chemical analysis.

Previous Work

Little published data exist on the trace element content of coal balls. Phillips, Kunz, and Mickish (1977) report data for 32 elements in 7 composite coal-ball samples. For most of the trace elements the values are at or below detection limits. For their zones 1 to 6, the values for composite samples of coal balls generally agree with our data, with much of the elemental distribution controlled by the pyrite content. For the uppermost zone 8, their values for composite samples of coal balls have much higher levels of Sr and Mn. The high Mn concentration is particularly questionable and may reflect a major bias in how the composite sample for each zone of coal balls was prepared and selected. A reporting of results on individual coal balls would have been more informative.

Results reported here agree with other published results on the major chemical constituents for coal balls. The absence of siderite in this study is the main exception and reflects the local formative conditions in the study area.

Mamay and Yochelson (1962) published the major chemical composition as well as semiquantitative spectroscopic results for 8 midwestern coal balls. The ranges are comparable to those in our study including excess iron, which remains after it is balanced with the sulfur to form pyrite. There is no sample in this study comparable to the faunal coal ball from Kansas with 61 percent pyrite.

Analytical Methods

The elements reported in this study are listed in figure 26. Included are elements of potential environmental concern (Harvey et al., 1983). All samples for geochemical analysis were ground to minus 60 mesh. Moisture was determined on each sample and the values reported are on a moisture-free basis. The methods used are as follows:

X-RAY FLUORESCENCE (XRF): Si, Al, Ca, Fe, Ti, Mg, P
GRAVIMETRIC PROCEDURES: total C, S, moisture, CO_2, loss on ignition (LOI); insoluble residue (In Res)
INSTRUMENTAL NEUTRON ACTIVATION ANALYSIS (INAA): K, Na, Mn, As, Br, Ce, Co, Cr, Cs, Dy, Eu, Ga, Hf, In, La, Lu, Mo, Rb, Sb, Sc, Se, Sm, Ta, Tb, Th, U, W, Yb
OPTICAL EMISSION (OE): Ag, B, Be, Ge, Tl, V
ATOMIC ABSORPTION (AA): Cd, Cu, Hg, Li, Ni, Pb, Zn
ENERGY DISPERSIVE X-RAY (EDX): Ba, Sr, Zr
ION SELECTIVE ELECTRODE (ISE): F

Details of the procedures are contained in Gluskoter et al. (1977).

The isotopic determinations were provided by T. F. Anderson using standard methodology (Anderson, Brownlee and Phillips, 1980) the δC^{13} and δO^{18} results for selected samples are reported in table 9.

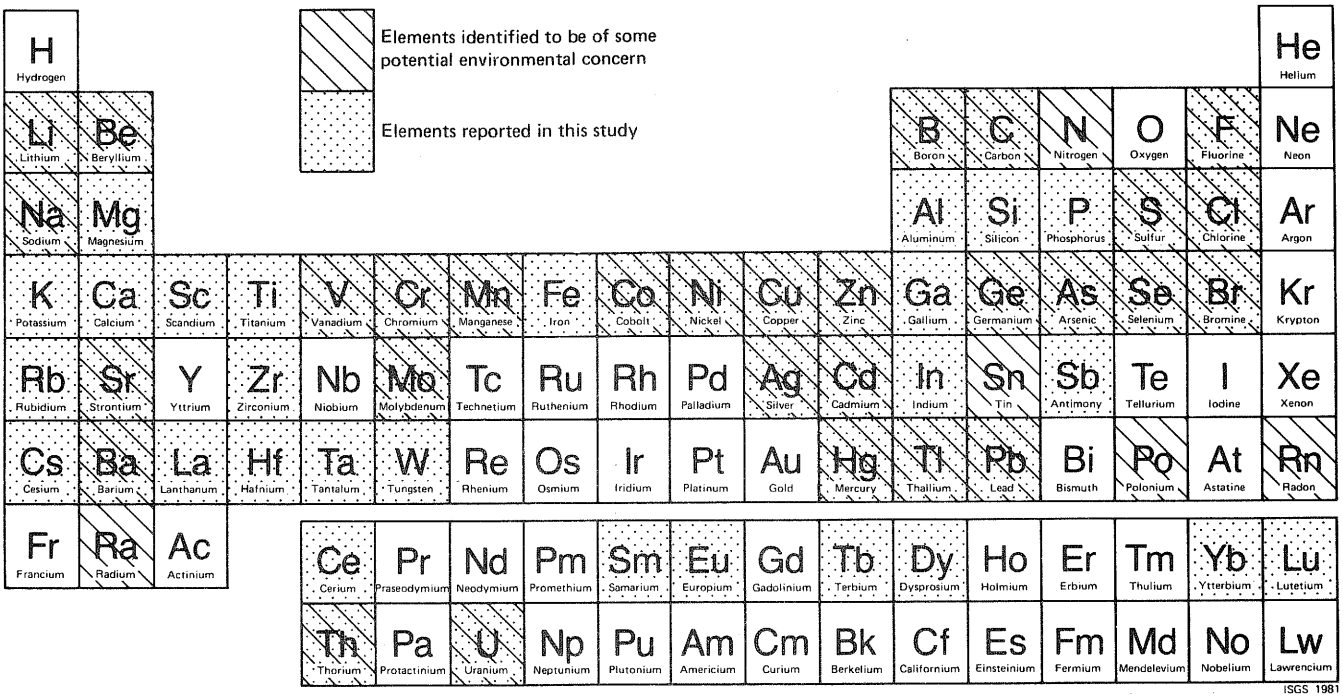

Figure 26
Elements reported in this study and those of some potential environmental concern.

Mineral Composition

The dominant minerals observed were calcite, dolomite, ferroan dolomite, and pyrite. Minerals of minor abundance included marcasite, gypsum, quartz, illite, kaolinite, and lepidocrocite. No siderite or barite was detected. No quantitative analysis was made for the minerals detected; however, the relative peak heights of the x-ray diffraction intensities are listed in table 4.

Major Elements

The major constituents in coal balls are CaO, MgO, Fe_2O_3, S, MnO, CO_2, and organic carbon. The major constituents reflect variations of the major minerals observed by x-ray diffraction: calcite ($CaCO_3$), dolomite ($CaMg(CO_3)_2$), ferroan dolomite $Ca(Mg,Fe,Mn)(CO_3)_2$, pyrite (FeS_2), and quartz (SiO_2).

The mineral composition of the 25 samples for which x-ray diffraction results had been obtained (table 4) were calculated using the chemical results (table 5). The calculation was based on these assumptions: (1) all of the Mg occurred in dolomite, (2) the Ca value was obtained from the Ca determination after the amount needed to produce dolomite had been subtracted, and (3) pyrite was calculated from the S determination. Included is a summation that approaches 100 percent, which provided a useful check on the mineralogy and the major elemental analyses. Figure 27 (dolomite relative to MgO) and Figure 28 (pyrite relative to total S) illustrate the correlation of these two data sets.

The amount of detrital minerals incorporated into the coal balls can be estimated from the concentrations of Al_2O_3 or K_2O, which were in most cases very low or undetectable. This observation was confirmed by x-ray diffraction results that indicated very weak or no reflections from the clay minerals, illite or

Table 4. Relative Heights: X-Ray Diffraction of Selected Coal Balls, Limestones, and Anna Shale Concretions

	Calcite 29.4*	Mg-Dolomite 30.9*	Fe-Dolomite 30.7*	Pyrite 40.8*	Marcasite 25.9*	Gypsum 11.6*	Quartz 26.6*	Illite 8.8*	Kaolinite 12.4*
COAL BALLS									
C21568	120.	--	9.5	9.3	1.1	--	--	--	--
C21569	135.	--	11.8	5.2	--	--	6.0	--	--
C21570	150.	--	14.7	4.6	--	2.0	1.5	--	--
C21571	150.	--	20.5	0.5	--	1.4	2.0	2.0	2.0
C21581	140.	--	5.7	5.0	1.5	2.0	2.0	2.5	2.0
C21582	140.	--	8.6	10.2	--	3.5	13.2	--	2.5
C21583	130.	--	23.3	7.0	4.0	4.0	10.6	--	--
C21584	120.	--	7.6	21.8	2.5	4.3	40.5	3.0	3.3
C21585	130.	--	45.0	4.0	--	3.0	2.8	--	--
C21586	9.6	--	130.	14.0	--	2.6	--	2.4	2.2
C21587	130.	--	78.0	2.4	--	--	1.5	--	--
C21588	140.	--	26.0	1.7	1.7	7.2	15.0	2.5	--
C21589	--	120	--	2.2	--	15.3	25.5	4.2	6.5
C21590	130.	--	14.3	3.0	--	--	--	--	--
C21591	34.0	--	--	10.2	--	--	150.	--	--
C21758	150.	--	17.8	3.7	--	2.2	8.0	--	2.2
C21765	2.9	--	--	4.	--	--	170.	--	--
C21766	150.	--	--	2.0	--	--	17.0	4.0	5.4
ASSOCIATED ROCKS									
C21626	22.4	--	150.	3.5	--	--	37.0	4.0	5.5
C21627	120.	--	9.0	6.1	6.5	4.3	83.5	4.8	3.5
C21628	93.5	--	11.1	8.2	1.5	9.5	115	4.0	4.5
C21629	120.	--	--	2.2	2.5	--	18.8	1.5	2.0
C21760	120.	--	4.2	8.6	--	19.0	120	12.5	9.8
C21761	15.0	--	5.2	7.6	6.7	--	150	6.8	4.0
C21767	115.	--	12.5	5.2	--	4.2	120	4.5	5.5

*Degrees 2 θ
Lepidocrocite found in C21587.
Plagioclase feldspar found in C21760.

Table 5. Predicted Mineral Composition Based on Chemical Analysis

	Calcite (%)	Dolomite (%)	Pyrite (%)	Quartz (%)	Organic carbon (%)	Al_2O_3 (%)	Total (%)
COAL BALLS AND SIMILAR MATERIALS							
C21568	65	7	26	<.1	3	< .1	101
C21569	81	12	6	1.5	3	< .1	103
C21570	74	14	12	<.1	4	< .1	104
C21571	84	17	2	0.8	2	< .1	106
C21581	81	6	12	0.4	3	< .1	102
C21582	64	6	25	2	3	< .1	100
C21583	70	12	16	2	1	0.8	102
C21584	38	5	39	12	2	2	98
C21585	66	20	8	0.9	6	< .1	101
C21586	18	39	33	<.1	1	< .1	91
C21587	69	26	0.3	0.4	1	< .1	97
C21588	77	14	2	2	4	< .1	99
C21589	9	55	2	7	15	2	90
C21590	83	7	4	0.2	7	< .1	101
C21591	1	1	5	70	22	< .1	99
C21758	82	15	4	2	5	< .2	108
C21765	0.5	< 1	2	89	13	0.2	105
C21766	5	43	5	2	31	0.6	87
ASSOCIATED ROCKS							
C21626	21	61	1	11	1	3	99
C21627	40	7	18	26	2	5	98
C21628	31	7	14	34	4	5	95
C21629	83	7	3	6	3	1	103
C21760	20	2	13	40	6	10	91
C21761	3	4	12	66	3	6	94
C21767	35	11	8	38	3	3	98

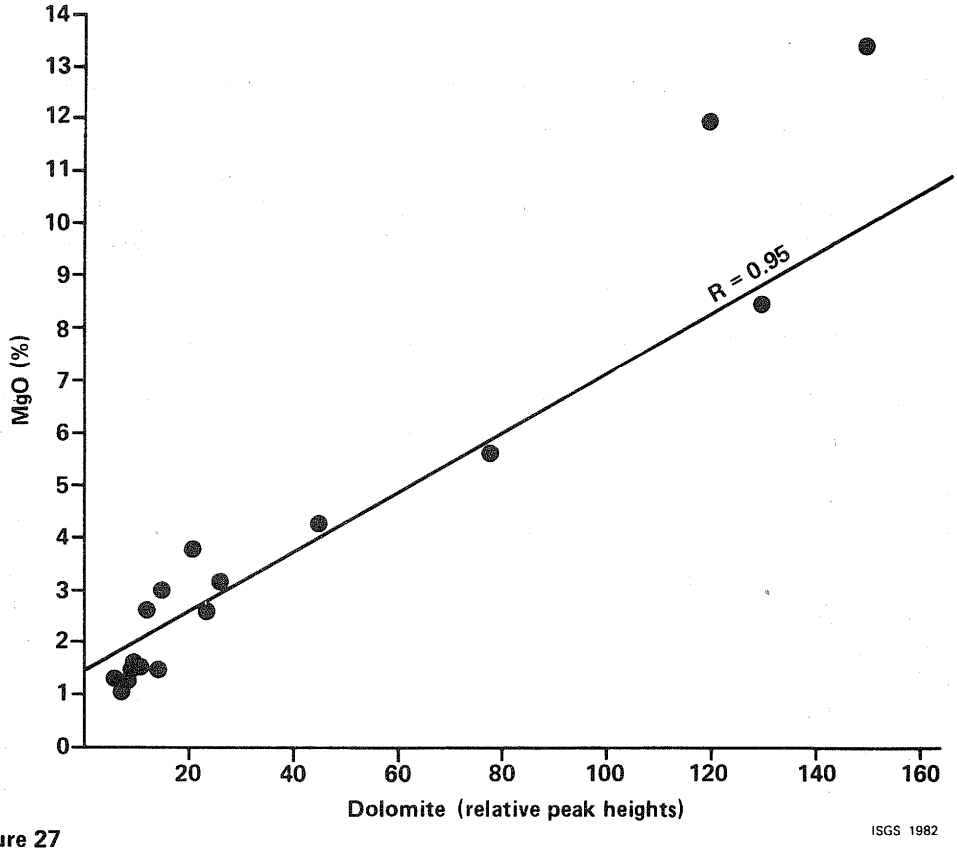

Figure 27
Relationship between percentage of MgO (XRF) and relative peak height of dolomite (XRD) in coal balls.

kaolinite. Plots of K_2O relative to intensities of illite or kaolinite, however, did not show a strong correlation; whereas plots of Al_2O_3 relative to peak heights of illite and kaolinite did, although only 6 samples had detectable Al_2O_3. This indicates that K may occur in other minerals present.

Based on major elemental analysis and x-ray diffraction, coal balls fell into four groups: the first contained 10 samples predominantly composed of calcite with less than 2 percent pyrite; the second contained 17 samples with pyrite levels ranging from 2 to 39 percent and lesser amounts of carbonate minerals than the first group; the third contained 2 samples (C21589 and C21766) with greater then 40 percent dolomite; and the fourth contained 2 samples (C21591 and C21765) with 70 and 89 percent quartz, respectively. Coal balls examined by Rao (1979) are mineralogically similar to our first two groups. Based on x-ray diffraction analysis, he reported ranges of calcite (31% to 98%), dolomite (0% to 21%), pyrite (1% to 54%), and quartz (0% to 4%) in 52 coal balls from North America and Europe.

Minor and Trace Elements

Concentration of many minor and trace elements are very low in our coal balls. This is reflected by the great number of "less than" values reported. The trace elements B, Be, Cd, Cs, Ga, Ge, Hf, In, Mo, Ni, Rb, Ta, Th, Tl, U, V, W and Zr are not included in table 6 or in the statistical treatment of the data because most of the values were below the upper detection limits. Mean values for the coal balls are listed in table 6. Also included are statistics based on

Table 6. Comparison of Mean Concentrations of Rock Materials Associated with Coal Ball Occurrences

	Anna Shale (8)*	Energy Shale (4)	Blue Band (6)	Underclay (3)	Limestone (6)	Total coal balls (31)	Pyritic coal balls (21)	Nonpyritic coal balls (10)
SiO_2	46.3 %	55.1 %	48.2 %	61.7 %	21.7 %	6.6 %	9.3 %	1.0 %
CaO	4.2 %	0.3 %	0.4 %	0.9 %	27.3 %	41.1 %	35.2 %	51.6 %
Fe_2O_3	4.8 %	6.9 %	2.6 %	2.7 %	7.6 %	7.1 %	10.3 %	1.3 %
MgO	1.4 %	1.6 %	0.4 %	1.3 %	5.2 %	3.5 %	3.2 %	4.2 %
K_2O	3.0 %	3.5 %	1.4 %	3.6 %	0.7 %	0.03 %	0.04 %	67.8 ppm
Na_2O	0.8 %	1.2 %	0.5 %	0.9 %	0.3 %	0.06 %	0.05 %	.07 %
P_2O_5	2.0 %	0.2 %	0.1 %	0.7 %	0.4 %	0.09 %	0.09 %	.07 %
MnO	0.03 %	0.05 %	.01%	0.01 %	0.1 %	0.08 %	0.08 %	.08 %
CO_2	0.9 %	0.07 %	0.2 %	0.09 %	25.6 %	32.9 %	29.4 %	41.6 %
Org Carbon	14.3 %	3.6 %	16.2 %	3.0 %	2.4 %	5.8 %	7.2 %	2.1 %
Sulfur	2.5 %	2.7 %	1.8 %	0.5 %	4.3 %	5.4 %	7.3 %	0.5 %
As	15.9 ppm	12.3 ppm	4.9 ppm	6.0 ppm	10.0 ppm	8.8 ppm	12.8 ppm	0.5 ppm
Ba	1472. ppm	556. ppm	380. ppm	307. ppm	1902. ppm	555. ppm	795. ppm	51. ppm
Br	2.5 ppm	2.8 ppm	2.4 ppm	3.1 ppm	1.7 ppm	2.0 ppm	1.6 ppm	2.7 ppm
Ce	83. ppm	72. ppm	92. ppm	94. ppm	46. ppm	15.0 ppm	14. ppm	15. ppm
Co	18. ppm	20. ppm	11. ppm	17. ppm	7. ppm	1.6 ppm	2.1 ppm	0.7 ppm
Cr	487. ppm	95. ppm	68. ppm	115. ppm	36. ppm	3.4 ppm	4.2 ppm	1.7 ppm
Cu	109. ppm	69. ppm	39. ppm	47. ppm	24. ppm	10.2 ppm	10.2 ppm	10.2 ppm
Dy	4.6 ppm	5.0 ppm	2.6 ppm	5.4 ppm	3.0 ppm	1.2 ppm	1.2 ppm	1.3 ppm
Eu	1.3 ppm	1.5 ppm	1.0 ppm	1.6 ppm	1.2 ppm	0.3 ppm	0.3 ppm	0.4 ppm
F	1714 ppm	520. ppm	301. ppm	1500. ppm	333. ppm	108. ppm	108. ppm	105. ppm
La	46. ppm	48. ppm	50. ppm	46. ppm	14.6 ppm	6.6 ppm	6.6 ppm	6.5 ppm
Li	32.5 ppm	51.5 ppm	164.7 ppm	26.3 ppm	9.2 ppm	3.6 ppm	3.7 ppm	3.4 ppm
Lu	0.6 ppm	0.6 ppm	0.4 ppm	0.6 ppm	0.3 ppm	0.1 ppm	0.2 ppm	0.08 ppm
Pb	30.6 ppm	31.0 ppm	28.3 ppm	36.3 ppm	29.0 ppm	54.4 ppm	54.0 ppm	55.3 ppm
Sb	6.0 ppm	1.0 ppm	0.7 ppm	1.4 ppm	1.3 ppm	0.5 ppm	0.7 ppm	0.07 ppm
Sc	15.3 ppm	18.0 ppm	9.0 ppm	17.3 ppm	7.2 ppm	1.9 ppm	2.0 ppm	1.7 ppm
Se	41.2 ppm	2.6 ppm	6.8 ppm	0.8 ppm	4.6 ppm	6.3 ppm	9.0 ppm	0.6 ppm
Sm	8.4 ppm	6.8 ppm	6.4 ppm	8.7 ppm	5.7 ppm	1.6 ppm	1.6 ppm	1.5 ppm
Sr	164. ppm	124. ppm	100. ppm	160. ppm	360. ppm	440. ppm	406. ppm	512. ppm
Tb	1.1 ppm	1.3 ppm	0.8 ppm	1.0 ppm	0.9 ppm	0.3 ppm	0.3 ppm	0.3 ppm
Yb	3.3 ppm	3.3 ppm	2.1 ppm	3.4 ppm	2.0 ppm	0.6 ppm	0.7 ppm	0.5 ppm
Zn	1000 ppm	69.5 ppm	17.3 ppm	25.3 ppm	13.2 ppm	9.8 ppm	10.3 ppm	8.6 ppm

*(N) = Number of samples in each group.

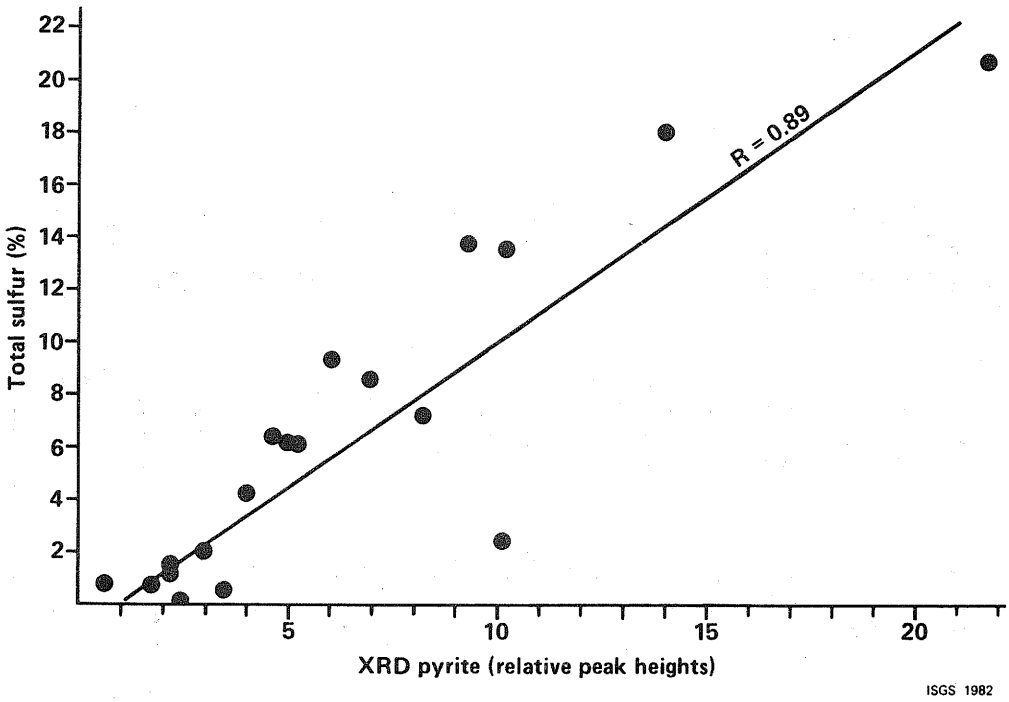

Figure 28
Relationship between percent sulfur (ASTM) and relative peak height of pyrite (XRD) in coal balls.

separating coal balls into those with greater than 2 percent and those with less than 2 percent pyrite. The choice of 2 percent for a cut-off was based on a histogram plot of frequency by pyrite percentage. Also included in table 6 are mean concentrations observed in the associated rock materials.

Elemental Associations

Inter-elemental associations in the coal balls were determined by simple correlation and clustering programs as well as R-mode factor analysis. These approaches gave comparable insights into controlling factors for the observed variations.

Correlation and factor analysis

Factor analysis is a statistical technique summarizing the relationships between variables in a matrix of factors. In general, enough factors are chosen to account for 90 percent of the system variance, with no prior assumptions made concerning the resulting factors (Cahill, 1981).

We chose 20 elements, which had sufficient analytical accuracy, for R-mode factor analysis. The elements, Si, Mg, Mn, and Ba, were excluded since their distribution was controlled by 1 or 2 samples with anomalously high levels, for example, from coal balls with high levels of quartz or dolomite. The Ba variance was controlled by C21561, which had a concentration of 1.1 percent compared to a range of 19 to 2000 ppm Ba in the other samples.

The results of factor analysis are shown in table 7; 4 factors have been extracted. Factor 1 shows high loadings of Sc and rare earth elements (REE). As discussed later, we think that the REE are associated with carbonate minerals.

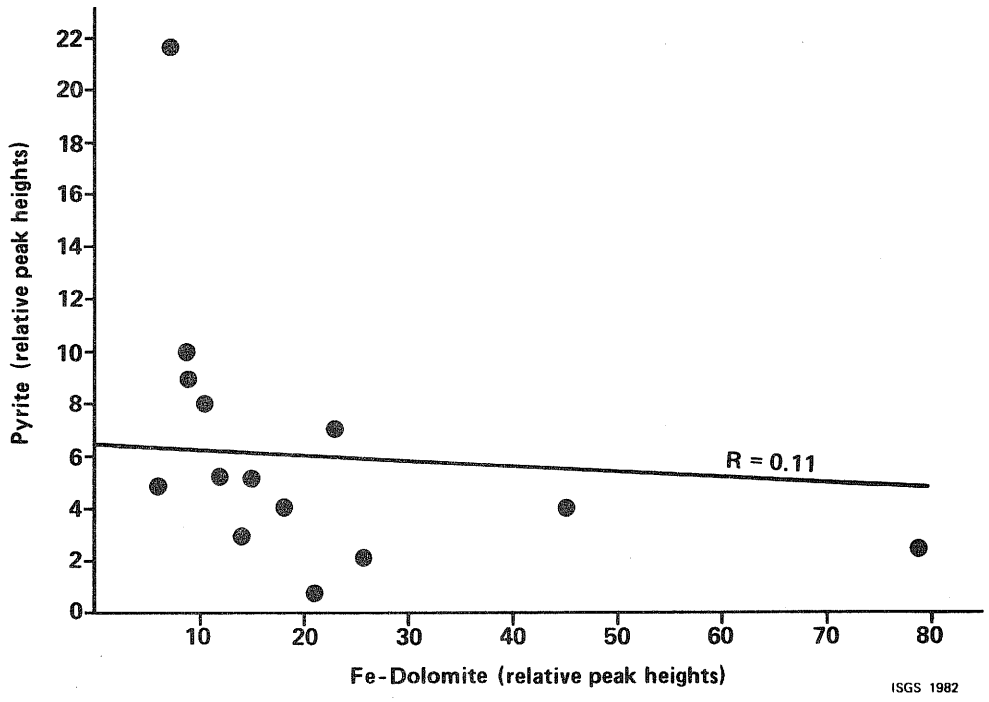

Figure 29
Relationship between pyrite in coall balls (XRD) and relative peak heights of dolomite (XRD).

Elements with high loadings in Factor 2 are Fe, S, Co, Cu, As, Se, and Pb; this factor is related to the pyrite formation. Factor 3 shows high loadings of Na, Al, K, and Cr, indicating the control of clay minerals. Elements with high loadings in Factor 4 are Ca, Sr, and CO_2, obviously due to carbonate minerals.

The results of the correlation and cluster program placed 34 elements into the following 8 clusters:

Si, organic carbon, total carbon, Mg and Mn
Na, Br
Ca, inorganic carbon, Sr
F
Ba, Co, Pb
Fe, S, As, Se
K, Cr, Cu, Li, Sb, P, Zn
Ce, La, Dy, Eu, Sm, Tb, Lu, Yb (rare earth elements), and Sc

Based on the statistical techniques the following geochemical associatons are apparent:

Pyritic Association. Iron and S have a high positive correlation (0.95) and in most samples the Fe/S ratio is close to the pyrite stoichiometric ratio of 0.87. This relationship confirms the observation in figure 28. The incorporation of iron into ferroan dolomite gives an indication of the secondary nature of pyrite formation. Figure 29 is a plot of the relationship of relative peak height of pyrite to peak height of ferroan dolomite. The relation is an inverse one indicating two things: when dolomite was forming iron was sufficiently available to substitute in the structure; conditions did not favor the formation of pyrite.

Table 7. R-Mode Factor Analysis Results for Selected Elements in Coal Balls*

	Factor 1	Factor 2	Factor 3	Factor 4
Al	0.18	0.27	0.84	-0.17
Ca	0.13	-0.16	-0.21	0.80
Fe	0.12	0.92	-0.03	-0.32
K	0.15	0.08	0.96	-0.10
Na	0.08	-0.13	0.50	0.03
CO	0.20	-0.28	-0.18	0.89
S	-0.07	0.89	0.00	-0.24
As	0.09	0.90	0.20	-0.23
Ce	0.82	-0.04	-0.01	0.08
Co	0.07	0.56	0.08	0.09
Cr	0.31	0.35	0.79	-0.35
Cu	0.01	0.51	0.52	0.15
Eu	0.93	-0.07	0.12	-0.01
La	0.74	0.11	0.05	0.22
Pb	-0.06	0.56	-0.14	0.58
Sc	0.78	0.09	0.40	-0.04
Se	0.06	0.53	0.12	-0.24
Sm	0.99	-0.02	0.07	-0.03
Sr	-0.19	-0.24	0.15	0.58
Tb	0.93	0.10	0.17	-0.08
Yb	0.94	0.18	0.12	-0.10

*Significant loadings are underscored.

The trace elements As and Se show expected high correlation with pyrite, so they are probably substituted into the pyrite structure.

Sulfur is also positively correlated with a few other chalcophile elements including Co, Cu, Mo, Pb and Sb. These relationships are to be expected if the chalcophile elements co-precipitated with iron during pyrite formation.

Lithophile Elements. Lithophile elements considered here are only those concentrated in silicate minerals; they are not the rare earth elements that have high loadings on a single factor but no high correlation with either the other lithophiles or the carbonate minerals. They will be considered separately.

As pointed out early in the previous section, the coal-ball samples generally contained less than a few percent silicate minerals. Among the major oxides, K_2O and Al_2O_3 are strongly correlated (0.97). Alumina and SiO_2 are not correlated due in part to some samples with very high levels of quartz.

Rare Earth Elements. The rare earth elements (REE) as a group had high loadings on Factor 1, high mutual correlations, and formed a distinct cluster. The lack of strong correlation between REE and other lithophile elements was not expected. Previous work on the Herrin Coal (Chou et al., 1982) indicated that REE distribution was controlled by clay minerals. Cahill (1981) also found that the REE were associated with other lithophilic elements and the clay-sized sediments in recent Lake Michigan sediments.

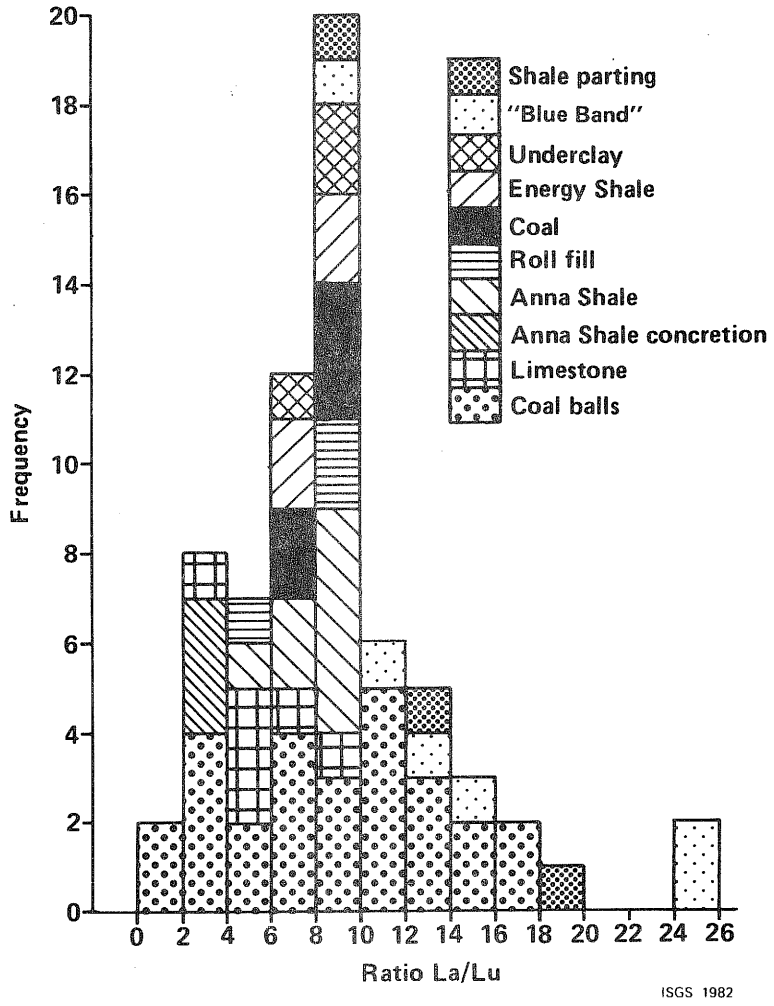

Figure 30
Frequency distribution of the La/Lu ratio for coal balls and associated materials.

The REE contents in the 31 coal-ball samples are variable in concentration (La 0.3 to 20 ppm, for example) and also in relative abundance patterns when normalized to the REE content of chondrites. One means of comparing the relative distribution patterns is to calculate a lanthanum/lutetium (La/Lu) ratio, which approximates the general slope of the REE normalized distribution pattern.

The range of La/Lu ratios is from 1.3 to 25.6. The distribution is plotted in terms of a frequency histogram (fig. 30) along with associated rock materials. The coal-ball La/Lu ratio distribution is much wider than that of the other rock types. Some coal balls have patterns similar to limestones or Anna Shale concretions while others have patterns more similar to shale partings in coal seams.

The wide range of La/Lu ratios and the statistically distinct grouping of REE indicates that their abundances are controlled by at least two factors. If the distribution is influenced partly by the clay minerals present in the coal balls, then in samples with no detectable Al and K, the REE abundances may reflect the REE composition of the original peat incorporated into carbonate minerals.

More work is needed to understand the significance of these REE distribution patterns. The analysis of the carbonate-free fraction (insoluble residue) may be one means of explaining the observed patterns.

Strontium and Carbonate Associations. The carbonate minerals--calcite, dolomite and ferroan dolomite--constitute the predominant portion of carbonate coal balls. The substitution of Sr into carbonate minerals will depend on the form of calcium carbonate precipitated as well as the temperature and composition of water. The correlation between strontium and calcium is high, showing that substitution has occurred.

Coal-Ball Formation: Implications of Geochemical Data

Geochemical data has seldom been used to interpret the formation of coal balls. Specifically, the application of Sr/Ca molar ratios has seldom been attempted. In most applications, biochemical effects associated with the co-precipitation of aragonite and calcite are more important than inorganic precipitation alone.

Excluding the coal balls with high dolomite content, the Sr/Ca molar ratios are 4 to 10.5 ($\times 10^{-4}$). The ratios in the limestones from this work, range from 4.5 to 12.3 ($\times 10^{-4}$) while that in the average limestone is 7 ($\times 10^{-4}$) and in marine carbonate ooze is 15 ($\times 10^{-4}$) (Wedepohl, 1978). From previous, unpublished results the Sr/Ca molar ratios for a series of cleat calcites from the Herrin Coal ranged from 1.4 to 3.6 ($\times 10^{-4}$). The overlap in ratios for limestones and coal balls indicate a similar mineralizing solution distinct from that which formed the cleat fillings.

Statistical tests were performed to test whether the Sr/Ca ratios could be used to distinguish two types of coal balls. Table 8 is a compilation of the Sr/Ca molar ratios and means of each group. It was found that at the 95 percent confidence level the two groups were statistically different. Despite the difficulty of having multiple mineral phases present in the samples analyzed, the Sr/Ca molar ratio indicates a marine source based on a comparison to the limestones in the area and that the top coal balls have probably undergone recrystallization, which explains their lower ratios. This supports the Old Ben 24 Model of coal-ball formation.

Kinsman (1969) provides a good summary of the interpretation of the Sr record in carbonate minerals and highlights the potential shortcomings. In applications to this study he notes that the Sr/Ca molar ratio can range as much as 0.6 to 1.3 $\times 10^{-2}$ in marine waters, although the Sr/Ca molar ratio is normally 0.9 $\times 10^{-2}$ in sea water. The median value for freshwater is much lower at 0.3 $\times 10^{-2}$.

Treese et al. (1981) evaluated the Sr/Ca molar ratios in carbonate sediments in a freshwater marl lake as indicators of different depositional environments and/or the extent of subsequent diagenetic alterations. They noted that the biochemical effect is the major control of the Sr/Ca molar ratio in the various groups of freshwater carbonates. They reported a range of Sr/Ca molar ratios of 5.9 to 8.8 ($\times 10^{-4}$).

Elderfield et al. (1982) measured the concentrations of Sr^{+2}, Mg^{+2}, and Ca^{+2} ions in interstitial solutions associated with deeply buried marine

Table 8. Statistical Test of Sr/Ca Molar Ratio for the Separation of two Coal Ball Groups

A. Top of Seam Coal Balls		Sr/Ca (10^{-4})	
C21533	LW-H-5	7.1	
C21568	LW-C-4B	4.8	
C21569	22600 E	4.8	Mean = 5.5
C21571	LW-K-1	6.2	Std. Dev. = 1.0
C21581	LW-H-7	4.9	
C21758	OB26-A-5	5.2	
B. Coal Balls from Vertical Section #3			
C21557	Zone BB3	5.3	
C21558	Zone 2	8.5	
C21559	Zone 3	5.9	Mean = 7.3
C21560	Zone 4	6.1	Std. Dev. = 1.6
C21561	Zone 4	9.3	
C21562	Zone BB4	7.4	
C21563	Zone 9A	6.7	
C21564	Zone 17/18	8.7	
C21565	Zone 20	10.3	
C21566	Zone 12	7.5	
C21567	Zone 16	7.2	
C21581	Zone BB2	4.9	

Analysis of variance by F test
Calculated critical F = 6.13 Degrees of Freedom = 16
Critical F at 99% F = 8.53
Critical F at 95% F = 4.49
Means are significantly different at 95% level.

sediments. They noted that as recrystallization of $CaCO_3$ occurred, a considerable increase in Sr^{+2} was found in the interstitial solution with depth. Lorens (1981) found that by increasing calcite precipitation rates the distribution coefficient for strontium also increased.

Boron has been used by many investigators as an indicator of paleosalinity (Schopf, 1980). However, B is predominately associated with clay minerals. The B content was below the detection limit in 23 of 31 coal balls studied here. The highest B content, 85 ppm, occurred in a transported coal ball (C21584) with the highest amount of clay present.

The fluorine distribution in coal balls is interesting because it formed a distinct cluster and in factor analysis (not shown) a high loading on a single factor. The concentration in the coal balls ranged from 10 to 260 ppm, which barely overlaps with the range of 250 to 476 ppm found in the limestones. Fluorine would be expected to substitute easily for hydroxyl groups and be present in fluorite, apatite, or clay minerals. Fluorine, however, has a weak correlation with Sr, Cu and Pb but not with P. Further work is needed to understand F importance as an environmental indicator element.

Manganese is a minor constituent in coal balls and ranges from 113 to 2100 ppm in the normal coal balls, and only about 20 ppm in two siliceous coal balls. The chemistry of Mn is complex because of its three oxidation states and hence its occurrence will be greatly affected by changing eH, pH and pCO_2 conditions. Manganese minerals, therefore, could be indicators of equilibrium conditions during coal-ball formation. There is a weak correlation between Mg and Mn (0.38) and Mn would be expected to substitute into dolomite over calcite. Rhodochrosite, $MnCO_3$, was not detected by x-ray diffraction, but its presence would indicate high pH and pCO_2 conditions. These conditions would also be favorable for siderite formation, but $FeCO_3$ was not detected. If a sharp eH gradient existed between the pore waters of the peat and the overlying solutions, a Fe, Mn oxide layer would form. This is particularly true where anaerobic sediments come in contact with water with a high pO_2. Such a layer was not observed, but it may not have been preserved. Under conditions where pyrite was being formed, manganese sulfides would be much more soluble. This is reflected by Fe/Mn ratios which range from 5 to 46 for coal balls with less than 2 percent pyrite to ratios of 17 to 600 in coal balls with pyrite levels of 2 to 39 percent.

Carbon and Oxygen Isotopes

Carbon and oxygen isotopes are often used in geochemical studies to determine the original environment of deposition. Limestones of marine origin normally have δC^{13} values near zero, while high negative δC^{13} values are typically found in terrestrial plants. The whole range of our samples is skewed toward the terrestrial end of the scale; even the open-marine Brereton Limestone has a negative δC^{13} value of -6.1 permil (fig. 31). Coal balls from mid- and low-seam in area L (vertical sections 3 and 5) have δC^{13} values from -15.7 permil -29.5 permil suggesting little or no marine influence. Coal balls from near the top of the seam range between -11.3 and -12.6 permil in their δC^{13} values. This would seem to support a different origin for these two types of coal balls, consistent with our model of coal-ball formation presented in the next chapter.

Another interesting relationship is that between samples B-5 and V-3 (table 9). The parent material filling the bioturbation trace in the Herrin Coal (LW-B-5) is the Brereton Limestone. The typical Brereton Limestone is represented here by LW-V-3. During the burrowing and infilling, bits of δC^{13} depleted peat were mixed with the Brereton Limestone. The δC^{13} value of B-5 was apparently lowered to -12.0 permil through recrystallization; its $\delta 0^{18}$ value of -8.9 permil was also the most terrestrial value of this data set.

In comparing these values to previous work, several parallels are obvious. The normal coal balls selected by Mamay for Weber and Keith (1962) fall in the same range as the full-seam coal balls at Old Ben Mine No. 24. Their Berryville coal ball with its marine core is similar (δC^{13} of -13.9 permil) to our sample B-5, which is a burrow filled with marine sediment (δC^{13} of -12.0 permil). However, adjacent normal coal balls have a δC^{13} of -20.7 permil suggesting a different carbon source. The values from the Amax Delta mine (Anderson, Brownlee, and Phillips, 1980) are similar to Old Ben Mine No. 24, although they are generally not as negative. Zone 8 from the Amax Delta mine is anomalous both chemically and isotopically. The δC^{13} and $\delta 0^{18}$ values for composite samples from Zone 8 are most similar to the values for the marine Anna Shale concretion and to the Brereton Limestone sample from Old Ben Mine No. 24; no coal ball from Franklin County has a δC^{13} value higher than -11.3 permil.

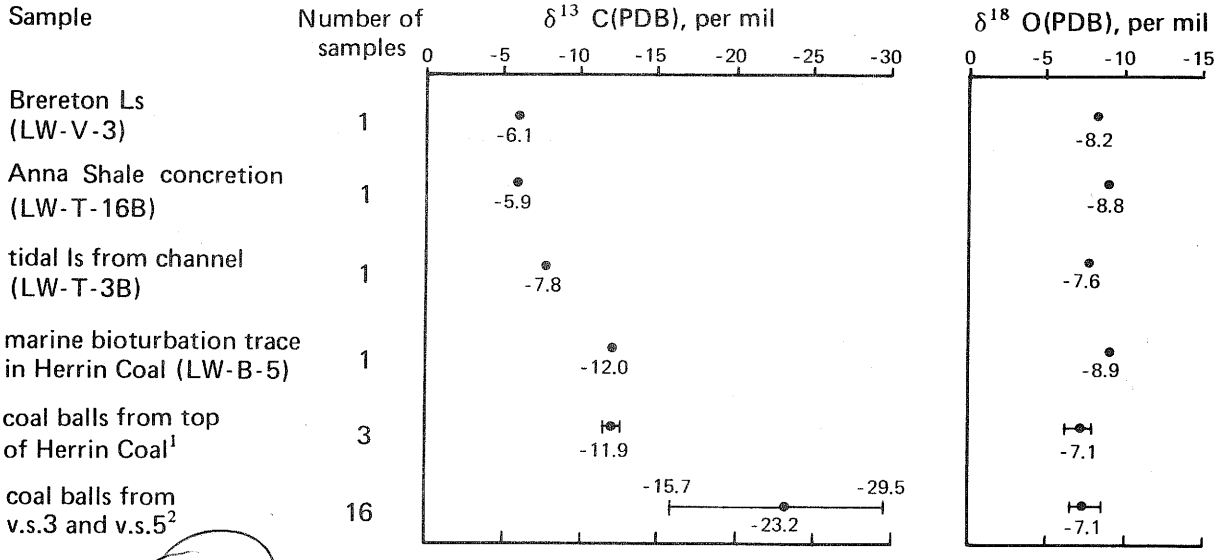

[1] Coal balls LW-H-5, 22600E and OB26-A-5. Mean and range bar shown.
[2] Coal balls from Old Ben No. 24 ranging from below the "blue band" to near the top of the seam. These values show no significant change from top to bottom (type II occurrence). Mean and range bar shown.

Figure 31
Stable carbon and oxygen isotope values (δC^{13} and δO^{18}) for coal balls and associated units from transitional roof areas. Carbon and oxygen isotope data provided by T. F. Anderson, University of Illinois (1982).

MODELS FOR THE FORMATION OF COAL BALLS AND THEIR PREDICTIVE VALUE

The Old Ben 24 Coal-Ball Model

Earlier explanations for coal-ball formation were limited. Until this investigation at Old Ben Mine No. 24, not enough data was available on coal balls and their geological settings to work out a comprehensive model--one that covers the development of several periods of coal-ball formation. In this section, we bring together the results of our field and laboratory work, and set out all the conditions and processes that produced coal balls. Later, we discuss models developed by others.

In the vast peat swamp of the Herrin Coal, the water table was generally high. There were some fluctuations; several relatively "dry" periods are recognizable by greater concentrations of fusain and certain plants occurring in distinct layers within the seam. Periods of flooding are marked by shale partings that originated from a major river to the west. Although there is no evidence of marine ingression during peat accumulation, the swamps were set in an extremely flat coastal plain and brackish conditions may have existed at times. Peat swamps and bogs are often characterized by acidic conditions with pH values of 4 to 6. Under these conditions Ca, Fe, Mg and other metals may be chelated into organic matter or dissolved as ionic compounds.

Probably as a result of a general rise in the base level of water as the sea transgressed, the Walshville river deposited mud that became the Energy Shale on adjacent flood plains where peat had accumulated. At Old Ben Mine No. 24 fossil remains of the last swamp forest are found in the carbonaceous facies of the

Table 9. δC^{13} and δO^{18} Isotope Data from Coal Balls and Associated Lithologies

Stratigraphic Unit	Sample Number	δC^{13} (°/oo)	δO^{18} (°/oo)
Brereton Limestone	V-3	- 6.1	- 8.2
Anna Shale concretion	T-16B	- 5.9	- 8.8
Fossiliferous limestone from "roll"	T-3B	- 7.8	- 7.6
Transported coal ball from "roll"	N-2	-15.6	- 6.3
Marine burrow-fill limestone in top of seam	B-5	-12.0	- 8.9
Top-of-seam coal ball, isolated	H-5	-11.3	- 7.3
Top-of-seam coal ball; edge of area L	22600E	-12.6	- 7.8
Top-of-seam coal ball, isolated	A-5	-11.7	- 6.1
Top-of-seam coal ball under "roll"	A-4	-15.9	- 7.5
Coal ball, Zone 20 (near roof)	22362B (V.S. 3)	-29.5	- 6.5
Coal ball, Zone 20	22347A "	-15.7	- 5.8
Coal ball, Zone 17/18	19541C "	-26.6	- 6.5
Coal ball, Zone 16	19526C "	-24.7	- 6.8
Coal ball, Zone 12	19478C "	-22.5	- 8.1
Coal ball, Zone 9A	22453B "	-24.9	- 7.4
Coal ball, Zone 4	22403D "	-23.5	- 7.7
Coal ball, Zone 3	22388B "	-21.4	- 7.6
Coal ball, Zone 2	22379B "	-22.3	- 7.7
Coal ball, Zone 2	19602A (V.S. 5)	-22.7	- 7.0
Coal ball, Zone 2	19602B "	-28.5	- 6.4
Coal ball, Zone 2	19602E "	-17.9	- 8.6
Coal ball, Zone BB4	19582B "	-26.2	- 7.0
Coal ball, Zone BB4	19576B "	-22.7	- 6.4
Coal ball, Zone BB3	19470C "	-17.2	- 7.7
Coal ball, Zone BB2 (near floor)	19557B "	-25.0	- 6.5

Data furnished by Dr. T. F. Anderson, Department of Geology, University of Illinois. Data is reported relative to the PDB standard.
Units are in rough stratigraphic order. All samples except A-4 and A-5 are from Old Ben No. 24 mine.
Samples have either a Coal Section field number or a five-digit petrifaction number from the Paleoherbarium, Botany Department, University of Illinois.

Energy Shale, deposited under freshwater conditions. A rapidly thickening layer of mud buried the peat, effectively sealing it and forming a closed system (fig. 32a). As the oxygen level dropped, anaerobic decomposition became dominant and the CO_2 generated became enriched in the δC^{13} isotope, due to microbial methanogenesis. The partial pressure of CO_2 may have increased substantially due to the relatively impermeable cover, perhaps reaching supersaturation, which would lead to low pH values and high carbonate solubility. Methane-producing bacteria could have used a significant amount of CO_2. Since they would preferentially use light CO_2, the remaining CO_2 might have a wide range of δC^{13} values, locally depending on the relative degree of methanogenesis.

Soon after the Energy Shale muds had been deposited, large-scale erosion occurred, apparently from the diversion of the Walshville river (fig. 32b). The peat was eroded and oxidized as it became exposed along a gradually widening path. The pH increased as freshwaters entering the peat increased Ca and Mg ion concentrations and removed organic acids, while CO_2 was released simultaneously. The shift in equilibrium resulted in precipitation of Ca and Ca/Mg carbonates within the peat: this was probably the main phase of coal-ball formation. Massive coal balls of type II probably developed at this time; but it is uncertain whether some coal balls of type I were also forming.

As the sea invaded the area, tidal channels developed, often re-using old channels (rolls), although new ones were also cut into the peat (fig. 32c). Coal balls, eroded from the peat, were redeposited in these tidal channels along with the carbonaceous, fossiliferous sediments that hardened into shale. Coal balls continued to form during this period; some type I coal balls exhibit collapsed cell structures, suggesting dehydration of the peat due to marine conditions. Also, some type I coal balls occur near the tidal channels (fig. 32c).

Widespread deposition of Anna Shale and Brereton Limestone followed as the water deepened (fig. 32d). Conditions in peat sealed by the Anna Shale mud probably were less conducive to carbonate permineralization. There is no preference for coal-ball formation under a limestone roof; coal balls seem to be randomly distributed under Anna Shale/Brereton Limestone roof. The only coal balls that definitely formed during the deposition of Brereton Limestone mud are the rare, mixed coal balls associated with an unknown burrowing animal (fig. 32d).

Predictive Value of Old Ben 24 Model

The Old Ben 24 model requires first sealing a peat deposit, then selectively eroding the protective sediment cover. Whether the initial seal has to be a nonmarine, rapidly accumulating mud is uncertain; and the subsequent erosion could probably have been accomplished by either fluvial channeling or by marine erosion. Although marine conditions occurring sometime after seam formation have been connected with most coal-ball finds around the world, marine sediments above the coal do not suffice for coal-ball formation--certainly not for the massive coal-ball aggregates of type II. In Illinois, more than 90 percent of the rocks overlying the Herrin Coal have a marine origin (Krausse et al., 1979); yet coal balls are only local phenomena.

At present, in-mine mapping distinguishes areas likely to have coal balls, especially type II, which are the more serious mining problem. In Old Ben Mine No. 24, in-mine mapping showed a strong relationship between type II coal ball occurrences and Anna Shale/Brereton Limestone roof (figs. 18, 19, 20; Part I, figs. 7, 9, 10). To predict the location of these type

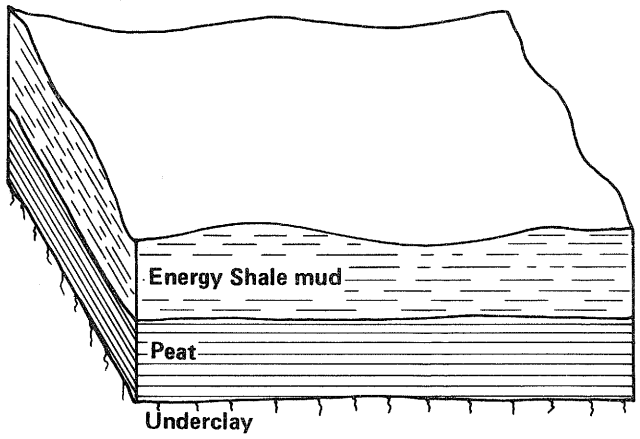

Figure 32
Schematic block diagrams showing geologic events leading to the formation of coal balls.

a. Peat was buried under a thick layer of mud (Energy Shale), which sealed it. Partial CO_2 pressure increased in the peat due to the mud seal.

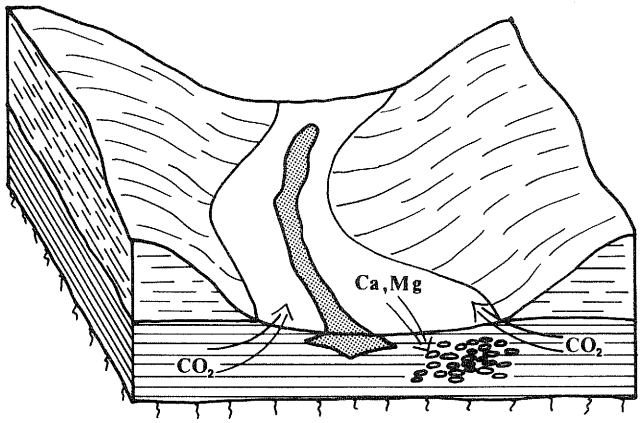

b. The Walshville river selectively eroded the sediments overlying the peat. Peat was oxidized and also partly eroded. CO_2 was released, and freshwaters containing Ca and Mg ions flushed organic acids out of the peat: the pH increased.

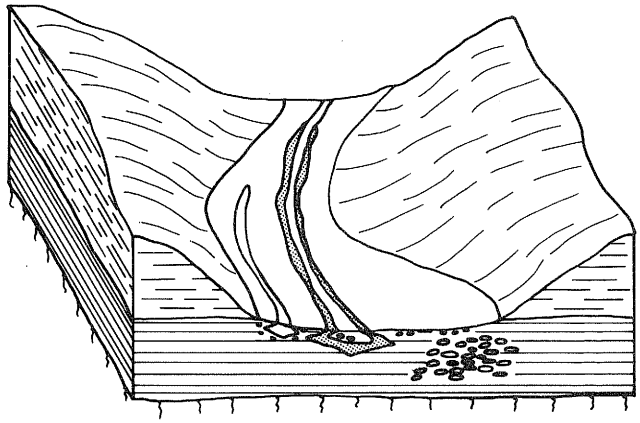

c. As the sea invaded, tidal channels were cut into both old channel fill and peat. Some coal balls were dislodged by erosion and redeposited in carbonaceous fossiliferous shale in tidal channels. Also some top-of-seam coal balls formed.

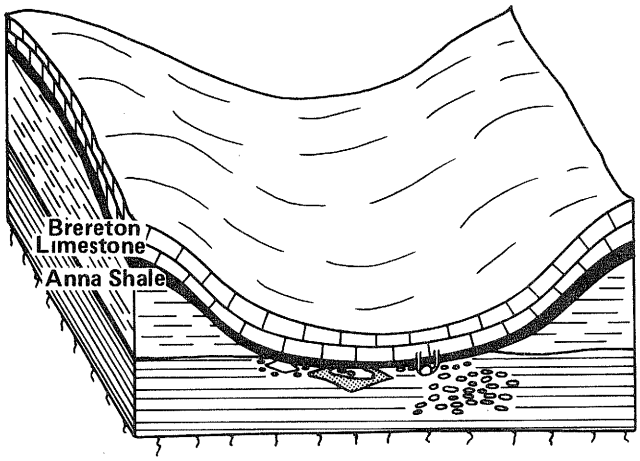

d. Sediments that became marine black shale and limestone were deposited. During the limestone environment, organisms burrowed into and through the Anna Shale sediments into the coal-forming peat. Mineralization around a burrow could form a mixed coal ball.

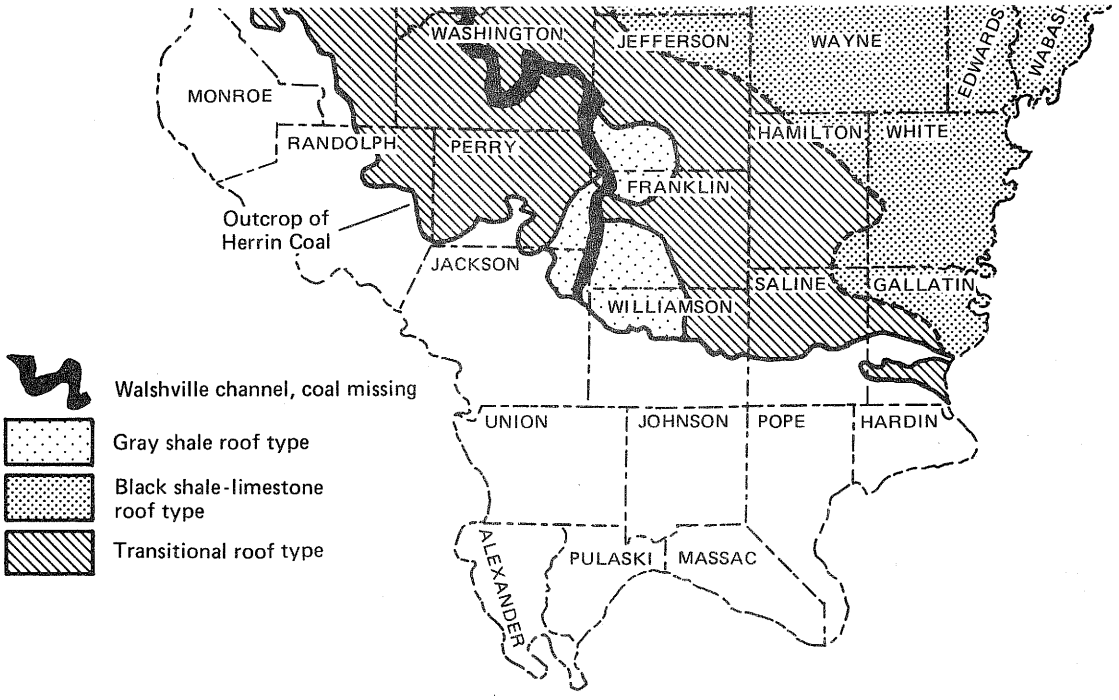

Figure 33
Transition roof areas near Franklin County (modified from Damberger, Nelson, and Krausse, 1980).

II coal balls, in-mine mapping was integrated with the developing depositional model. In Old Ben Mine No. 24, 16 of the 17 type II coal-ball areas were found along a continuous, sinuous, channel exposure of Anna Shale/Brereton Limestone roof; the one other exposure was in a new section of the mine. As mining advances, however, we expect to identify a second subparallel sinuous exposure of Anna Shale/Brereton Limestone roof. At Old Ben Mine No. 27, a short segment of a similar linear exposure was mapped; it contained two type II occurrences (fig. 20). Orientation may also be characteristic of these linear exposures. The exposure at No. 24 mine trends WNW-ESE; the short segment at No. 27 mine trends roughly NW-SE. In fact, several sub-parallel erosional channels, which are likely sites of coal-ball mineralization, may be found in the Energy Shale of Franklin County.

Exploratory drilling will normally permit the identification of transitional roof lithology; however, the small size of the channel-shaped windows in the gray shale associated with massive coal balls at Old Ben Mine No. 24 (fig. 18; Part 1, fig. 9) makes it prohibitively expensive to delineate them by exploratory drilling.

Most vulnerable to massive coal balls is the longwall mining system: the face must advance no matter what obstacles are present in the panel. In Illinois, support entries are first developed around longwall panels for mining on retreat, so ample time exists to map the roof of the future panel. As data are accumulated and evaluated by means of the Old Ben 24 model, mine plans may be altered to avoid probable coal-ball areas as well as identify potential roof control problems.

The model may also be extended to other areas of Herrin Coal with transitional roof (fig. 33). As noted previously, the Clarkson Mine (Washington County) has a roof similar to that of the Old Ben Mine No. 24, but perhaps with a

different distribution of the dark gray, fossiliferous shale. In areas of transitional roof south and east of the Old Ben sites, a number of type II coal-ball sites have been found, particularly in the Sahara Mine No. 6 and the Amax Delta mine. In these mines the ratio of Anna Shale/Brereton Limestone roof to Energy Shale roof is higher than at the Old Ben mines. Although the Old Ben 24 model may still apply, the more extensive erosion of the Energy Shale may make it more difficult to identify linear, eroded areas. Also, the model may not apply to areas never completely covered by Energy Shale.

Fluvial mud deposits on the Herrin Coal, like those at Old Ben Mine No. 24, are known to exist at several locations along the Walshville channel (fig. 33) and channels of similar origin associated with other coals in the Illinois Basin (Treworgy and Jacobson, in press). These are potential sites for transitional roof and thus coal balls.

Our model for formation of type II coal balls does not depend on marine conditions; the windows in the original cover might be filled with nonmarine sediments. Massive coal balls, which may be similar to type II areas, have been reported from nonmarine rock sequences in both the USSR and Australia.

Review of Literature on Coal Balls

Paleobotanists and geologists have studied coal balls for a long time. Stopes and Watson (1909) in England and Kukuk (1909) in Germany recognized that these concretions preserved peat at an early stage of coal seam formation. Both studies found that roots of succeeding plants penetrated previously deposited peat composed predominantly of aerial plant material. Coal balls formed in place of autochthonous peat; they were not formed elsewhere and subsequently deposited in the peat.

A definite association of coal balls with marine roof shales was noted by early researchers. Stopes and Watson (1909) found coal balls under marine shale roof and not under freshwater sediments (fig. 34). They thought the carbonate

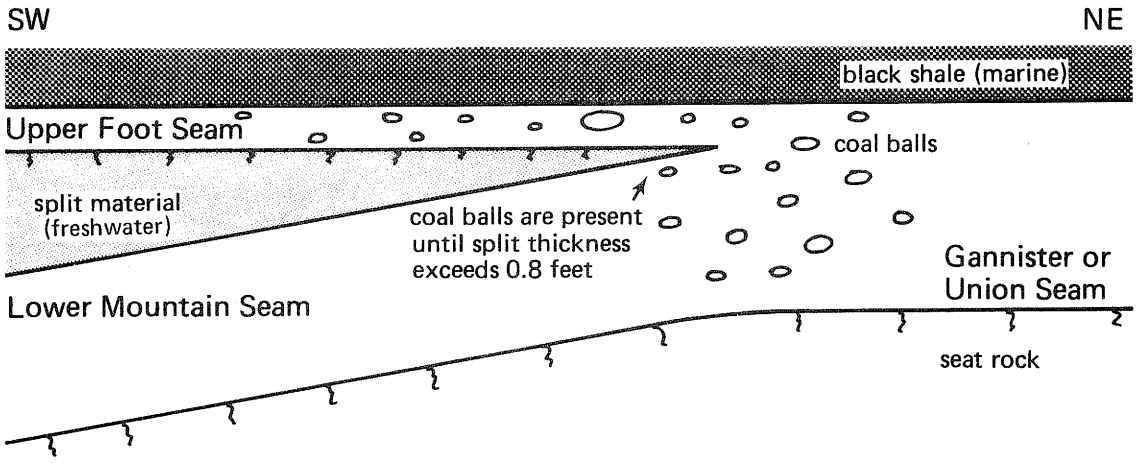

Figure 34
Distribution of coal balls in the Upper Foot and Gannister Coals in Lancashire, England (Watson, 1907; Stopes and Watson, 1909). Coal balls formed only in areas below marine roof.

was primarily derived from decaying plants and became fixed as a result of sulfate reduction. Seawater provided a large pool of Ca and Mg and permitted the formation of coal balls over a long time. Kukuk (1909) noted that while two seams with a marine roof had coal balls, other seams with a marine roof had none. He suggested coal balls may have been associated with a particular facies of marine roof, since he found certain fossils and roof concretions together with coal balls.

Cady and Schopf performed the earliest detailed examination of coal balls in the Herrin Coal during research at the Clarkson Mine in Nashville, Illinois. Cady (1936b) described the coal and roof units and Schopf (1938) studied the coal balls. Schopf (1938) believed the Stopes and Watson model was applicable to the Nashville sites and also that coal balls were formed in situ during the peat stage.

Cady and other investigators (1936a, 1940) noted that coal balls were associated with neither the gray Energy Shale nor the black Anna Shale, but a roof of dark gray, very argillaceous limestone or calcareous shale of marine origin (fig. 35). The original notes from the Clarkson Mine show this material also occurred as channel fill, just at Old Ben Mine No. 24. Photos and descriptions in a paper by Cady et al. (1940) show depositional sequences in the roof similar to those as at Old Ben Mine No. 24. Both mines have Anna Shale deposited on the eroded Energy Shale surface or directly on the coal where the Energy Shale is absent. Specifically, the coal balls in the Clarkson Mine were all found in the top 3 feet of the coal seam, probably a type I occurrence.

Evans and Amos (1961) visited three coal-ball sites in the Sahara Coal Company Mine No. 6 in the Herrin Coal in southern Illinois. Because of the bowl or funnel shape of some massive coal-balls deposits, they speculated that blow wells--hydrologically connected to the sea through the sandstone unit below the underclay--had excavated (eroded) funnel-shaped areas of peat 9.5 to 171 feet across. The carbonate-laden waters of the blow well rotated the eroded peat, forming the coal balls. Also, the coal balls were supposed to be supported and rotated by water pressure, so that a humic coating, which later turned to coal, could be deposited around the coal balls. Yet the authors show that even under these great water pressures, the 2- to 3-foot thick underclay between the sandstone and coal seam remained intact. Although Evans and Amos state that the coal-ball sites had a marine shale roof, no detailed descriptions of the geologic settings were given.

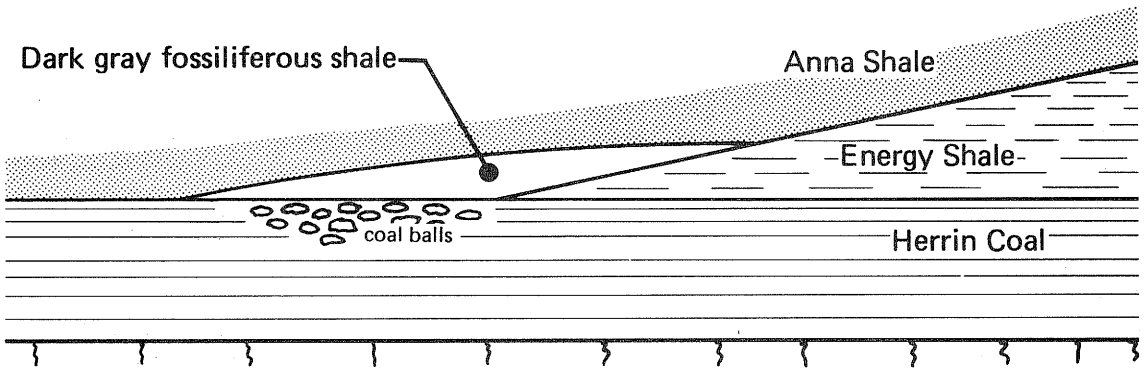

Figure 35
Coal-ball locations in Clarkson Mine (Cady, 1936a; Cady et al., 1940). Coal balls are found only under dark gray, fossiliferous shale.

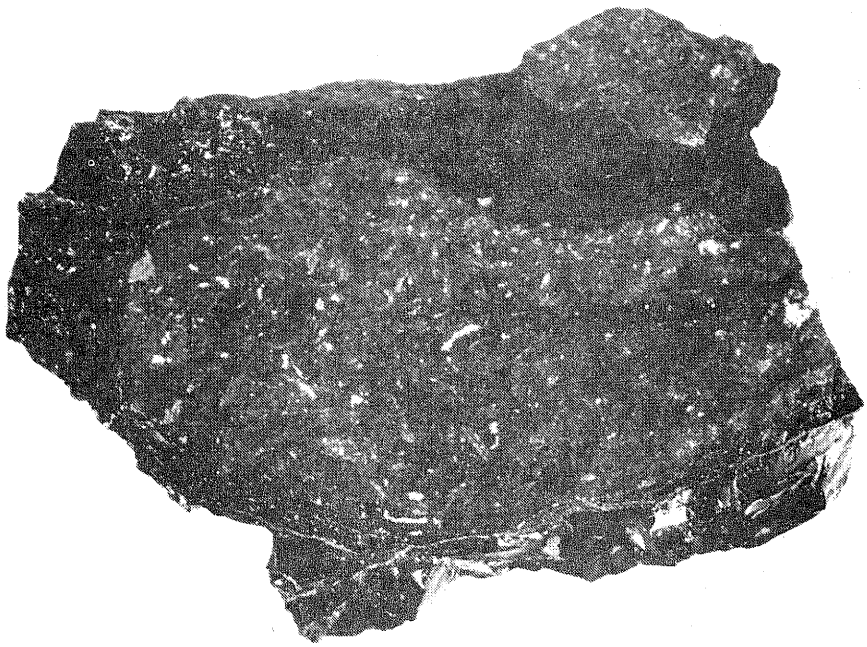

Figure 36
Bioturbation trace surrounded by coal from the top of the Herrin Coal (sample LW-B-5). Original orientation unknown. (1.3 x)

Many coal-ball studies have been conducted by individuals primarily interested in the plant assemblages preserved in the coal balls and the swamp ecology they reflect (Phillips, Kunz, and Mickish, 1977; Phillips and DiMichele, 1981). Phillips, Kunz, and Mickish (1977) developed a coal-ball model based on four study sites in the Herrin Coal, including both the Sahara Coal Company Mine No. 6 and the Amax Delta Mine. Their model assumes coal-ball sites were relative lows within the swamp, so that permineralization occurred whenever carbonate was introduced into the swamp, either from freshwater or marine sources. Unfortunately, the majority of coal ball sites used in these studies were in strip mines, where it is very difficult to relate the spatial association of coal balls to roof type. It is difficult, therefore, to compare this model with the model developed at Old Ben Mine No. 24.

Mixed Coal Balls

Mamay and Yochelson (1962) differentiated four types of coal balls: normal (plants only), mixed heterogeneous (plants and animals, segregated), mixed homogeneous (plants and animals, mixed), and faunal (animal fossils only). They recognized mixed coal balls for the first time, identifying the marine components in detail. After considering and rejecting a burrowing mechanism, they offered a "mud roller" hypothesis for the origin of mixed coal balls. They speculated that during storms marine mud might have been carried onshore and deposited in recesses in the peat. Even within the context of their paleoenvironmental scenario, however, it is difficult to picture a marine mud ball entering a slightly compacted peat, and the limestone mud remaining undissolved in the acidic environment of the living swamp.

We believe bioturbation produced the mixed coals and "faunal" coal balls observed in Franklin County. Burrowing traces produced by a marine

organism begin at the base of the Brereton Limestone, extend into and through the Anna Shale, and occasionally into the top of the Herrin Coal (fig. 36). These traces of 1 to 2 inches in diameter were found up to 1.5 feet below the Brereton, extending as much as 5 feet horizontally. In Tazewell County, Smith et al. (1970) illustrated similar traces at the base of the Oak Grove Limestone. If these burrows were filled with marine mud and found in a coal seam, they would be considered "faunal" coal balls by Mamay and Yochelson. However, we do not consider these "faunal" coal balls to be legitimate because they contain no permineralized peat. In contrast, mixed coal balls contain permineralized peat, although the nucleation for peat permineralization is clearly different than for normal coal balls, which have no obvious core.

CONCLUSIONS

Coal balls in the Herrin Coal are predictable at two distinct levels: Generally; they are associated with Anna Shale/Brereton Limestone roof in transitional roof areas; transitional roof can be identified from typical drill-hole densities used (1 to 2 holes/mi^2) during exploration. Specifically, the type II coal-ball areas that cause mining problems are located under a linear exposure of Anna Shale/Brereton Limestone roof at Old Ben Mine No. 24. Preliminary evidence suggests similar linear exposures may be linked to type II coal-ball areas found elsewhere. These linear exposures can be mapped in mine without difficulty.

A depositional model explains the distribution of coal balls at Old Ben Mine No. 24. In this model, freshwater sediments covered the top of the peat, sealing it. Continued decomposition of the peat produced high partial CO_2 pressures in the sealed peat. Selective erosion of the cover by river waters containing Ca and Mg ions flushed out the organic acids and increased the pH; as the CO_2 outgassed, the equilibrium shifted toward carbonate precipitation, which created coal balls. Later, marine mud was deposited on both freshwater sediments and exposed peat, producing the association of coal balls and marine shale roof. This model may apply to other coal-ball sites.

RECOMMENDATIONS

In-mine mapping located type II coal balls under specific linear exposures of Anna Shale/Brereton Limestone roof. Ideally, these linear exposures could be identified during the development of main entries, so that panel layout (especially longwall panels) could avoid areas of maximum risk. Further mapping around coal-ball areas is needed to broaden the data base.

Further geochemical work may lead to advances in prediction of coal balls; their stratigraphic setting is now largely known. To refine the depositional model, the critical ranges of partial CO_2 pressures and pH values as well as the availability of calcium for carbonate precipitation should be determined. The timing of coal-ball formation relative to pyrite generation needs to be examined, as does the problem of when dolomite formed in the coal balls. Further analysis of coal-ball mineralogy by petrography is also needed. Finally, the association of type II coal-ball areas with certain segments of the linear exposures should be investigated. Under marine roof in coal-ball locations, the peat at the top of the seam may show distinct geochemical differences; samples from adjacent sites should be checked. Analysis of top benches instead of full channel samples may accentuate these differences and aid in evaluating the utility of this information for predicting coal-ball areas.

At other coal-ball sites in Illinois, some geochemical, isotopic, and/or paleobotanical work has been performed. No detailed geological evaluations have been made. Geologic mapping in these areas and other areas of known transitional roof is needed to test the capability of the model to predict coal balls.

REFERENCES

Anderson, T., M. E. Brownlee, and T. L. Phillips, 1980, A Stable isotope study on the origin of permineralized peat zones in the Herrin Coal: Journal of Geology, v. 88, p. 713-722.

Berner, R. A., 1971, Principles of Chemical Sedimentology, McGraw-Hill, New York, 240 p.

Cady, G. H., 1936a, The occurrence of coal balls in No. 6 coal bed of Nashville, Illinois - Draft versions: Illinois State Geological Survey unpublished manuscript no. 48.

Cady, G. H., 1936b, The occurrence of coal balls in No. 6 coal bed at Nashville, Illinois: Transactions, Illinois Academy of Science, v. 29, no. 2, p. 157-158.

Cady, G. H., L. C. McCabe, J. M. Schopf, and C. C. Ball, 1940, Report on the Herrin (No. 6) Coal at Nashville, Washington County, Illinois: Illinois Geological Survey unpublished manuscript no. 49, copy 2, p. 83.

Cahill, R. A., 1981, Geochemistry of Recent Lake Michigan Sediments, Illinois State Geological Survey Circular 517, 94 p.

Chou, C.-L., R. A. Cahill, R. R. Ruch and R. D. Harvey, 1982, Geochemistry of a Bituminous Coal Seam in Illinois (Abstract): Transactions American Nuclear Society, v. 41, p. 187-188.

Damberger, H. H., W. J. Nelson and H.-F. Krausse, 1980, Effects of geology on roof stability in room-and-pillar mines in the Herrin (No. 6) Coal of Illinois, in Proceedings: First Conference on Ground Control problems in the Illinois Coal Basin, Southern Illinois University, Carbondale, Illinois, June 1980, Yoginder P. Chugh and A. Van Besien (eds.) p. 14-32; also Illinois State Geological Survey Reprint 1980P.

DeMaris, P. J., 1982, Erosional channels in the Herrin (No. 6) Coal at Old Ben No. 24 Mine, Franklin County, Illinois: Abstracts with Programs North-Central Section of the Geological Society of America, April 1982, p. 258.

Elderfield, H., J. M. Gieskes, P. A. Baker, R. K. Oldfield, C. J. Hawkesworth, and R. Miller, 1982, $^{87}Sr/^{86}Sr$ and $^{18}0/^{16}0$ ratios, interstitial water chemistry and diagenesis in deep-sea carbonate sediments of the Ontong Java Plateau, Geochimica et Cosmochimica Acta, v. 46, p. 2259-2268.

Evans, W. D., and D. H. Amos, 1961, An example of the origin of coal balls, Proceedings of Geologist's Association, London, v. 72, part 4, p. 445-454.

Garrels, R. M., and C. L. Christ, 1965, Solutions, Minerals, and Equilibria, Freeman, Cooper and Company, San Francisco, 450 p.

Givens, T. J., 1968, Paleoecology and environment of deposition of part of the Brereton and Jamestown Cyclothems (Middle Pennsylvanian) of Williamson County, Illinois: Southern Illinois University Master's thesis, Carbondale, 184 p.

Gluskoter, H. J., R. R. Ruch, W. G. Miller, R. A. Cahill, G. B. Dreher, and J. K. Kuhn, 1977, Trace elements in coal: Occurrence and distribution: Illinois State Geological Survey Circular 499, 154 p.

Harvey R. D., R. A. Cahill, C.-L. Chou and J. D. Steele, 1983, Mineral matter and trace elements in the Herrin and Springfield Coals, Illinois Basin Coal Field: Final Report to U.S. Environmental Protection Agency, Grant R806654, Illinois State Geological Survey Contract/Grant Report 1983-4, 162 p.

Heckel, P. H., 1977, Origin of phosphatic black shale facies in Pennsylvanian cyclothems of mid-continent North America: AAPG Bulletin, v. 61, p. 1045-1068.

Johnson, P. R., 1979, Petrology and environments of deposition of the Herrin (No. 6) Coal Member, Carbondale Formation, at the Old Ben Coal Company Mine No. 24, Franklin County, Illinois: University of Illinois Master's thesis, Urbana-Champaign, 169 p.

Johnson, D. O., 1972, Stratigraphic analysis of the interval between the Herrin (No. 6) Coal and the Piasa Limestone in southwestern Illinois: University of Illinois Ph.D. dissertation, Urbana-Champaign, 105 p.

Kinsman, D. J., 1969, Interpretation of Sr^{+2} concentrations in carbonate minerals and rocks: Journal of Sedimentary Petrology, v. 39, no. 2, p. 486-508.

Krausse, H.-K., H. H. Damberger, W. J. Nelson, S. R. Hunt, C. T. Ledvina, C. G. Treworgy, and W. A. White, 1979, Engineering study of structural geologic features of the Herrin (No. 6) Coal and associated rock in Illinois: Contract Report for U.S. Bureau of Mines, Contract No. H0242017, p. 205.

Kukuk, P., 1909, Concerning peat dolomites in the seams of the lower Rhine-Westphalian bituminous coal deposit: Glueckauf, Berg-und Huettenmaennische Zeitschrift, Nr. 32, p. 1137-1150. (German).

Lorens, R. B. 1981, Sr, Cd, Mn and Co distribution coefficients in calcite as a function of calcite precipitation rate: Geochemica et Cosmochimica Acta, v. 45, p. 553-561.

Mamay, S. S., and E. L. Yochelson, 1962, Occurrence and significance of marine animal remains in american coal balls: U.S. Geological Society Professional Paper 354-I.

Phillips, T. L., and W. A. DiMichele, 1981, Paleoecology of Middle Pennsylvanian age coal swamps in southern Illinois -- Herrin Coal Member at Sahara Mine No. 6, in Paleobotany, Paleoecology, and Evolution, Karl J. Niklas (ed.), Praeger, New York, 297 p.

Phillips, T. L., A. B. Kunz, and D. J. Mickish, 1977, Paleobotany of permineralized peat (coal balls) from the Herrin (No. 6) Coal member of the Illinois Basin, in P. H. Given and A. D. Cohen (eds.), Interdisciplinary Studies of Peat and Coal Origins: Geological Society of America Microform Publication 7, p. 18-49.

Rao, C. Prasada, 1979, Origin of coal balls of the Illinois Basin: Illinois State Geological Survey unpublished manuscript no. 2.

Schopf, J. M., 1938, Coal balls as an index to the constituion of coal: Transactions, Illinois Academy of Science, v. 31, p. 187-189; reprinted as Illinois State Geological Survey Circular 51, 1939.

Schopf, T. J. M., 1980, Paleoceanography, Harvard University Press, Cambridge, Massachusetts, 341 p.

Smith, W. H., R. B. Nance, M. E. Hopkins, R. G. Johnson and C. W. Shabica, 1970, Depositional environments in parts of the Carbondale Formation -- western and northern Illinois: Illinois State Geological Survey Guidebook Series No. 8, p. 10-11.

Stopes, M. C., and D. M. S. Watson, 1909, On the present distribution and origin of the calcareous concretions in coal seams, known as "coal balls": Philosophical Transaction of the Royal Society of London, Series B, v. 200, London, p. 167-218.

Teichmuller, R., 1955, Sedimentation und Setzung im Ruhrkarbon: Neues Jahrbuch fur Geologie und Palaeontologie Mh. 4., p. 145-168.

Treese, T. N., R. M. Owen, and B. H. Wilkinson, 1981, Sr/Ca and Mg/Ca ratios in polygenetic carbonate allochems from a Michigan marl lake: Geochemica et Cosmochimica Acta, v. 45, p. 439-445.

Treworgy, C. G., and R. J. Jacobson (in press), Paleoenvironments and distribution of low-sulfur coal in Illinois: Compte Rendu, IX-ICC.

Watson, D. M. S., 1907, The formation of coal-balls in the coal measures: Manchester Geological and Mining Society, Transactions v. 30, p. 135-137.

Weber, J. N., and M. L. Keith, 1962, Carbon-isotope composition and the origin of calcareous coal balls: Science, v. 138, p. 900-902.

Wedepohl, K. H., 1978, Handbook of Geochemistry, Vol. II/2 and II/4, Springer Verlag, Berlin, West Germany.

Woodland, B. G., and C. K. Richardson, 1975, Time factors of differentially preserved wood in two calcitic concretions in Pennsylvanian black shale from Indiana: Fieldiana, Geology, v. 33, No. 10, p. 179-192.

Zangerl, R., and E. S. Richardson, Jr., 1963, The paleoecological history of two Pennsylvanian black shales: Fieldiana, Geology Memoirs Volume, v. 4, Chicago Natural History Museum, 352 p.

Zaritsky, P. V., 1975, On thickness decrease of parent substance of coal: Seventh International Congress of Carboniferous Stratigraphy and Geology, Compte Rendu, v. 4, p. 393-397.

APPENDIX A. Geochemistry Sample Reference List

C#	Sample #	Description
C21533	LW-H-5	Coal ball, pyritic; near top of Herrin Coal
C21634	LW-B-2C	Coal ball; upper of 2 from midseam block
C21535	LW-J-10	Energy Shale; light gray near contract with Herrin Coal
C21536	LM-S-32	Anna Shale; 0.2' above contact and just above calcite/apatite band
C21537	LW-V-3	Brereton Limestone - roughly middle of unit
C21538	LM-C-01	Herrin Coal; top 0.65' under Brereton roof
C21539	LM-W-13	"Blue band," rather carbonaceous, under Anna roof
C21540	LM-Z-09	Underclay, top 0.15', under Anna roof
C21557	19582B	Coal ball, composite section[1], tissue specific; partial anal. - see C21572 (Zone BB4)
C21558	22379B	Coal ball, composite section, tissue specific; partial anal. - see C21573 (Zone 3)
C21559	22388D	Coal ball, composite section, tissue specific; partial anal. only (Zone 3)
C21560	22403D	Coal ball, composite section, tissue specific, middle c.b.; partial anal. - see C21574 (Zone 4)
C21561	22403D	Coal ball, composite section, tissue specific, bottom c.b.; partial anal. only (Zone 4)
C21562	19576B	Coal ball, composite section, tissue specific; partial anal. - see C21575 (Zone BB4)
C21563	22453B	Coal ball, composite section, tissue specific; partial anal. only (Zone 9A)
C21564	19541C	Coal ball, composite section, tissue specific; partial anal. only (Zone 17/18)
C21565	22362B	Coal ball, composite section, tissue specific; partial anal. only (Zone 20)
C21566	19478C	Coal ball, composite section, tissue specific; partial anal. only (Zone 12)
C21567	19526C	Coal ball, composite section, tissue specific; partial anal. - see C21576 (Zone 16)
C21568	LW-C-4B	Coal ball, upper third of seam, tissue specific

APPENDIX A. continued

C#	Sample #	Description
C21569	22600E	Coal ball from top coal over mid-seam c.b.'s
C21570	LW-A-1	Coal ball from mid-seam, pyritic at base; coal traces present in sample
C21571	LW-K-1	Coal ball from top coal, isolated
C21572	19582B	Coal ball, composite section, tissue specific (Zone BB4)
C21573	22379B	Coal ball, composite section, tissue specific (Zone 2)
C21574	22403D	Coal ball, composite section, tissue specific (Zone 4)
C21575	19576B	Coal ball, composite section, tissue specific (Zone BB4)
C21576	19526C	Coal ball, composite section, tissue specific (Zone 16)
C21581	LW-H-7	Coal ball under erosional channel tissue specific, coal traces present in sample
C21582	19557	Coal ball below blue band, very pyritic, composite section (Zone BB2)
C21583	LW-N-2	Coal ball in erosional channel (also C.B. 22928)
C21584	LW-Z-7	Coal ball in erosional channel, trace of exterior clastics in sample
C21585	22067F	Coal ball in top coal, fusainized, tissue specific, probably sub-adjacent to C21690
C21586	22062B	Coal ball in top coal, pyritic and small, isolated
C21587	OR3-C-3	Coal ball from upper part of deposit, traces only of coal and secondary calcite in sample
C21588	OR3-C-2	Coal ball from lower part of deposit, traces only of coal and secondary calcite in sample
C21589	OR6-C-5	Dolomitic material in coal, some coal in sample
C21590	22067F	Dolomitic material in coal, some coal in sample. Probably super adjacent to C21585
C21591	LW-E-3	Coal ball, silicate permineralization of fusain
C21626	C2-M-12	Limestone (Brereton)
C21627	LW-T-3A	Argillaceous limestone from an erosional channel

APPENDIX A. continued

C#	Sample #	Description
C21628	LW-H-5	Concretion from Anna Shale
C21629	LW-T-16	Concretion from Anna Shale
C21630	LW-S-7	Black (Anna) shale, upper portion
C21631	OR-6-D-2	Dark gray shale; carb. facies of Energy Shale
C21632	C2-N-10	"Blue band," coaly, from Herrin Coal
C21633	C2-N-12	Shale parting in Herrin Coal
C21634	OB27-A-2	Channel-fill material; medium gray shale
C21635	LW-T-11	Black (Anna) shale, basal portion
C21652	C2-M-11B	Black (Anna) shale, top
C21653	C2-M-11C	Black (Anna) shale, middle
C21654	C2-M-11D	Black (Anna) shale, bottom
C21655	C2-M-13	Light gray (Energy) shale
C21656	LW-T-12	Black (Anna) shale, top (partial anal. only)
C21657	C2-L-12A	Coal from Anvil Rock channel (partial anal. only)
C21658	C2-F-6	Coal from Anvil Rock channel
C21659	26524C	Argillaceous Limestone with permin. plants
C21660	LM-W-2	"Blue band" of Herrin Coal under coal balls
C21661	LM-PW-1	"Blue band" of Herrin Coal under Energy roof
C21662	LM-PZ-1A	Underclay, 2-4" deep (under Energy roof)
C21663	LM-PZ-1B	Underclay, 10-12" deep (under Energy roof)
C21664	C2-0-1	"Blue band" from Herrin Coal (under Energy roof)
C21665	C2-0-2	Shale parting from Herrin Coal, mid-seam
C21666	C2-0-3	Shale parting from Herrin Coal, B2/B3 marker
C21721		Face channel coal, Anna roof (Site F)

APPENDIX A. continued

C#	Sample #	Description
C21722		Face channel coal, Energy roof (Site S)
C21758	OB26-A-5	Coal-ball from top coal
C21759	OB26-A-8	Black (Anna) shale; roof over C21721
C21760	OB26-A-12	Argillaceous limestone from an erosional channel
C21761	OB26-A-16B	Anna Shale concretion formed on limestone filled trace
C21762	OB26-A-20	"Blue band" of Herrin Coal
C21763	OB26-A021	Channel-fill material (shale)
C21764	OB26-A-26	Energy Shale; roof over C21722
C21765	1893	Silicate "coal ball" (apparently of late mineralization)
C21766	C2-K-11	Dolomitic material in coal, some coal in sample
C21767	LW-S-5	Brereton limestone
C21768	LW-W-2	Channel-fill material (impure coal)

[1]Composite Section means the combination of coal-ball vertical sections 3 and 5 (which do not overlap), and thus extends from slightly below the blue band to near the top of the seam.

APPENDIX B. Analyses of Coal Balls and Similar Materials

LAB.NO.	GEOL.NO.	SIO2	AL203	CAO	FE203	TIO2	MGO	K20	NA20	P205
C21533	LW-H-5	0.73%	1.11%	20.51%	37.29%	0.08%	0.81%	50 PPM	400 PPM	0.05%
C21534	LW-B-2C	0.73%	0.79%	54.03%	1.06%	0.08%	3.93%	50 PPM	400 PPM	0.14%
C21557	19582B	1.1 %	<0.02%	51.35%	1.3 %	<0.08%	5.6 %	38 PPM	150 PPM	0.14%
C21558	22379B	<0.02%	<0.02%	50.8 %	2.4 %	<0.08%	3.3 %	43 PPM	516 PPM	0.02%
C21559	223880	2.1 %	<0.02%	53.2 %	1.1 %	<0.08%	2.8 %	106 PPM	1260 PPM	0.07%
C21560	224030	<0.02%	<0.02%	53.7 %	0.4 %	<0.08%	3.1 %	70 PPM	865 PPM	0.09%
C21561	224030	1.1 %	<0.02%	43.1 %	9.1 %	<0.08%	3.3 %	52 PPM	690 PPM	0.02%
C21562	19576B	1.3 %	0.6 %	24.5 %	31.3 %	<0.08%	1.3 %	67 PPM	540 PPM	0.07%
C21563	22453B	1.1 %	<0.02%	48.8 %	5.9 %	<0.08%	13.0 %	35 PPM	330 PPM	0.07%
C21564	19541C	0.4 %	<0.02%	51.5 %	0.6 %	<0.08%	5.0 %	47 PPM	290 PPM	<0.02%
C21565	22362B	1.7 %	<0.02%	51.3 %	1.7 %	<0.08%	4.5 %	59 PPM	530 PPM	0.07%
C21566	19478C	1.1 %	<0.02%	51.5 %	3.1 %	<0.08%	3.3 %	20 PPM	320 PPM	<0.02%
C21567	19526C	0.8 %	<0.02%	53.3 %	0.3 %	<0.08%	4.0 %	55 PPM	577 PPM	0.02%
C21568	LW-C-4B	<0.02%	<0.02%	38.8 %	17.9 %	<0.08%	1.6 %	<12 PPM	500 PPM	0.02%
C21569	22600E	1.5 %	<0.02%	49.2 %	4.1 %	<0.08%	2.6 %	49 PPM	820 PPM	0.07%
C21570	LW-A-1	<0.02%	<0.02%	45.7 %	8.3 %	<0.08%	3.0 %	40 PPM	580 PPM	0.04%
C21571	LW-K-1	0.8 %	<0.02%	52.5 %	1.4 %	<0.08%	3.8 %	60 PPM	674 PPM	0.07%
C21572	19582B			51.4%	1.16%					
C21573	22379B			49.32%	2.77%					
C21574	224030			52.05%	1.09%					
C21575	19576B			49.32%	2.70%					
C21576	19526C			52.05%	1.86%					
C21581	LW-H-7	0.43%	<0.02%	47.01%	8.15%	<0.08%	1.33%	33 PPM	280 PPM	0.23%
C21582	19557	2.14%	<0.02%	37.64%	16.73%	<0.08%	1.33%	58 PPM	300 PPM	0.05%
C21583	LW-N-2	2.35%	0.76%	42.68%	11.15%	<0.08%	2.60%	660 PPM	400 PPM	0.14%
C21584	LW-Z-7	12.41%	1.89%	23.09%	25.45%	0.07%	1.16%	2390 PPM	1100 PPM	0.09%
C21585	22067F	0.86%	<0.02%	42.96%	6.86%	<0.08%	4.31%	<10 PPM	200 PPM	0.11%
C21586	22062B	<0.02%	<0.02%	22.11%	25.16%	<0.08%	8.45%	<10 PPM	140 PPM	0.02%
C21587	OR3-C-3	0.43%	<0.02%	46.45%	2.86%	<0.08%	5.64%	63 PPM	1400 PPM	0.07%
C21588	OR3-C-2	2.14%	<0.02%	47.29%	2.43%	<0.08%	3.15%	130 PPM	690 PPM	0.05%
C21589	OR6-C-5	6.85%	2.46%	21.83%	4.15%	0.10%	11.94%	3330 PPM	1270 PPM	0.14%
C21590	22067F	0.21%	<0.02%	48.55%	3.72%	<0.08%	1.49%	70 PPM	200 PPM	0.09%
C21591	LW-E-3	69.75%	<0.02%	<0.10%	3.29%	<0.08%	0.16%	84 PPM	500 PPM	0.05%
C21758	OB26-A-5	2.1 %	<0.2 %	50.5 %	3.3 %	<0.2 %	3.3 %	300 PPM	700 PPM	<0.2 %
C21765	1893	88.6 %	0.2 %	0.2 %	0.8 %	<0.2 %	<0.2 %	200 PPM	540 PPM	<0.2 %
C21766	C2-K-11	2.1 %	0.6 %	16.1 %	4.0 %	<0.2 %	9.4 %	470 PPM	960 PPM	<0.2 %

LAB.NO.	GEOL.NO.	MNO		CO2	TOT C	ORG C	TOT S	H2O	LOI	IN RES	AG
C21533	LW-H-5	520	PPM	15.65%	6.39%	2.12%	18.33%	0.40%	22.89%		<0.04PPM
C21534	LW-B-2C	850	PPM	43.62%	12.83%	0.93%	0.03%	0.25%	44.88%		<0.04PPM
C21557	19582B	509	PPM								<0.05PPM
C21558	22379B	478	PPM								<0.05PPM
C21559	22388D	1042	PPM								<0.05PPM
C21560	22403D	806	PPM								<0.05PPM
C21561	22403D	555	PPM								<0.05PPM
C21562	19576B	740	PPM								<0.05PPM
C21563	22453B	429	PPM								<0.05PPM
C21564	19541C	323	PPM								<0.05PPM
C21565	22362B	352	PPM								<0.05PPM
C21566	19478C	356	PPM								<0.05PPM
C21567	19526C	440	PPM								<0.05PPM
C21568	LW-C-4B	1033	PPM	30.69%	10.94%	2.56%	13.80%	0.30%	31.06%	19.33%	<0.3 PPM
C21569	22600E	1020	PPM	39.27%	13.28%	2.56%	3.45%	0.30%	38.96%	5.42%	<0.3 PPM
C21570	LW-A-1	1007	PPM	35.00%	13.39%	3.84%	6.52%	0.30%	37.24%	8.89%	<0.3 PPM
C21571	LW-K-1	1343	PPM	41.16%	12.74%	1.51%	0.86%	0.10%	42.40%	1.72%	<0.3 PPM
C21572	19582B			42.98%	12.75%	1.02%	0.13%	0.10%	44.33%	0.16%	
C21573	22379B			38.32%	16.82%	6.36%	2.24%	0.10%	43.21%	3.41%	
C21574	22403D			40.84%	14.32%	3.17%	0.55%	0.30%	43.77%	1.37%	
C21575	19576B			38.57%	14.57%	4.04%	1.80%	0.40%	40.62%	5.67%	
C21576	19526C			41.38%	13.72%	2.43%	0.93%	0.40%	42.69%	1.43%	
C21581	LW-H-7	556	PPM	35.64%	12.65%	2.90%	6.26%	0.1 %	36.77%		<0.2 PPM
C21582	19557	146	PPM	29.35%	10.98%	2.95%	13.63%	0.3 %	31.95%		<0.2 PPM
C21583	LW-N-2	400	PPM	32.86%	10.09%	1.07%	8.68%	0.6 %	33.62%		<0.2 PPM
C21584	LW-Z-7	564	PPM	17.33%	6.55%	1.80%	20.73%	0.6 %	24.48%		<0.2 PPM
C21585	22067F	2760	PPM	37.40%	15.92%	5.68%	4.30%	0.3 %	40.14%		<0.2 PPM
C21586	22062B	2120	PPM	27.37%	8.80%	1.30%	17.89%	0.4 %	27.23%		<0.2 PPM
C21587	OR3-C-3	1500	PPM	42.48%	13.22%	1.48%	0.19%	1.0 %	45.09%	0.49%	<0.2 PPM
C21588	OR3-C-2	1250	PPM	38.57%	15.03%	4.37%	0.87%	0.2 %	44.30%	2.51%	<0.2 PPM
C21589	OR6-C-5	880	PPM	30.77%	23.73%	15.24%	1.22%	1.3 %	49.78%	10.64%	<0.2 PPM
C21590	22067F	660	PPM	37.56%	17.02%	6.68%	2.11%	0.6 %	44.39%		<0.2 PPM
C21591	LW-E-3	22	PPM		21.87%	21.87%	2.55%	0.5 %	25.27%		<0.2 PPM
C21758	OB26-A-5	1930	PPM	30.97%	13.11%	4.66%	1.99%	0.20%	39.55%		<0.2 PPM
C21765	1893	27	PPM	<0.1 %	13.02%	13.02%	1.11%	0.75%	18.23%		<0.2 PPM
C21766	C2-K-11	1610	PPM	22.45%	37.22%	31.09%	2.61%	1.76%	65.40%		<0.1 PPM

APPENDIX B. continued

LAB.NO.	GEOL.NO.	AS	B	BA	BE	BR	CD	CE	CO	CR
C21533	LW-H-5	55 ppm	<28 ppm	46 ppm	1.9 ppm	2.4 ppm	<1.7 ppm	16 ppm	0.9 ppm	6 ppm
C21534	LW-B-2C	0.08ppm	<33 ppm	45 ppm	<0.04ppm	1.8 ppm	<1.5 ppm	33 ppm	0.2 ppm	2 ppm
C21557	19582B	0.2 ppm	<10 ppm	63 ppm	<5 ppm	1.5 ppm	<1.4 ppm	32 ppm	0.6 ppm	1.8 ppm
C21558	22379B	5.8 ppm	<10 ppm	43 ppm	<5 ppm	1.6 ppm	<1.4 ppm	6 ppm	0.6 ppm	0.6 ppm
C21559	22388D	0.7 ppm	<10 ppm	56 ppm	<5 ppm	3.2 ppm	<1.2 ppm	17 ppm	1.4 ppm	1.0 ppm
C21560	22403D	<0.1 ppm	<10 ppm	86 ppm	<5 ppm	2.5 ppm	<1.4 ppm	10 ppm	2.2 ppm	0.7 ppm
C21561	22403D	10 ppm	<10 ppm	1.13%	<5 ppm	2.3 ppm	<1.4 ppm	7 ppm	4.7 ppm	1.3 ppm
C21562	19576B	40 ppm	<8 ppm	64 ppm	<5 ppm	1.8 ppm	<1.2 ppm	14 ppm	15 ppm	4.3 ppm
C21563	22453B	3.4 ppm	<8 ppm	29 ppm	<5 ppm	1.2 ppm	<1.4 ppm	6 ppm	1.6 ppm	1.0 ppm
C21564	19541C	0.2 ppm	<8 ppm	48 ppm	<5 ppm	1.6 ppm	<1.4 ppm	4 ppm	0.1 ppm	0.4 ppm
C21565	22362B	1.4 ppm	<8 ppm	38 ppm	<5 ppm	1.0 ppm	<1.4 ppm	3 ppm	0.5 ppm	1.4 ppm
C21566	19478C	2.1 ppm	<8 ppm	48 ppm	<5 ppm	1.7 ppm	<1.4 ppm	1 ppm	0.4 ppm	0.8 ppm
C21567	19526C	0.1 ppm	<8 ppm	45 ppm	<5 ppm	1.4 ppm	<1.4 ppm	3 ppm	0.1 ppm	0.4 ppm
C21568	LW-C-4B	19 ppm	<10 ppm	162 ppm	<6 ppm	1.6 ppm	<1.3 ppm	18 ppm	0.2 ppm	3.4 ppm
C21569	22600E	4.0 ppm	<10 ppm	61 ppm	<6 ppm	2.6 ppm	<1.4 ppm	13 ppm	0.3 ppm	1.5 ppm
C21570	LW-A-1	7.5 ppm	<10 ppm	34 ppm	<6 ppm	1.6 ppm	<1.4 ppm	14 ppm	1.0 ppm	1.7 ppm
C21571	LW-K-1	1.1 ppm	<10 ppm	50 ppm	<6 ppm	2.0 ppm	<1.4 ppm	18 ppm	0.3 ppm	1.0 ppm
C21572	19582B									
C21573	22379B									
C21574	22403D									
C21575	19576B									
C21576	19526C									
C21581	LW-H-7	11 ppm	32 ppm	27 ppm	<6 ppm	1.9 ppm	<2.7 ppm	10 ppm	0.2 ppm	1.7 ppm
C21582	19557	17 ppm	54 ppm	33 ppm	<6 ppm	1.4 ppm	<2.7 ppm	17 ppm	7.5 ppm	2.2 ppm
C21583	LW-N-2	20 ppm	30 ppm	2674 ppm	<6 ppm	1.1 ppm	<2.7 ppm	27 ppm	2.0 ppm	8.9 ppm
C21584	LW-Z-7	55 ppm	85 ppm	1792 ppm	<6 ppm	<1 ppm	<2.5 ppm	15 ppm	3.7 ppm	19 ppm
C21585	22067F	0.8 ppm	14 ppm	40 ppm	<6 ppm	0.5 ppm	<2.7 ppm	8 ppm	0.06ppm	1.8 ppm
C21586	22062B	7 ppm	10 ppm	24 ppm	<6 ppm	0.5 ppm	<2.2 ppm	11 ppm	0.1 ppm	4.6 ppm
C21587	OR3-C-3	0.5 ppm	15 ppm	23 ppm	<6 ppm	9 ppm	<2.6 ppm	15 ppm	0.2 ppm	2 ppm
C21588	OR3-C-2	0.4 ppm	<10 ppm	59 ppm	<6 ppm	2.9 ppm	<2.5 ppm	19 ppm	0.9 ppm	6 ppm
C21589	OR6-C-5	2.8 ppm	<10 ppm	104 ppm	12 ppm	3.3 ppm	<1.7 ppm	18 ppm	2.8 ppm	14 ppm
C21590	22067F	<0.1 ppm	<10 ppm	30 ppm	<6 ppm	1.3 ppm	<2.6 ppm	15 ppm	0.1 ppm	1.1 ppm
C21591	LW-E-3	2.3 ppm	<10 ppm	19 ppm	<6 ppm	2.5 ppm	<2.0 ppm	0.4 ppm	0.2 ppm	1.0 ppm
C21758	OB26-A-5	3.2 ppm	<3 ppm	133 ppm	<3 ppm	0.8 ppm	<5 ppm	80 ppm	1.1 ppm	4.1 ppm
C21765	1893	1.9 ppm	<8 ppm	27 ppm	<2 ppm	1.2 ppm	<4 ppm	5 ppm	0.6 ppm	6.5 ppm
C21766	C2-K-11	0.7 ppm	52 ppm	21 ppm	<2 ppm	1.8 ppm	<3 ppm	9 ppm	1.4 ppm	3.4 ppm

LAB.NO.	GEOL.NO.	CS	CU	DY	EU	F	GA	GE	HF
C21533	LW-H-5	<1 ppm	11.5 ppm	1.5 ppm	0.52ppm	73 ppm	0.7 ppm	39 ppm	<0.2 ppm
C21534	LW-B-2C	0.15ppm	9.7 ppm	<1 ppm	0.25ppm	125 ppm	<0.3 ppm	<16 ppm	<0.1 ppm
C21557	19582B	0.4 ppm	15 ppm	3.1 ppm	0.32ppm	209 ppm	<1 ppm	<7 ppm	0.07ppm
C21558	22379B	<0.1 ppm	10 ppm	0.3 ppm	0.10ppm	183 ppm	<1 ppm	<7 ppm	<0.05ppm
C21559	22388D	<0.1 ppm	10 ppm	1.1 ppm	0.35ppm	175 ppm	<1 ppm	<7 ppm	
C21560	22403D	<0.1 ppm	12 ppm	0.5 ppm	0.20ppm	146 ppm	<1 ppm	<7 ppm	<0.05ppm
C21561	22403D	0.04ppm	12 ppm	0.5 ppm	0.15ppm	183 ppm	<0.5 ppm	<7 ppm	<0.1 ppm
C21562	19576B	<0.1 ppm	12 ppm	2.5 ppm	0.41ppm	195 ppm	<0.5 ppm	<5 ppm	<0.1 ppm
C21563	22453B	<0.1 ppm	15 ppm	<0.3 ppm	0.12ppm	146 ppm	<0.5 ppm	<7 ppm	<0.1 ppm
C21564	19541C	<0.1 ppm	10 ppm	0.12ppm	0.05ppm	122 ppm	<0.2 ppm	<7 ppm	<0.05ppm
C21565	22362B	<0.1 ppm	13 ppm	<0.2 ppm	0.06ppm	259 ppm	<0.1 ppm	<7 ppm	<0.1 ppm
C21566	19478C	<0.1 ppm	9 ppm	0.1 ppm	0.03ppm	58 ppm	<0.4 ppm	<7 ppm	0.1 ppm
C21567	19526C	<0.1 ppm	8 ppm	<0.3 ppm	0.04ppm	180 ppm	<0.2 ppm	<7 ppm	<0.1 ppm
C21568	LW-C-4B	<0.1 ppm	12 ppm	<0.8 ppm	0.30ppm	68 ppm	<1 ppm	<7 ppm	<0.1 ppm
C21569	22600E	<0.1 ppm	10 ppm	<1 ppm	0.24ppm	52 ppm	<1 ppm	<7 ppm	<0.1 ppm
C21570	LW-A-1	<0.1 ppm	12 ppm	<2 ppm	0.23ppm	183 ppm	<0.4 ppm	<7 ppm	<0.1 ppm
C21571	LW-K-1	<0.1 ppm	10 ppm	<0.8 ppm	0.27ppm	189 ppm	<0.4 ppm	<7 ppm	<0.1 ppm
C21572	19582B								
C21573	22379B								
C21574	22403D								
C21575	19576B								
C21576	19526C								
C21581	LW-H-7	<0.1 ppm	5 ppm	<0.4 ppm	0.07ppm	130 ppm	<0.5 ppm	<7 ppm	<0.1 ppm
C21582	19557	<0.1 ppm	7 ppm	1.3 ppm	0.4 ppm	87 ppm	0.5 ppm	<7 ppm	<0.1 ppm
C21583	LW-N-2	0.3 ppm	17 ppm	1.0 ppm	0.6 ppm	183 ppm	0.7 ppm	<7 ppm	<0.1 ppm
C21584	LW-Z-7	0.9 ppm	27 ppm	1.2 ppm	0.3 ppm	141 ppm	3 ppm	<7 ppm	0.5 ppm
C21585	22067F	<0.1 ppm	5 ppm	1.7 ppm	0.3 ppm	54 ppm	0.5 ppm	<7 ppm	<0.1 ppm
C21586	22062B	<0.1 ppm	7 ppm	0.8 ppm	0.4 ppm	35 ppm	1.9 ppm	<7 ppm	<0.1 ppm
C21587	OR3-C-3	0.1 ppm	6 ppm	2.5 ppm	0.3 ppm	76 ppm	<1 ppm	<7 ppm	<0.1 ppm
C21588	OR3-C-2	0.1 ppm	8 ppm	2.9 ppm	1.7 ppm	19 ppm	<1 ppm	<7 ppm	<0.1 ppm
C21589	OR6-C-5	1.2 ppm	12 ppm	3.1 ppm	0.9 ppm	126 ppm	3.8 ppm	<7 ppm	1.0 ppm
C21590	22067F	<0.1 ppm	6 ppm	1.9 ppm	0.5 ppm	49 ppm	<1 ppm	<7 ppm	<0.1 ppm
C21591	LW-E-3	<0.2 ppm	2 ppm	0.04ppm	0.03ppm	32 ppm	<0.5 ppm	<7 ppm	<0.1 ppm
C21758	OB26-A-5	<0.1 ppm	7 ppm	4.0 ppm	1.5 ppm	195 ppm	<0.2 ppm	<7 ppm	<0.1 ppm
C21765	1893	0.15ppm	7 ppm	0.10ppm	0.03ppm	10 ppm	0.4 ppm	<6 ppm	0.1 ppm
C21766	C2-K-11	0.5 ppm	8 ppm	0.5 ppm	0.16ppm	95 ppm	1.0 ppm	<4 ppm	0.2 ppm

APPENDIX B. continued

LAB.NO.	GEOL.NO.	IN	LA	LI	LU	MO	NI	PB	RB	SB
C21533	LW-H-5	<500 ppb	6.0 ppm	<7.1 ppm	0.45ppm	27 ppm	<20 ppm	<45 ppm	<10 ppm	0.2 ppm
C21534	LW-B-2C	<260 ppb	12 ppm	<6.4 ppm	0.1 ppm	<1 ppm	<8 ppm	53 ppm	<2 ppm	<0.1 ppm
C21557	19582B	<20 ppb	9.8 ppm	<3 ppm	0.10ppm	<2 ppm	<10 ppm	70 ppm	<0.5 ppm	<0.01ppm
C21558	22379B	<8 ppb	3.9 ppm	4 ppm	0.03ppm	<2 ppm	<10 ppm	60 ppm	<0.5 ppm	0.05ppm
C21559	22388D	<50 ppb	8.5 ppm	3 ppm	0.08ppm	<3 ppm	<10 ppm	70 ppm	<1 ppm	<0.05ppm
C21560	22403D	<100 ppb	6.5 ppm	3 ppm	0.04ppm	<2 ppm	<5 ppm	60 ppm	<1 ppm	<0.05ppm
C21561	22403D	<200 ppb	4.7 ppm	<2 ppm	0.05ppm	2 ppm	<10 ppm	110 ppm	2.5 ppm	0.1 ppm
C21562	19576B	<100 ppb	8.1 ppm	<2 ppm	0.31ppm	8 ppm	24 ppm	140 ppm	13 ppm	0.2 ppm
C21563	22453B	<20 ppb	3.1 ppm	<3 ppm	0.03ppm	<2 ppm	<10 ppm	70 ppm	<1 ppm	0.04ppm
C21564	19541C	<7 ppb	2.5 ppm	<3 ppm	0.02ppm	<2 ppm	<10 ppm	60 ppm	<1 ppm	<0.1 ppm
C21565	22362B	<20 ppb	1.4 ppm	<3 ppm	0.03ppm	<1 ppm	<10 ppm	50 ppm	<1 ppm	0.1 ppm
C21566	19478C	<10 ppb	1.3 ppm	<3 ppm	0.02ppm	<1 ppm	<10 ppm	<40 ppm	<1 ppm	0.02ppm
C21567	19526C	<100 ppb	1.5 ppm	<3 ppm	0.01ppm	5 ppm	<10 ppm	<40 ppm	<1 ppm	<0.05ppm
C21568	LW-C-4B	<400 ppb	10 ppm	<3 ppm	0.14ppm	21 ppm	<10 ppm	70 ppm	10 ppm	0.2 ppm
C21569	22600E	<100 ppb	6.8 ppm	<3 ppm	0.08ppm	<5 ppm	<10 ppm	40 ppm	<1 ppm	0.3 ppm
C21570	LW-A-1	<100 ppb	7.2 ppm	<3 ppm	0.09ppm	<3 ppm	<10 ppm	70 ppm	4 ppm	0.1 ppm
C21571	LW-K-1	<100 ppb	10.2 ppm	<3 ppm	0.06ppm	9 ppm	<10 ppm	40 ppm	<1 ppm	0.07ppm
C21572	19582B									
C21573	22379B									
C21574	22403D									
C21575	19576B									
C21576	19526C									
C21581	LW-H-7	<100 ppb	3.6 ppm	3 ppm	0.05ppm	15 ppm	<10 ppm	50 ppm	4 ppm	0.8 ppm
C21582	19557	<10 ppb	11 ppm	4 ppm	0.15ppm	<2 ppm	14 ppm	80 ppm	<2 ppm	0.1 ppm
C21583	LW-N-2	<50 ppb	11 ppm	4 ppm	0.36ppm	44 ppm	<10 ppm	50 ppm	4 ppm	3.0 ppm
C21584	LW-Z-7	<300 ppb	7.7 ppm	7 ppm	0.31ppm	51 ppm	<30 ppm	50 ppm	23 ppm	8.3 ppm
C21585	22067F	<100 ppb	6.3 ppm	4 ppm	0.16ppm	<2 ppm	<5 ppm	50 ppm	<2 ppm	<0.1 ppm
C21586	22062B	<5 ppb	4.5 ppm	3 ppm	0.31ppm	5 ppm	<10 ppm	30 ppm	<3 ppm	<0.1 ppm
C21587	OR3-C-3	<100 ppb	7.2 ppm	3 ppm	0.05ppm	<7 ppm	<10 ppm	50 ppm	<1 ppm	<0.1 ppm
C21588	OR3-C-2	<40 ppb	5.6 ppm	4 ppm	0.31ppm	<5 ppm	<15 ppm	60 ppm	<2 ppm	0.03ppm
C21589	OR6-C-5	<100 ppb	8.7 ppm	7 ppm	0.24ppm	<5 ppm	<10 ppm	40 ppm	20 ppm	<0.1 ppm
C21590	22067F	<20 ppb	8.5 ppm	3 ppm	0.13ppm	<4 ppm	<5 ppm	60 ppm	2 ppm	0.3 ppm
C21591	LW-E-3	<20 ppb	0.3 ppm	3 ppm	<0.05ppm	<4 ppm	<5 ppm	30 ppm	<1 ppm	<0.1 ppm
C21758	OB26-A-5	<800 ppb	20 ppm	<2 ppm	0.38ppm	18 ppm	<10 ppm	<19 ppm	3 ppm	0.4 ppm
C21765	1893	<10 ppb	2.5 ppm	4 ppm	<0.05ppm	19 ppm	<8 ppm	<15 ppm	<1 ppm	<0.05ppm
C21766	C2-K-11	<300 ppb	2.9 ppm	3 ppm	0.03ppm	12 ppm	<5 ppm	<15 ppm	<1 ppm	0.13ppm

LAB.NO.	GEOL.NO.	SC	SE	SM	SR	TA	TB	TH	TL	U
C21533	LW-H-5	1.3 ppm	27 ppm	2.4 ppm	228 ppm	<0.1 ppm	0.6 ppm	<0.5 ppm	17 ppm	1.0 ppm
C21534	LW-B-2C	1.9 ppm	0.5 ppm	1.3 ppm	433 ppm	<0.04ppm	0.2 ppm	0.3 ppm	<4.5 ppm	<0.1 ppm
C21557	19582B	1.8 ppm	0.4 ppm	1.8 ppm	429 ppm	<0.02ppm	0.4 ppm	0.2 ppm	<12 ppm	<0.2 ppm
C21558	22379B	0.4 ppm	4.6 ppm	0.5 ppm	677 ppm	<0.02ppm	0.05ppm	0.3 ppm	<12 ppm	<0.3 ppm
C21559	22388D	1.2 ppm	1.2 ppm	1.5 ppm	491 ppm	<0.01ppm	0.3 ppm	<0.1 ppm	<12 ppm	<0.3 ppm
C21560	22403D	0.5 ppm	0.2 ppm	0.9 ppm	510 ppm	<0.02ppm	0.1 ppm	<0.1 ppm	<12 ppm	<0.3 ppm
C21561	22403D	0.7 ppm	1.8 ppm	0.7 ppm	628 ppm	<0.02ppm	0.1 ppm	0.1 ppm	<12 ppm	1.5 ppm
C21562	19576B	2.3 ppm	6.7 ppm	1.8 ppm	283 ppm	<0.01ppm	0.3 ppm	0.1 ppm	<10 ppm	<0.2 ppm
C21563	22453B	0.6 ppm	1.0 ppm	0.6 ppm	509 ppm	<0.01ppm	0.06ppm	0.2 ppm	<10 ppm	<0.1 ppm
C21564	19541C	0.4 ppm	0.2 ppm	0.3 ppm	698 ppm	<0.05ppm	0.03ppm	0.1 ppm	<10 ppm	<0.2 ppm
C21565	22362B	0.4 ppm	1.3 ppm	0.3 ppm	828 ppm	<0.1 ppm	0.06ppm	0.2 ppm	<10 ppm	<1 ppm
C21566	19478C	0.2 ppm	0.7 ppm	0.15ppm	678 ppm	<0.05ppm	0.01ppm	<0.1 ppm	<10 ppm	<1 ppm
C21567	19526C	0.3 ppm	0.2 ppm	0.2 ppm	603 ppm	<0.02ppm	0.03ppm	<0.1 ppm	<10 ppm	<0.2 ppm
C21568	LW-C-4B	1.3 ppm	23 ppm	1.5 ppm	291 ppm	<0.05ppm	0.2 ppm	<0.05ppm	<10 ppm	1.7 ppm
C21569	22600E	0.5 ppm	6.3 ppm	1.0 ppm	369 ppm	<0.05ppm	0.15ppm	<0.1ppm	<10 ppm	<0.5 ppm
C21570	LW-A-1	1.0 ppm	6.2 ppm	1.1 ppm	433 ppm	<0.05ppm	0.15ppm	0.1 ppm	<10 ppm	<0.5 ppm
C21571	LW-K-1	0.5 ppm	1.6 ppm	1.7 ppm	511 ppm	<0.05ppm	0.2 ppm	<0.1 ppm	<10 ppm	7 ppm
C21572	19582B									
C21573	22379B									
C21574	22403D									
C21575	19576B									
C21576	19526C									
C21581	LW-H-7	0.6 ppm	38 ppm	0.6 ppm	361 ppm	<0.1 ppm	<0.1 ppm	<0.1 ppm		6.3 ppm
C21582	19557	1.8 ppm	3.8 ppm	2.0 ppm	382 ppm	<0.2 ppm	0.4 ppm	<0.5 ppm	<10 ppm	<0.5 ppm
C21583	LW-N-2	8.5 ppm	25 ppm	2.8 ppm	428 ppm	<0.1 ppm	0.4 ppm	1.0 ppm	<10 ppm	6.7 ppm
C21584	LW-Z-7	5.0 ppm	28 ppm	1.7 ppm	241 ppm	0.08ppm	0.5 ppm	2.6 ppm	<10 ppm	5.2 ppm
C21585	22067F	0.5 ppm	0.8 ppm	1.0 ppm	535 ppm	<0.1 ppm	0.2 ppm	<0.1 ppm	<10 ppm	0.6 ppm
C21586	22062B	2.5 ppm	4.1 ppm	2.0 ppm	260 ppm	<0.1 ppm	0.3 ppm	0.1 ppm	<10 ppm	1.6 ppm
C21587	OR3-C-3	0.6 ppm	0.3 ppm	1.3 ppm	300 ppm	<0.1 ppm	0.2 ppm	<0.1 ppm	<10 ppm	<0.7 ppm
C21588	OR3-C-2	9.7 ppm	0.3 ppm	6.0 ppm	324 ppm	<0.1 ppm	1.1 ppm	0.2 ppm	<10 ppm	<0.5 ppm
C21589	OR6-C-5	6.4 ppm	0.8 ppm	3.2 ppm	650 ppm	0.2 ppm	0.6 ppm	1.6 ppm	<10 ppm	11 ppm
C21590	22067F	0.5 ppm	0.4 ppm	1.8 ppm	488 ppm	<0.1 ppm	0.3 ppm	<0.1 ppm	<10 ppm	<0.6 ppm
C21591	LW-E-3	0.10ppm	0.6 ppm	0.1 ppm	<5 ppm	<0.1 ppm	0.02ppm	<0.1 ppm	<10 ppm	<0.5 ppm
C21758	OB26-A-5	6.6 ppm	2.2 ppm	7.6 ppm	408 ppm	<0.01ppm	1.1 ppm	0.7 ppm	<12 ppm	7 ppm
C21765	1893	0.4 ppm	4.8 ppm	0.2 ppm	<5 ppm	<0.1 ppm	0.03ppm	0.4 ppm	<10 ppm	1.2 ppm
C21766	C2-K-11	0.7 ppm	3.1 ppm	0.7 ppm	670 ppm	<0.1 ppm	0.1 ppm	0.5 ppm	<7 ppm	<1 ppm

APPENDIX B. continued

LAB.NO.	GEOL.NO.	V	W	YB	ZN	ZR
		PPM	PPM	PPM	PPM	PPM
C21533	LW-H-5	63	<0.5	1.0	<5	<5
C21534	LW-B-2C	<7.6	<0.3	0.4	<5	<5
C21557	19582B	<3	<0.2	0.7	10	<5
C21558	22379B	<3	<0.2	0.12	8	<5
C21559	22388D	<3	<0.2	0.4	10	<5
C21560	22403D	<3	<0.2	0.2	9	<5
C21561	22403D	<3	<0.2	0.3	6	<5
C21562	19576B	10	<0.2	0.8	7	<5
C21563	22453B	<3	<0.1	0.16	7	<5
C21564	19541C	<3	<0.1	0.07	5	<5
C21565	22362B	<3	<0.1	0.11	6	<5
C21566	19478C	<3	<0.1	0.05	8	<5
C21567	19526C	<3	<0.1	0.05	6	<5
C21568	LW-C-4B	<5	<0.1	0.62	11	<5
C21569	22600E	<5	<0.2	0.44	7	<5
C21570	LW-A-1	<5	<0.2	0.32	10	<5
C21571	LW-K-1	<5	<0.2	0.38	7	<5
C21572	19582B					
C21573	22379B					
C21574	22403D					
C21575	19576B					
C21576	19526C					
C21581	LW-H-7	<10	<0.1	0.3	15	<5
C21582	19557	<10	<0.1	0.6	17	<5
C21583	LW-N-2	<10	<0.1	1.7	17	<5
C21584	LW-Z-7	<10	<0.3	1.0	15	19
C21585	22062B	<10	<0.1	0.6	12	<5
C21586	22062B	<10	<0.2	1.2	11	<5
C21587	ORJ-C-3	<10	<0.5	0.4	16	<5
C21588	OR3-C-2	<10	<0.3	1.8	12	<5
C21589	OR6-C-5	<10	<0.2	1.1	14	43
C21590	22067F	<10	<0.2	0.8	12	<5
C21591	LW-E-3	<10	<0.5	<0.1	8	<5
C21758	OB26-A-5	<5	<0.5	2.3	7	<5
C21765	1893	<4	<0.5	0.07	16	<5
C21766	C2-K-11	<3	<0.3	0.2	4	<5

LAB.NO.	GEOL.NO.	SIO2	AL2O3	CAO	FE2O3	TIO2	MGO	K2O	NA2O	P2O5
					UNDERCLAY					
C21540	LM-Z-09	65.55%	15.85%	1.22%	2.63%	0.65%	1.04%	3.47%	.86%	0.76%
C21662	LM-PZ-1A	59.9 %	18.3 %	0.7 %	2.4 %	1.0 %	1.3 %	3.4 %	.79%	0.7 %
C21663	LM-PZ-1B	59.5 %	19.1 %	0.7 %	3.0 %	1.0 %	1.5 %	3.8 %	.95%	0.7 %
					COAL					
C21538	LM-C-01	3.27%	1.34%	1.05%	1.19%	0.06%	0.10%	.18%	.13%	0.01%
C21657	C2-L-12A	5.1 %	1.5 %	4.2 %	7.9 %	0.2 %	0.3 %	.4 %	.36%	3.2 %
C21658	C2-F-5	4.3 %	1.3 %	2.8 %	8.1 %	<0.1 %	<0.2 %	.2 %	.12%	0.5 %
C21721	OB26-1	4.5 %	1.7 %	1.0 %	2.0 %	<0.2 %	0.2 %	.21%	.14%	<0.2 %
C21722	OB26-2	4.7 %	1.7 %	0.7 %	2.7 %	<0.2 %	0.2 %	.20%	.13%	<0.2 %
					ENERGY SHALE					
C21535	LW-J-10	56.23%	18.34%	0.53%	5.62%	0.88%	1.54%	3.63%	1.77%	0.23%
C21631	OR6-D-2	52.8 %	19.3 %	0.1 %	5.7 %	0.8 %	2.0 %	3.8 %	1.05%	<0.2 %
C21655	C2-M-13	53.3 %	14.0 %	0.4 %	9.7 %	0.5 %	0.5 %	3.0 %	1.34%	0.2 %
C21764	OB26-A26	58.2 %	19.3 %	0.3 %	6.4 %	1.0 %	2.3 %	3.6 %	.80%	0.2 %
					CHANNEL FILL MATERIALS					
C21627	LW-T-3A	25.7 %	4.9 %	24.8 %	12.6 %	0.2 %	1.5 %	.9 %	.36%	<0.2 %
C21634	OB27-A-2	58.8 %	19.3 %	0.1 %	6.3 %	0.8 %	2.3 %	4.1 %	1.20%	<0.2 %
C21760	OB26-A12	39.6 %	9.6 %	12.2 %	9.6 %	0.5 %	0.5 %	1.8 %	.69%	0.2 %
C21763	OB26-A21	62.5 %	16.4 %	0.3 %	5.1 %	0.8 %	0.8 %	3.2 %	1.22%	0.2 %
C21768	LW-W-2	20.3 %	5.5 %	0.3 %	4.6 %	0.3 %	0.8 %	1.05%	.38%	<0.1 %
					ANNA SHALE					
C21536	LM-S-32	52.67%	15.36%	0.36%	4.73%	0.77%	1.04%	3.78%	1.39%	0.17%
C21630	LW-S-7	56.0 %	17.2 %	2.4 %	5.9 %	0.3 %	1.8 %	3.4 %	.91%	<0.2 %
C21635	LW-T-11	55.0 %	16.8 %	0.1 %	4.9 %	0.7 %	0.8 %	3.1 %	1.12%	<0.2 %
C21652	C2-M-11B	43.4 %	16.1 %	5.0 %	5.7 %	0.7 %	1.3 %	3.2 %	.71%	3.4 %
C21653	C2-M-11C	51.3 %	16.2 %	1.1 %	4.7 %	0.8 %	1.8 %	3.4 %	.80%	0.7 %
C21654	C2-M-11D	25.2 %	8.7 %	5.7 %	3.9 %	0.3 %	1.8 %	2.0 %	.33%	3.9 %
C21656	LW-T-12	52.2 %	15.7 %	5.2 %	5.6 %	0.8 %	1.2 %	3.3 %	.84%	0.2 %
C21759	OB26-A8	34.6 %	10.8 %	13.6 %	2.8 %	0.5 %	1.5 %	2.0 %	.56%	6.9 %
					"BLUE BAND"					
C21539	LM-W-13	53.27%	20.18%	1.87%	4.36%	1.08%	0.22%	1.87%	.58%	<0.01%
C21632	C2-N-10	26.3 %	8.9 %	0.1 %	1.7 %	0.5 %	<0.2 %	.8 %	.18%	<0.2 %
C21660	LM-W-2	55.8 %	24.6 %	0.1 %	1.6 %	1.3 %	0.2 %	1.6 %	.58%	<0.1 %
C21661	LM-PW-1	56.5 %	19.3 %	0.1 %	1.3 %	1.2 %	1.0 %	1.4 %	.47%	<0.1 %
C21664	C2-O-1	47.9 %	17.9 %	0.3 %	5.3 %	0.8 %	0.5 %	1.4 %	.37%	<0.1 %
C21762	OB26-A20	49.6 %	21.0 %	<0.2 %	1.4 %	1.0 %	0.3 %	1.5 %	.63%	<0.2 %
					OTHER SHALE PARTINGS					
C21633	C2-N-12	31.4 %	13.2 %	0.1 %	14.7 %	0.7 %	1.2 %	1.3 %	.25%	<0.2 %
C21665	C2-O-2	30.6 %	12.3 %	0.1 %	11.0 %	0.7 %	0.8 %	1.4 %	.26%	<0.1 %
C21666	C2-O-3	30.0 %	12.5 %	0.1 %	18.7 %	0.7 %	0.7 %	.8 %	.48%	<0.1 %
					LIMESTONE AND RELATED MATERIALS					
C21537	LM-V-31	9.91%	1.49%	44.80%	1.35%	0.15%	4.13%	.37%	.17%	1.67%
C21626	C2-M-12	11.3 %	2.6 %	30.6 %	4.1 %	0.2 %	13.4 %	.4 %	.17%	<0.2 %
C21659	26524C	5.1 %	1.5 %	28.8 %	11.7 %	<0.1 %	9.3 %	.2 %	.11%	0.2 %
C21767	LW-S-5	38.5 %	3.2 %	22.8 %	6.4 %	0.2 %	2.3 %	.56%	.23%	0.2 %
					ANNA SHALE CONCRETIONS					
C21628	LW-H-5	34.4 %	5.3 %	19.6 %	10.7 %	0.2 %	1.5 %	1.1 %	.36%	<0.2 %
C21629	LW-T-16	6.2 %	1.1 %	48.4 %	2.3 %	<0.2 %	1.5 %	.2 %	.09%	<0.2 %
C21761	OB26A16B	66.3 %	6.2 %	2.7 %	9.4 %	0.3 %	0.8 %	1.4 %	.43%	<0.2 %

LAB.NO.	GEOL.NO.	MNO		CO2	TOT C	ORG C	TOT S	H2O	LOI	AG
						UNDERCLAY				
C21540	LM-Z-09	165	ppm	0.08%	0.96%	0.94%	0.45%	4.67%	6.81%	0.21ppm
C21662	LM-PZ-1A	61	ppm	0.12%	5.49%	5.46%	0.25%	2.4 %	11.47%	<0.2 ppm
C21663	LM-PZ-1B	93	ppm	<0.08%	2.59%	2.59%	0.77%	2.9 %	9.44%	<0.2 ppm
						COAL				
C21538	LM-C-01	41	ppm	0.50%	72.58%	72.44%	2.69%	2.6 %	91.72%	0.04ppm
C21657	C2-L-12A	259	ppm							<0.05ppm
C21658	C2-F-5	869	ppm	0.19%	53.70%	53.65%	9.77%	4.5 %	82.70%	<0.06ppm
C21721	OB26-1	37	ppm				3.25%	2.26%		<0.03ppm
C21722	OB26-2	39	ppm				2.76%	2.39%		<0.03ppm
						ENERGY SHALE				
C21535	LW-J-10	545	ppm	0.03%	0.94%	0.70%	1.29%	3.20%	8.42%	<0.04ppm
C21631	OR6-D-2	353	ppm	<0.08%	6.26%	6.26%	1.30%	0.9 %	12.49%	<0.25ppm
C21655	C2-M-13	461	ppm	0.07%	5.36%	5.34%	7.86%	2.7 %		<0.2 ppm
C21764	OB26-A26	675	ppm	<0.1 %	2.04%	2.04%	0.17%	0.76%	8.01%	<0.2 ppm
						CHANNEL FILL MATERIALS				
C21627	LW-T-3A	1173	ppm	20.40%	7.81%	2.24%	9.39%	1.1 %	20.53%	<0.25ppm
C21634	OB27-A-2	455	ppm	<0.07%	0.62%	0.62%	2.96%	1.0 %	6.71%	<0.25ppm
C21760	OB26-A12	1322	ppm	7.05%	7.55%	5.62%	6.96%	2.39%	17.90%	<0.2 ppm
C21763	OB26-A21	397	ppm	<0.1 %	1.72%	1.72%	2.79%	1.31%	8.59%	<0.2 ppm
C21768	LW-W-2	68	ppm	<0.1 %	54.95%	54.95%	4.14%	1.80%	68.68%	<0.08ppm
						ANNA SHALE				
C21536	LM-S-32	137	ppm	0.04%	8.60%	8.59%	1.71%	3.20%	16.10%	6.7 ppm
C21630	LW-S-7	225	ppm	2.33%	3.39%	2.75%	2.91%	1.2 %	10.79%	<0.25ppm
C21635	LW-T-11	505	ppm	0.10%	8.25%	8.25%	3.03%	0.9 %	15.89%	<0.25ppm
C21652	C2-M-11B	198	ppm	0.20%	11.32%	11.27%	3.65%	7.0 %		<0.2 ppm
C21653	C2-M-11C	300	ppm	<0.04%	13.03%	13.03%	2.14%	4.3 %		<0.2 ppm
C21654	C2-M-11D	149	ppm	0.78%	38.38%	38.17%	2.70%	1.5 %		<0.1 ppm
C21656	LW-T-12	313	ppm							<0.2 ppm
C21759	OB26-A8	192	ppm	3.14%	18.84%	17.98%	1.60%	1.16%	25.71%	<0.2 ppm
						"BLUE BAND"				
C21539	LM-W-13	87	ppm	1.03%	4.54%	4.25%	2.61%	3.26%	15.06%	0.17ppm
C21632	C2-N-10	72	ppm	<0.08%	52.09%	52.09%	2.48%	6.7 %	66.60%	<0.25ppm
C21660	LM-W-2	71	ppm	<0.10%	3.69%	3.69%	0.60%	1.6 %	13.27%	<0.2 ppm
C21661	LM-PW-1	25	ppm	<0.08%	11.60%	11.60%	0.20%	1.5 %	20.73%	<0.2 ppm
C21664	C2-O-1	223	ppm	<0.08%	11.39%	11.39%	3.85%	3.7 %	24.98%	<0.2 ppm
C21762	OB26-A20	55	ppm	<0.1 %	14.40%	14.40%	0.85%	2.51%	24.51%	<0.2 ppm
						OTHER SHALE PARTINGS				
C21633	C2-N-12	155	ppm	<0.07%	19.93%	19.93%	11.31%	3.1 %	37.67%	<0.25ppm
C21665	C2-O-2	83	ppm	<0.08%	26.28%	26.28%	8.89%	3.6 %	44.83%	<0.2 ppm
C21666	C2-O-3	124	ppm	<0.08%	15.85%	15.85%	15.85%	3.0 %	36.24%	<0.2 ppm
						LIMESTONE AND RELATED MATERIALS				
C21537	LM-V-31	622	ppm	37.00%	10.93%	0.83%	0.54%	<0.3 %	38.69%	0.4 ppm
C21626	C2-M-12	2605	ppm	36.55%	10.73%	0.75%	0.65%	0.2 %	37.80%	<0.25ppm
C21659	26524C	1907	ppm	34.98%	11.35%	1.80%	3.73%	0.9 %	35.11%	<0.2 ppm
C21767	LW-S-5	593	ppm	17.56%	8.23%	3.44%	4.53%	0.45%	21.70%	<0.25ppm
						ANNA SHALE CONCRETIONS				
C21628	LW-H-5	545	ppm	13.50%	7.70%	4.01%	7.36%	1.5 %	17.66%	<0.25ppm
C21629	LW-T-16	919	ppm	38.33%	13.87%	3.41%	1.43%	0.2 %	39.02%	<0.25ppm
C21761	OB26A16B	156	ppm	2.00%	3.68%	3.13%	6.33%	0.63%	11.45%	<0.2 ppm

LAB.NO.	GEOL.NO.	AS	B	BA	BE	BR	CD	CE	CO	CR
					UNDERCLAY					
C21540	LM-Z-09	3.7 ppm	240 ppm	262 ppm	8.4 ppm	2.2 ppm	<1.5 ppm	82 ppm	12 ppm	111 ppm
C21662	LM-PZ-1A	1.4 ppm	153 ppm	320 ppm	9 ppm	3 ppm	<0.9 ppm	92 ppm	10 ppm	115 ppm
C21663	LM-PZ-1B	13 ppm	184 ppm	340 ppm	10 ppm	4 ppm	<0.9 ppm	109 ppm	28 ppm	119 ppm
					COAL					
C21538	LM-C-01	.7 ppm	300 ppm	3130 ppm	1.6 ppm	14 ppm	<0.1 ppm	3.7 ppm	1.3 ppm	8 ppm
C21657	C2-L-12A	21 ppm	16 ppm	100 ppm	<1 ppm	8 ppm	<0.3 ppm	60 ppm	8 ppm	31 ppm
C21658	C2-F-5	15 ppm	14 ppm	63 ppm	<4 ppm	3 ppm	1.1 ppm	8 ppm	9 ppm	9 ppm
C21721	OB26-1	2.7 ppm	75 ppm	40 ppm	0.7 ppm	12 ppm	<0.5 ppm	10 ppm	3.1 ppm	10 ppm
C21722	OB26-2	12 ppm	92 ppm	35 ppm	0.5 ppm	15 ppm	<0.6 ppm	11 ppm	4.4 ppm	12 ppm
					ENERGY SHALE					
C21535	LW-J-10	16 ppm	170 ppm	614 ppm	11 ppm	2.3 ppm	<1.5 ppm	99 ppm	24 ppm	110 ppm
C21631	OR6-D-2	10 ppm	55 ppm	539 ppm	<3 ppm	5 ppm	<1.6 ppm	93 ppm	20 ppm	105 ppm
C21655	C2-M-13	13 ppm	34 ppm	480 ppm	<5 ppm	< 2 ppm	1.2 ppm	74 ppm	11 ppm	68 ppm
C21764	OB26-A26	10 ppm	95 ppm	592 ppm	3.3 ppm	< 2 ppm	<4 ppm	108 ppm	24 ppm	98 ppm
					CHANNEL FILL MATERIALS					
C21627	LW-T-3A	16 ppm	<10 ppm	7653 ppm	<6 ppm	1.2 ppm	<1.8 ppm	49 ppm	7.6 ppm	32 ppm
C21634	OB27-A-2	13 ppm	32 ppm	615 ppm	<3 ppm	< 1 ppm	<1.7 ppm	88 ppm	24 ppm	100 ppm
C21760	OB26-A12	24 ppm	<9 ppm	2758 ppm	<3 ppm	2 ppm	<4 ppm	112 ppm	17 ppm	67 ppm
C21763	OB26-A21	12 ppm	110 ppm	548 ppm	<3 ppm	1.4 ppm	<4 ppm	100 ppm	19 ppm	90 ppm
C21768	LW-W-2	24 ppm	38 ppm	169 ppm	0.7 ppm	6.9 ppm	<2 ppm	47 ppm	10 ppm	288 ppm
					ANNA SHALE					
C21536	LM-S-32	18 ppm	230 ppm	426 ppm	11 ppm	3.4 ppm	13.9 ppm	49 ppm	20 ppm	693 ppm
C21630	LW-S-7	10 ppm	<10 ppm	2429 ppm	<3 ppm	< 2 ppm	<1.7 ppm	71 ppm	22 ppm	248 ppm
C21635	LW-T-11	27 ppm	21 ppm	498 ppm	<3 ppm	1.9 ppm	<1.6 ppm	76 ppm	21 ppm	304 ppm
C21652	C2-M-11B	10 ppm	37 ppm	500 ppm	<5 ppm	< 1 ppm	25 ppm	109 ppm	19 ppm	417 ppm
C21653	C2-M-11C	16 ppm	38 ppm	484 ppm	<5 ppm	< 2 ppm	0.9 ppm	70 ppm	16 ppm	417 ppm
C21654	C2-M-11D	12 ppm	29 ppm	280 ppm	<3 ppm	4 ppm	19 ppm	66 ppm	13 ppm	905 ppm
C21656	LW-T-12	22 ppm	42 ppm	470 ppm	<5 ppm	2 ppm	<1.0 ppm	63 ppm	24 ppm	217 ppm
C21759	OB26-A8	12 ppm	94 ppm	6692 ppm	3.5 ppm	4 ppm	68 ppm	157 ppm	10 ppm	698 ppm
					"BLUE BAND"					
C21539	LM-W-13	9.4 ppm	260 ppm	351 ppm	5.4 ppm	2.2 ppm	<1.3 ppm	119 ppm	13 ppm	90 ppm
C21632	C2-N-10	1.7 ppm	12 ppm	246 ppm	1.4 ppm	1.9 ppm	<0.7 ppm	53 ppm	8.7 ppm	47 ppm
C21660	LM-W-2	7 ppm	160 ppm	480 ppm	5 ppm	1 ppm	<0.9 ppm	45 ppm	19 ppm	71 ppm
C21661	LM-PW-1	1.4 ppm	123 ppm	320 ppm	5 ppm	2 ppm	<0.8 ppm	102 ppm	4.6 ppm	67 ppm
C21664	C2-O-1	3.3 ppm	123 ppm	600 ppm	3.8 ppm	< 1 ppm	<0.8 ppm	97 ppm	9 ppm	60 ppm
C21762	OB26-A20	6.8 ppm	132 ppm	285 ppm	3.3 ppm	6 ppm	<4 ppm	138 ppm	12 ppm	75 ppm
					OTHER SHALE PARTINGS					
C21633	C2-N-12	10 ppm	31 ppm	263 ppm	2 ppm	< 2 ppm	<1.2 ppm	49 ppm	8.1 ppm	47 ppm
C21665	C2-O-2	7.8 ppm	81 ppm	280 ppm	1.8 ppm	1 ppm	<0.6 ppm	41 ppm	8 ppm	46 ppm
C21666	C2-O-3	10 ppm	145 ppm	320 ppm	1.8 ppm	.9 ppm	<0.7 ppm	82 ppm	6 ppm	45 ppm
					LIMESTONE AND RELATED MATERIALS					
C21537	LM-V-31	4.8 ppm	<33 ppm	292 ppm	1.8 ppm	1.6 ppm	<1.3 ppm	16 ppm	3.4 ppm	40 ppm
C21626	C2-M-12	2 ppm	<10 ppm	65 ppm	<6 ppm	.8 ppm	<1.8 ppm	12 ppm	3.2 ppm	32 ppm
C21659	26524C	4 ppm	<9 ppm	107 ppm	<5 ppm	2 ppm	<0.9 ppm	48 ppm	3.5 ppm	10 ppm
C21767	LW-S-5	9.3 ppm	<10 ppm	540 ppm	<3 ppm	2.6 ppm	<4 ppm	37 ppm	9.7 ppm	33 ppm
					ANNA SHALE CONCRETIONS					
C21628	LW-H-5	17 ppm	<10 ppm	300 ppm	<3 ppm	2.5 ppm	15 ppm	26 ppm	14 ppm	185 ppm
C21629	LW-T-16	6 ppm	<10 ppm	66 ppm	<3 ppm	1.5 ppm	11 ppm	22 ppm	2.4 ppm	123 ppm
C21761	OB26A16B	20 ppm	<9 ppm	313 ppm	<3 ppm	< 2 ppm	<4 ppm	27 ppm	9 ppm	221 ppm

LAB.NO.	GEOL.NO.	CS	CU	DY	EU	F	GA	GE	HF	HG
					UNDERCLAY					
C21540	LM-Z-09	12 ppm	34 ppm	4.6 ppm	1.4 ppm	1509 ppm	23 ppm	<8 ppm	1.7 ppm	
C21662	LM-PZ-1A	12 ppm	46 ppm	5.5 ppm	1.5 ppm	1798 ppm	24 ppm	<6 ppm	6.7 ppm	
C21663	LM-PZ-1B	15 ppm	61 ppm	6.2 ppm	2.0 ppm	1231 ppm	26 ppm	<6 ppm	5.9 ppm	
					COAL					
C21538	LM-C-01	.8 ppm	5.5 ppm	.2 ppm	.08ppm	132 ppm	2.2 ppm	<7 ppm	.3 ppm	
C21657	C2-L-12A	.8 ppm	15 ppm	6.3 ppm	1.9 ppm	1011 ppm	6 ppm	<5 ppm	.7 ppm	
C21658	C2-F-5	.5 ppm	17 ppm	.5 ppm	.17ppm	230 ppm	3 ppm	<5 ppm	.3 ppm	
C21721	OB26-1	1.1 ppm	8 ppm	.5 ppm	.20ppm	72 ppm	2.8 ppm	<0.8 ppm	.4 ppm	0.09 ppm
C21722	OB26-2	.8 ppm	8 ppm	.3 ppm	.18ppm	56 ppm	2.3 ppm	<0.8 ppm	.5 ppm	0.09 ppm
					ENERGY SHALE					
C21535	LW-J-10	9.8 ppm	30.5 ppm	7.3 ppm	1.5 ppm	589 ppm	24 ppm	<14 ppm	6 ppm	
C21631	OR6-D-2	10 ppm	20 ppm	3.6 ppm	1.4 ppm	348 ppm	27 ppm	<6 ppm	4.8 ppm	
C21655	C2-M-13	7.7 ppm	186 ppm	4.4 ppm	1.4 ppm	517 ppm	15 ppm	<5 ppm	3.4 ppm	0.10 ppm
C21764	OB26-A26	9 ppm	42 ppm	4.5 ppm	1.5 ppm	625 ppm	25 ppm	<7 ppm	6.0 ppm	
					CHANNEL FILL MATERIALS					
C21627	LW-T-3A	2.5 ppm	24 ppm	6.1 ppm	2.5 ppm	354 ppm	5.5 ppm	<6 ppm	1.6 ppm	
C21634	OB27-A-2	10 ppm	40 ppm	3.7 ppm	1.5 ppm	490 ppm	24 ppm	<6 ppm	4.6 ppm	
C21760	OB26-A12	7 ppm	35 ppm	6.8 ppm	1.6 ppm	476 ppm	12 ppm	<6 ppm	5.2 ppm	
C21763	OB26-A21	11 ppm	30 ppm	2.6 ppm	1.0 ppm	906 ppm	18 ppm	<7 ppm	6.0 ppm	
C21768	LW-W-2	4.8 ppm	32 ppm	1.2 ppm	.4 ppm	112 ppm	12 ppm	<2 ppm	3.7 ppm	0.18 ppm
					ANNA SHALE					
C21536	LM-S-32	12 ppm	113 ppm	2.2 ppm	.4 ppm	1318 ppm	20 ppm	<8 ppm	5.3 ppm	0.23 ppm
C21630	LW-S-7	10 ppm	51 ppm	2.7 ppm	1.2 ppm	1478 ppm	23 ppm	<6 ppm	4.8 ppm	0.09 ppm
C21635	LW-T-11	8.3 ppm	92 ppm	3.0 ppm	1.1 ppm	696 ppm	21 ppm	<5 ppm	5.6 ppm	0.24 ppm
C21652	C2-M-11B	6.4 ppm	149 ppm	9.4 ppm	2.6 ppm	1760 ppm	19 ppm	<5 ppm	4.3 ppm	0.31 ppm
C21653	C2-M-11C	8.8 ppm	120 ppm	3.6 ppm	1.3 ppm	1455 ppm	20 ppm	<5 ppm	4.5 ppm	
C21654	C2-M-11D	3.6 ppm	179 ppm	5.1 ppm	1.2 ppm	1552 ppm	10 ppm	<5 ppm	1.7 ppm	0.36 ppm
C21656	LW-T-12	8.9 ppm	72 ppm	3.4 ppm	1.0 ppm	1288 ppm	20 ppm	<5 ppm	4.4 ppm	0.12 ppm
C21759	OB26-A8	9 ppm	100 ppm	7.3 ppm	1.9 ppm	4165 ppm	12 ppm	<5 ppm	3.7 ppm	
					"BLUE BAND"					
C21539	LM-W-13	11 ppm	35 ppm	4.5 ppm	1.6 ppm	412 ppm	24 ppm	<8 ppm	5.0 ppm	
C21632	C2-N-10	4.9 ppm	34 ppm	1.5 ppm	.8 ppm	118 ppm	7.3 ppm	<6 ppm	2.1 ppm	
C21660	LM-W-2	11 ppm	53 ppm	1.0 ppm	.3 ppm	518 ppm	20 ppm	<6 ppm	4.5 ppm	
C21661	LM-PW-1	10 ppm	32 ppm	4.0 ppm	1.2 ppm	218 ppm	19 ppm	<6 ppm	4.4 ppm	
C21664	C2-O-1	9 ppm	27 ppm	2.1 ppm	1.1 ppm	182 ppm	12 ppm	<5 ppm	3.2 ppm	
C21762	OB26-A20	11 ppm	56 ppm	2.6 ppm	1.0 ppm	359 ppm	21 ppm	<5 ppm	3.8 ppm	
					OTHER SHALE PARTINGS					
C21633	C2-N-12	8.3 ppm	16 ppm	1.3 ppm	.59ppm	258 ppm	9.3 ppm	<4 ppm	3.1 ppm	
C21665	C2-O-2	8 ppm	16 ppm	1.7 ppm	.5 ppm	337 ppm	9 ppm	<4 ppm	2.8 ppm	
C21666	C2-O-3	7 ppm	43 ppm	1.9 ppm	.7 ppm	247 ppm	6 ppm	<5 ppm	2.9 ppm	
					LIMESTONE AND RELATED MATERIALS					
C21537	LM-V-31	.8 ppm	18.1 ppm	1.0 ppm	.3 ppm	269 ppm	2.1 ppm	11 ppm	.5 ppm	
C21626	C2-M-12	1.1 ppm	23 ppm	1.0 ppm	.28ppm	261 ppm	2.7 ppm	<6 ppm	.4 ppm	
C21659	26524C	.6 ppm	14 ppm	1.7 ppm	1.9 ppm	252 ppm	2 ppm	<5 ppm	.5 ppm	
C21767	LW-S-5	2.3 ppm	33 ppm	1.4 ppm	.5 ppm	387 ppm	3.6 ppm	<7 ppm	1.0 ppm	
					ANNA SHALE CONCRETIONS					
C21628	LW-M-5	2.7 ppm	79 ppm	1.2 ppm	.38ppm	629 ppm	6.0 ppm	<6 ppm	1.3 ppm	
C21629	LW-T-16	.4 ppm	32 ppm	1.3 ppm	.41ppm	606 ppm	1.1 ppm	<6 ppm	.2 ppm	0.08 ppm
C21761	OB26A16B	7 ppm	75 ppm	.3 ppm	.16ppm	372 ppm	8 ppm	<7 ppm	2.7 ppm	

APPENDIX C. continued

LAB.NO.	GEOL.NO.	IN	LA	LI	LU	MO	NI	PB	RB	SB
					UNDERCLAY					
C21540	LM-Z-09	35 ppb	36 ppm	19 ppm	.54ppm	3 ppm	<27 ppm	49 ppm	224 ppm	.5 ppm
C21662	LM-PZ-1A	31 ppb	48 ppm	32 ppm	.6 ppm	16 ppm	24 ppm	<30 ppm	220 ppm	1.7 ppm
C21663	LM-PZ-1B	<206 ppb	54 ppm	28 ppm	.6 ppm	< 10 ppm	45 ppm	<30 ppm	232 ppm	2.1 ppm
					COAL					
C21538	LM-C-01	< 10 ppb	2.6 ppm	4.5 ppm	.03ppm	54 ppm	8 ppm	5 ppm	10 ppm	.3 ppm
C21657	C2-L-12A	<104 ppb	29 ppm	4 ppm	.4 ppm	< 8 ppm	18 ppm	<10 ppm	15 ppm	.3 ppm
C21658	C2-F-5	<209 ppb	6 ppm	3 ppm	.08ppm	< 5 ppm	12 ppm	<10 ppm	15 ppm	.6 ppm
C21721	OB26-1	< 5 ppb	5.6 ppm	7 ppm	.07ppm	5 ppm	7 ppm	4 ppm	12 ppm	.2 ppm
C21722	OB26-2	< 10 ppb	5.6 ppm	14 ppm	.07ppm	7 ppm	17 ppm	33 ppm	12 ppm	.6 ppm
					ENERGY SHALE					
C21535	LW-J-10	8 ppb	50 ppm	58 ppm	.63ppm	< 2 ppm	<28 ppm	46 ppm	188 ppm	1.0 ppm
C21631	OR6-D-2	908 ppb	49 ppm	66 ppm	.7 ppm	< 10 ppm	33 ppm	<30 ppm	202 ppm	.4 ppm
C21655	C2-M-13	<409 ppb	42 ppm	19 ppm	.6 ppm	159 ppm	27 ppm	<30 ppm	113 ppm	1.8 ppm
C21764	OB26-A26	< 1 ppm	51 ppm	63 ppm	.56ppm	< 12 ppm	32 ppm	<18 ppm	175 ppm	.7 ppm
					CHANNEL FILL MATERIALS					
C21627	LW-T-3A	<506 PPB	20 ppm	10 ppm	.61ppm	18 ppm	24 ppm	<30 ppm	51 ppm	1.6 ppm
C21634	OB27-A-2	2828 ppb	49 ppm	43 ppm	.6 ppm	< 9 ppm	39 ppm	<30 ppm	202 ppm	1.0 ppm
C21760	OB26-A12	<410 PPB	37 ppm	16 ppm	.39ppm	60 ppm	52 ppm	<16 ppm	87 ppm	2.0 ppm
C21763	OB26-A21	< 1 ppm	47 ppm	28 ppm	.53ppm	20 ppm	20 ppm	<18 ppm	158 ppm	2.6 ppm
C21768	LW-W-2	<143 ppb	13 ppm	11 ppm	.22ppm	153 ppm	89 ppm	<6 ppm	45 ppm	4.5 ppm
					ANNA SHALE					
C21536	LM-S-32	31 ppb	33 ppm	36 ppm	.65ppm	81 ppm	131 ppm	55 ppm	210 ppm	5.9 ppm
C21630	LW-S-7	66 ppb	39 ppm	39 ppm	.5 ppm	21 ppm	92 ppm	<30 ppm	176 ppm	2.1 ppm
C21635	LW-T-11	<303 ppb	45 ppm	36 ppm	.5 ppm	50 ppm	101 ppm	<30 ppm	147 ppm	6.4 ppm
C21652	C2-M-11B	73 ppb	74 ppm	34 ppm	.8 ppm	26 ppm	264 ppm	<30 ppm	125 ppm	4.7 ppm
C21653	C2-M-11C	<410 ppb	37 ppm	31 ppm	.5 ppm	33 ppm	204 ppm	<30 ppm	152 ppm	6.7 ppm
C21654	C2-M-11D	61 ppb	54 ppm	25 ppm	.7 ppm	86 ppm	468 ppm	<20 ppm	76 ppm	8.7 ppm
C21656	LW-T-12	<202 ppb	35 ppm	34 ppm	.4 ppm	79 ppm	136 ppm	<35 ppm	146 ppm	6.1 ppm
C21759	OB26-A8	<405 ppb	52 ppm	25 ppm	.67ppm	182 ppm	217 ppm	<15 ppm	101 ppm	7.6 ppm
					"BLUE BAND"					
C21539	LM-W-13	< 25 ppb	52 ppm	109 ppm	.62ppm	5 ppm	<25 ppm	45 ppm	94 ppm	.3 ppm
C21632	C2-N-10	13 ppb	25 ppm	44 ppm	.17ppm	< 6 ppm	19 ppm	<15 ppm	41 ppm	.3 ppm
C21660	LM-W-2	<102 ppb	29 ppm	233 ppm	.3 ppm	< 12 ppm	64 ppm	<35 ppm	77 ppm	.4 ppm
C21661	LM-PW-1	24 ppb	67 ppm	380 ppm	.5 ppm	< 10 ppm	17 ppm	<30 ppm	73 ppm	1.3 ppm
C21664	C2-O-1	125 ppb	47 ppm	79 ppm	.2 ppm	< 8 ppm	21 ppm	<30 ppm	63 ppm	1.3 ppm
C21762	OB26-A20	16 ppb	79 ppm	143 ppm	.32ppm	< 10 ppm	59 ppm	<15 ppm	78 ppm	.5 ppm
					OTHER SHALE PARTINGS					
C21633	C2-N-12	31 ppb	27 ppm	48 ppm	.3 ppm	< 10 ppm	12 ppm	<20 ppm	93 ppm	.4 ppm
C21665	C2-O-2	< 10 ppb	24 ppm	40 ppm	.2 ppm	< 6 ppm	11 ppm	<25 ppm	74 ppm	.5 ppm
C21666	C2-O-3	< 31 ppb	54 ppm	59 ppm	.3 ppm	48 ppm	21 ppm	<25 ppm	48 ppm	.7 ppm
					LIMESTONE AND RELATED MATERIALS					
C21537	LM-V-31	< 6 ppb	6.3 ppm	7.1 ppm	.14ppm	24 ppm	<25 ppm	44 ppm	22 ppm	.6 ppm
C21626	C2-M-12	<100 ppb	8 ppm	9 ppm	.19ppm	7 ppm	21 ppm	<30 ppm	22 ppm	1.0 ppm
C21659	26524C	<303 ppb	20 ppm	5 ppm	.5 ppm	< 7 ppm	<14 ppm	<35 ppm	20 ppm	1.8 ppm
C21767	LW-S-5	< 40 ppb	14 ppm	8 ppm	.20ppm	< 20 ppm	55 ppm	<19 ppm	29 ppm	.7 ppm
					ANNA SHALE CONCRETIONS					
C21628	LW-H-5	46 ppb	17 ppm	16 ppm	.51ppm	108 ppm	82 ppm	<30 ppm	53 ppm	6.7 ppm
C21629	LW-T-16	< 80 ppb	13 ppm	7 ppm	.41ppm	30 ppm	54 ppm	<30 ppm	8 ppm	5.2 ppm
C21761	OB26A16B	< 50 ppb	11 ppm	21 ppm	.30ppm	102 ppm	75 ppm	<17 ppm	70 ppm	11 ppm

LAB.NO.	GEOL.NO.	SC	SE	SM	SR	TA	TB	TH	TL	U
					UNDERCLAY					
C21540	LM-Z-09	16 PPM	< .5 PPM	7 PPM	164 PPM	1.1 PPM	.9 PPM	16 PPM	<4.5 PPM	3.2 PPM
C21662	LM-PZ-1A	17 PPM	< .5 PPM	9.0 PPM	140 PPM	1.4 PPM	.9 PPM	16 PPM	<10 PPM	2 PPM
C21663	LM-PZ-1B	19 PPM	1.4 PPM	10.0 PPM	180 PPM	1.3 PPM	1.2 PPM	16 PPM	<10 PPM	< 2 PPM
					COAL					
C21538	LM-C-01	1.0 PPM	1.2 PPM	.8 PPM	47 PPM	.06PPM	.05PPM	.8 PPM	1.2 PPM	7.5 PPM
C21657	C2-L-12A	5 PPM	1.7 PPM	9.5 PPM	150 PPM	.1 PPM	1.4 PPM	2 PPM	<3 PPM	< 1 PPM
C21658	C2-F-5	1.3 PPM	3.3 PPM	.9 PPM	61 PPM	.08PPM	.07PPM	1 PPM	<3 PPM	3 PPM
C21721	OB26-1	1.8 PPM	1.6 PPM	.8 PPM	31 PPM	.12PPM	.10PPM	1.6 PPM	<1 PPM	.8 PPM
C21722	OB26-2	2.4 PPM	1.8 PPM	.8 PPM	27 PPM	.12PPM	.15PPM	2.0 PPM	<1 PPM	< .8 PPM
					ENERGY SHALE					
C21535	LW-J-10	21 PPM	< .5 PPM	2.8 PPM	107 PPM	1.3 PPM	1.3 PPM	17 PPM	<4.5 PPM	3.3 PPM
C21631	OR6-D-2	19 PPM	1.8 PPM	7.8 PPM	119 PPM	1.1 PPM	1.0 PPM	14 PPM	<10 PPM	5 PPM
C21655	C2-N-13	12 PPM	7 PPM	8.3 PPM	130 PPM	.5 PPM	.8 PPM	13 PPM	<10 PPM	7 PPM
C21764	OB26-A26	20 PPM	1.0 PPM	8.2 PPM	139 PPM	1.4 PPM	1.2 PPM	18 PPM	<12 PPM	3.0 PPM
					CHANNEL FILL MATERIALS					
C21627	LW-T-3A	15 PPM	3.7 PPM	10.7 PPM	238 PPM	.3 PPM	1.6 PPM	4.2 PPM	<10 PPM	5.2 PPM
C21634	OB27-A-2	20 PPM	2.0 PPM	8.2 PPM	92 PPM	1.1 PPM	1.3 PPM	13 PPM	<10 PPM	< 2 PPM
C21760	OB26-A12	11 PPM	12 PPM	8.8 PPM	194 PPM	1.3 PPM	1.2 PPM	17 PPM	<10 PPM	22 PPM
C21763	OB26-A21	17 PPM	3.4 PPM	6.0 PPM	109 PPM	1.4 PPM	0.6 PPM	17 PPM	<12 PPM	< 1.5 PPM
C21768	LW-W-2	6.6 PPM	44 PPM	4.7 PPM	51 PPM	.7 PPM	.3 PPM	7 PPM	<4 PPM	45 PPM
					ANNA SHALE					
C21536	LM-S-32	20 PPM	29 PPM	2.9 PPM	99 PPM	1.2 PPM	.6 PPM	16 PPM	10 PPM	14 PPM
C21630	LW-S-7	18 PPM	6.5 PPM	6.4 PPM	165 PPM	1.1 PPM	.7 PPM	13 PPM	<10 PPM	10 PPM
C21635	LW-T-11	16 PPM	45 PPM	6.6 PPM	85 PPM	1.1 PPM	1.0 PPM	12 PPM	<10 PPM	17 PPM
C21652	C2-M-11B	17 PPM	15 PPM	14 PPM	196 PPM	.8 PPM	2.1 PPM	14 PPM	<10 PPM	22 PPM
C21653	C2-M-11C	16 PPM	41 PPM	8.2 PPM	100 PPM	1.1 PPM	1.1 PPM	12 PPM	<10 PPM	20 PPM
C21654	C2-M-11D	10 PPM	121 PPM	8.6 PPM	140 PPM	.9 PPM	1.1 PPM	6 PPM	<6 PPM	52 PPM
C21656	LW-T-12	14 PPM	10 PPM	6.2 PPM	165 PPM	1.2 PPM	.6 PPM	13 PPM	<10 PPM	17 PPM
C21759	OB26-A8	11 PPM	62 PPM	14 PPM	362 PPM	1.2 PPM	1.5 PPM	14 PPM	<9 PPM	95 PPM
					"BLUE BAND"					
C21539	LM-W-13	12 PPM	5.5 PPM	10 PPM	76 PPM	1.8 PPM	.7 PPM	20 PPM	4.7 PPM	33 PPM
C21632	C2-N-10	5.6 PPM	7.5 PPM	4.5 PPM	59 PPM	.4 PPM	.4 PPM	8.8 PPM	<10 PPM	< 1 PPM
C21660	LM-W-2	8.4 PPM	8 PPM	1.9 PPM	93 PPM	1.6 PPM	.2 PPM	15 PPM	<10 PPM	< 2 PPM
C21661	LM-PW-1	10 PPM	3.6 PPM	7.8 PPM	110 PPM	1.4 PPM	.8 PPM	15 PPM	<10 PPM	< 1.5 PPM
C21664	C2-O-1	8.0 PPM	6 PPM	7.3 PPM	120 PPM	1.1 PPM	.5 PPM	15 PPM	<10 PPM	< 1 PPM
C21762	OB26-A20	10 PPM	10 PPM	7.1 PPM	142 PPM	1.3 PPM	0.5 PPM	23 PPM	<9 PPM	< 1 PPM
					OTHER SHALE PARTINGS					
C21633	C2-N-12	7.2 PPM	13 PPM	3.5 PPM	71 PPM	.8 PPM	.3 PPM	8.6 PPM	<10 PPM	1.9 PPM
C21665	C2-O-2	7.0 PPM	9 PPM	3.1 PPM	70 PPM	.7 PPM	.3 PPM	9 PPM	<7 PPM	< 1 PPM
C21666	C2-O-3	5.4 PPM	13 PPM	4.7 PPM	160 PPM	.7 PPM	.3 PPM	8 PPM	<8 PPM	< 1 PPM
					LIMESTONE AND RELATED MATERIALS					
C21537	LM-V-31	2.3 PPM	4.3 PPM	1.8 PPM	877 PPM	.15PPM	.19PPM	1.9 PPM	<6.7 PPM	9 PPM
C21626	C2-M-12	5.5 PPM	1.7 PPM	1.5 PPM	393 PPM	.1 PPM	.2 PPM	1.9 PPM	<10 PPM	2.4 PPM
C21659	26524C	5.8 PPM	.8 PPM	8.3 PPM	210 PPM	.09PPM	1.4 PPM	1 PPM	<10 PPM	< .8 PPM
C21767	LW-S-5	3.5 PPM	5.0 PPM	3.0 PPM	252 PPM	.3 PPM	.4 PPM	6 PPM	<12 PPM	6 PPM
					ANNA SHALE CONCRETIONS					
C21628	LW-H-5	13 PPM	88 PPM	2.9 PPM	251 PPM	.3 PPM	.3 PPM	4.6 PPM	<10 PPM	14 PPM
C21629	LW-T-16	5.6 PPM	58 PPM	2.2 PPM	930 PPM	< .1 PPM	.3 PPM	.7 PPM	<10 PPM	6.1 PPM
C21761	OB26A16B	13 PPM	60 PPM	1.2 PPM	61 PPM	.7 PPM	.3 PPM	9 PPM	<11 PPM	7.8 PPM

LAB.NO.	GEOL.NO.	V		W		YB		ZN		ZR	
					UNDERCLAY						
C21540	LM-Z-09	330	PPM	2.1	PPM	2.9	PPM	32	PPM	329	PPM
C21662	LM-PZ-1A	63	PPM	1.4	PPM	3.6	PPM	23	PPM	210	PPM
C21663	LM-PZ-1B	87	PPM	2	PPM	3.6	PPM	21	PPM	185	PPM
					COAL						
C21538	LM-C-01	31	PPM	.6	PPM	.1	PPM	193	PPM	14	PPM
C21657	C2-L-12A	67	PPM	< .5	PPM	2.2	PPM	11	PPM	22	PPM
C21658	C2-F-5	13	PPM	< .3	PPM	.2	PPM	433	PPM	<5	PPM
C21721	OB26-1	10	PPM	< .5	PPM	.5	PPM	40	PPM	20	PPM
C21722	OB26-2	12	PPM	.4	PPM	.4	PPM	15	PPM	23	PPM
					ENERGY SHALE						
C21535	LW-J-10	400	PPM	1.9	PPM	3.6	PPM	117	PPM	181	PPM
C21631	OR6-D-2	114	PPM	1.1	PPM	3.5	PPM	57	PPM	178	PPM
C21655	C2-M-13	60	PPM	< 1	PPM	2.5	PPM	55	PPM	93	PPM
C21764	OB26-A26	71	PPM	2.4	PPM	3.7	PPM	49	PPM	176	PPM
					CHANNEL FILL MATERIALS						
C21627	LW-T-3A	9	PPM	< .4	PPM	3.5	PPM	16	PPM	49	PPM
C21634	OB27-A-2	61	PPM	1.4	PPM	3.3	PPM	44	PPM	179	PPM
C21760	OB26-A12	33	PPM	< 1	PPM	2.5	PPM	16	PPM	103	PPM
C21763	OB26-A21	73	PPM	< 2	PPM	3.0	PPM	20	PPM	190	PPM
C21768	LW-W-2	330	PPM	< .5	PPM	1.1	PPM	21	PPM	103	PPM
					ANNA SHALE						
C21536	LM-S-32	1500	PPM	< 2	PPM	2.5	PPM	633	PPM	135	PPM
C21630	LW-S-7	63	PPM	1	PPM	2.6	PPM	75	PPM	179	PPM
C21635	LW-T-11	161	PPM	1.3	PPM	3.0	PPM	28	PPM	207	PPM
C21652	C2-M-11B	58	PPM	< .6	PPM	4.5	PPM	4790	PPM	135	PPM
C21653	C2-M-11C	113	PPM	1.7	PPM	3.0	PPM	297	PPM	146	PPM
C21654	C2-M-11D	310	PPM	.4	PPM	3.6	PPM	1098	PPM	76	PPM
C21656	LW-T-12	130	PPM	1	PPM	2.6	PPM	29	PPM	139	PPM
C21759	OB26-A8	700	PPM	.7	PPM	4.5	PPM	1050	PPM	78	PPM
					"BLUE BAND"						
C21539	LM-W-13	240	PPM	3.0	PPM	2.9	PPM	<4	PPM	142	PPM
C21632	C2-N-10	54	PPM	< 1	PPM	1.1	PPM	15	PPM	87	PPM
C21660	LM-W-2	53	PPM	3	PPM	1.4	PPM	9	PPM	155	PPM
C21661	LM-PW-1	49	PPM	2.8	PPM	3.1	PPM	49	PPM	155	PPM
C21664	C2-O-1	29	PPM	2	PPM	1.6	PPM	17	PPM	94	PPM
C21762	OB26-A20	41	PPM	2	PPM	2.2	PPM	10	PPM	126	PPM
					OTHER SHALE PARTINGS						
C21633	C2-N-12	64	PPM	.9	PPM	1.4	PPM	11	PPM	102	PPM
C21665	C2-O-2	20	PPM	1.1	PPM	1.2	PPM	13	PPM	84	PPM
C21666	C2-O-3	29	PPM	1.1	PPM	1.4	PPM	8	PPM	88	PPM
					LIMESTONE AND RELATED MATERIALS						
C21537	LM-V-31	88	PPM	< .5	PPM	.6	PPM	<4	PPM	7	PPM
C21626	C2-M-12	12	PPM	< .3	PPM	.7	PPM	24	PPM	10	PPM
C21659	26524C	54	PPM	< .3	PPM	3.6	PPM	13	PPM	<5	PPM
C21767	LW-S-5	5	PPM	< .5	PPM	.8	PPM	6	PPM	16	PPM
					ANNA SHALE CONCRETIONS						
C21628	LW-H-5	<10	PPM	< 1	PPM	2.0	PPM	404	PPM	37	PPM
C21629	LW-T-16	120	PPM	< 1	PPM	2.1	PPM	596	PPM	<5	PPM
C21761	OB26A16B	188	PPM	< .5	PPM	.9	PPM	12	PPM	53	PPM